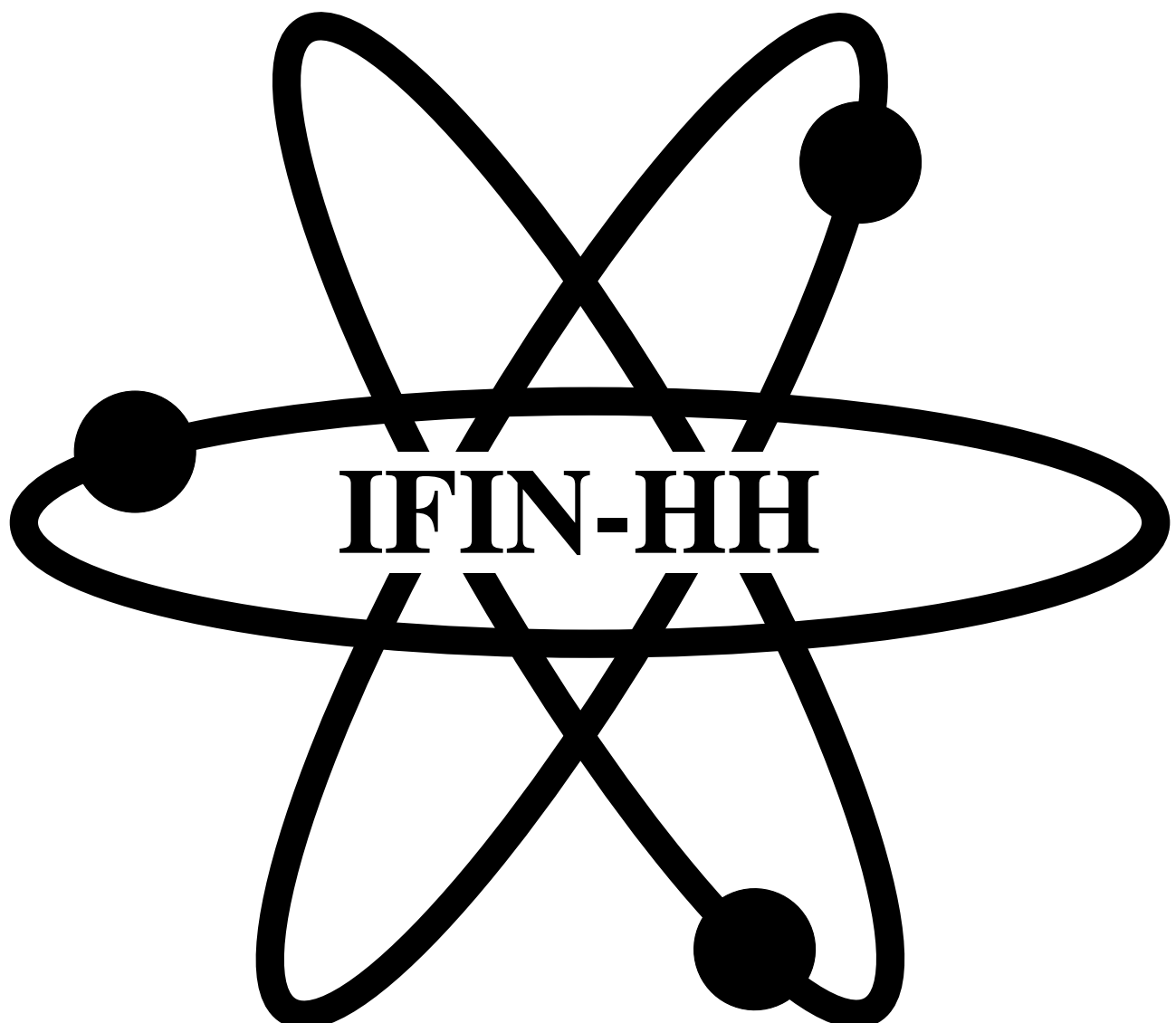


SCIENTIFIC REPORT 2003-2004



Bucharest, Romania, 2005

ISSN 1454-2714
IFIN-HH-AR-2005

Publisher: "Horia Hulubei" National Institute for Physics and Nuclear Engineering
Printing, Publishing, and Documentation Office
Str. Atomistilor no. 109
P.O. Box MG-6
RO-077125 Bucharest-Măgurele
Romania
Telephone: +40 1 404 23 00
Fax: +40 1 457 44 40
E-mail: anuar@ifin.nipne.ro
WWW home page: <http://www.nipne.ro>

Editors: Dan Grecu, Margareta Oancea, Claudiu Schiaua, Marinela Dumitriu

Printed by: Gelu Chisnăr

Cover: Adrian Socolov

The editors have not modified the text of the contributions, not even for spelling or grammar. Changes were only made in the title of some contributions by converting some capital-case letters to lower-case for case uniformity, in the placement of some pictures, and in the spelling of some author's names to assure the correct building of the author index.

FOREWORD

Physical research is probably one of the oldest occupations on earth, as old as the human need to take some control in relation with *physis*. From this perspective, two more years of researches in physics may not seem very significant. Besides, I suspect that the most amazing breakthroughs in this area happened thousands of years ago when the Nobel Prize had not yet been invented to reward them. On the other hand, as we found out and this report will show, there is still plenty left for us, physicists, to do. Human power over nature is still far from impressive and has often done more harm than good. So, on a global scale, we must start mending errors of the past, expand our understanding, and think of gentler ways to impose our control in the future.

Moreover, as Romanian physicists, we have our work cut out for us if we are to help put local society on a steady course to development. This is what the government, via the National Plan for Research, Development & Innovation, expects us to do, and this is precisely what IFIN-HH did pretty successfully, I'd say, in 2003-2004. Progress has been made at both ends of this bilateral relation. The government has learned how to spell out sensible demands, although funding has a tendency to atomize and lose some effectiveness by trying to accommodate too many small-time projects. The Plan, nevertheless, has rather straightforward goals and a number of equally clear programs, including a basic research program CERES and others such as RELANSIN, which aims to jumpstart the economy by research and innovation; VIASAN (life and health), BIOTECH (biotechnologies), MENER (energy and environment), and others that are of interest to IFIN-HH and under which public financing is available by annual project competitions. Our institute in turn has learned to meet the public demands halfway and beat competitors by putting forth more articulate project proposals.

Perhaps the best piece of news in 2003 was the launch of government financing for the national R&D institutes as a consequence of the 2002 Research Act. Funding under this Core Program is designed to help such institutes, including ours, to implement their own policies in their respective fields. As far as IFIN-HH is concerned, 26 projects we submitted were approved for funding under this program for the period 2003-2005. In terms of research objectives, the 26 fall into six categories, namely 1) quantum system-modeling of fundamental processes by analytical, computational, and experimental methods; 2) basic research in nuclear and atomic physics; developments and applications of accelerated particle beams; 3) life and environmental physics; 4) improving competence, adequacy, and competitiveness in the areas of services and micro-production; 5) consolidating R&D in areas with a potential for micro-production and services; and 6) radioactive waste management and the decommissioning of nuclear facilities. In the meantime, IFIN-HH units have tried to raise their market profile. In 2004, for example, ACTIVA-N won accreditation as a materials testing lab and IRASM Microbiology Laboratory was licensed for drug quality control.

Our IDRANAP (Inter-Disciplinary Research and Applications based on Nuclear and Atomic Physics) continued to operate as a European Center of Excellence through 2003 and wrapped up its activity in May 2004. Its most remarkable results included putting into operation and improving performance of several experimental facilities entirely developed by our specialists such as the tandem use as an accelerator mass spectrometer; a 14 GHz electronic cyclotron resonance source; the rotatable muon detector WILLI, and the high temperature facility TS-3000 K for neutron scattering. Over 300 experts attended the three international workshops and conference organized during the 39-month activity of IDRANAP. More than 80 foreign guests

(experts, post-docs, PhD students) mostly from European countries came to the center, and about as many visits abroad were made by our own staff. Despite some difficulties we faced, the project can be considered a success story. The European Center of Excellence title promoted IFIN-HH as a leading center for research, development, and training in nuclear physics, bringing together basic and applied research into a multidisciplinary approach.

In another piece of good news in 2003-2004 public financing for our collaboration with CERN began coming in under the National RD&I Program CORINT. It was about time since IFIN-HH researchers had long been actively involved in many CERN experiments. During the reporting period, our participation in ATLAS consisted in helping to build Tilecal subdetector, beam testing, validation of the GEANT4 hadronic physics library, trigger activities and data acquisition, as well as theoretical studies on LHC physics. Our ALICE group was involved in GRID activities and dedicated software installation and development. Most remarkably, our Nuclear Interactions and Hadronic Matter Center of Excellence set up its own Detector Laboratory that went into operation in November 2003. Twenty percent of the ALICE-TRD modules, or a total 108 individual modules, covering a 147 sq.m area and including 232,000 read-out channels, will be made at this IFIN-HH facility. Also during the reporting period, the group involved in LHCb was strengthened which boosted their contribution to calibrating ECAL modules and making ready for their installation on site. At the same time, our participation in CERN's DIRAC experiment continued with data acquisition and processing at the experimental facility that includes the preshower detector fully made at IFIN-HH.

Aside from our ties with CERN, we continued our longstanding collaborations with JINR Dubna, France's IN2P3, and INFN in Italy, and cooperated with dozens of other institutes, universities, and research centers around the world. We hosted conferences and workshops, and were represented at numerous meetings abroad. Our researchers published hundreds of papers in international scientific journals. They haven't won the Nobel yet, but they sure did a lot of useful things, as this report will prove.

Dr. Nicolae Victor Zamfir

Director General

Contents

Theoretical Physics	7
Nuclear & Particle Physics	39
Health and Environmental Physics	65
Waste Management	83
Miscellaneous Applications	95
 Appendix	 107
Publications	109
In Journals	109
Books and Chapter in Books	113
Preprints	113
International Conferences	114
PhD Theses	118
Scientific Exchanges	119
Foreign Visitors	119
Visits Abroad	119
Seminars Abroad	120
Research Staff	121
Author Index	125

Results included in the following are progress reports of research projects and therefore should be considered as preliminary communications.

Theoretical Physics

Phase transitions in ternary amphiphilic systems

D. Buzatu¹, F.D. Buzatu², D.A. Huckaby³

¹ University Politehnica, Bucharest, Romania

² Horia Hulubei National Institute for Physics and Nuclear Engineering, Bucharest, Romania

³ Texas Christian University, Fort Worth, US

Two almost immiscible liquids (e.g., water and chloroform) may become partially miscible in the presence of a solvent (ethanol, acetic acid). In order to describe this phenomenon, Wheeler and Widom [1] introduced a microscopic model in which each bond of a lattice is occupied by a bifunctional molecule of type AA, BB, or AB. The AB type molecule acts as an amphiphile that increases the mutual solubility of AA and BB. In the original model, only A or only B atoms may meet at a given site (infinite repulsion between A and B atoms of a common site; no interaction otherwise). The model reduces to the standard (spin 1/2, nearest-neighbor interaction) Ising model on the same lattice, its ferromagnetic transition corresponding to a phase-separation transition for the ternary solution. The original model has been extended to include temperature effects by allowing finite interactions between any two atoms near a common site [2], in which case the model becomes equivalent to the standard Ising model on an associated lattice.

A further extension of the model, describing more realistic cases (asymmetric coexistence curves), assumes three-body interactions between the atoms near a common site of the honeycomb or three-coordinated Bethe-lattice [3]. In this case, the molecular model is equivalent to the Ising model on an associated lattice with both two-body and three-body interactions. Nevertheless, it can be transformed via a star-triangle transformation to an Ising model on an intermediate lattice, then via a double-decoration to an Ising model on the original honeycomb or Bethe lattice with only two-body interactions. For strong three-body interactions, the parameters of the model on the intermediate lattice must get complex values, the appropriate transformations being determined in Ref. [4].

A ternary amphiphilic system can undergo a transi-

tion to an ordered amphiphile-rich phase. Within the Wheeler-Widom model, it corresponds to the antiferromagnetic transition of the equivalent Ising model. An accurate approximation to the boundary in temperature-composition space of the molecular model was calculated by transforming a closed-form approximation of the antiferromagnetic critical frontier in the equivalent Ising model [5].

A solution suddenly quenched from an initial one-phase state in the two-phase region reaches its equilibrium either through a nucleation or a spinodal decomposition process. The states below the coexistence curve can be then classified as metastable and unstable, separated in a mean-field description by the spinodal curve. A new microscopic derivation of the spinodal curve for ternary solutions within the extended Wheeler-Widom model has been presented in Ref. [6].

References

- [1] J. C. Wheeler and B. Widom, *J. Am. Chem. Soc.*, 90 (1968) 3064
- [2] D. A. Huckaby and M. Shinmi, *J. Stat. Phys.* 45 (1986) 135
- [3] D.L.Strout, D. A. Huckaby, and F. Y. Wu, *Physica A* 173 (1991) 60
- [4] F. D. Buzatu and D. A. Huckaby, *Physica A* 299 (2001) 427
- [5] D. A. Huckaby, A. Pekalski, D. Buzatu, and F. D. Buzatu, *J. Chem. Phys.* 115 (2001) 6775
- [6] F.D.Buzatu, D.Buzatu, and J.G.Albright, *J.Sol.Chem.*11 (2001) 969

Two-dimensional solitons in quasi-phase-matched quadratic crystals

N.C. Panoiu^{1,2}, D. Mihalache^{2,3}, D. Mazilu², F. Lederer³, R.M. Osgood¹

¹ Department of Applied Physics and Applied Mathematics, Columbia University, New York, New York 10027, USA

² Department of Theoretical Physics, Institute of Atomic Physics, P.O. Box MG-6, Bucharest, Romania

³ Institute of Solid State Theory and Theoretical Optics, Friedrich Schiller University Jena, Max-Wien-Platz 1, Jena, D-07743, Germany

We study the existence and dynamics of two-dimensional spatial solitons in crystals that exhibit a periodic modulation of both the refractive index and the second-order susceptibility for achieving quasi-phase matching. Far from resonances between the domain length of the periodic crystal and the diffraction length of the beams, it is demonstrated that the properties of the solitons in this quasi-pase-matched geometry are strongly influenced by induced third-order nonlinearities. The stability properties of the two-dimensional

solitons are analyzed as a function of the total power, the effective wave vector-mismatch between the first and second harmonic, and the relative strength between the induced third-order nonlinearity and the effective second-order nonlinearity. Finally, the formation of two-dimensional solitons from a Gaussian beam excitation is investigated numerically.

Published in: *Physical Review E*, v. 68, 016608 (2003)

Stable spatiotemporal spinning solitons in a bimodal cubic-quintic medium

D. Mihalache^{1,3}, D. Mazilu¹, I. Towers², B.A. Malomed², F. Lederer³

¹ Department of Theoretical Physics, Institute of Atomic Physics, P.O. Box MG-6, Bucharest, Romania

² Department of Interdisciplinary Studies, Faculty of Engineering, Tel Aviv University, Tel Aviv 69978, Israel

³ Institute of Solid State Theory and Theoretical Optics, Friedrich Schiller University Jena, Max-Wien-Platz 1, Jena, D-07743, Germany

We investigate the formation of stable spatiotemporal three-dimensional (3D) solitons (“light bullets”) with internal vorticity (“spin”) in a bimodal system described by coupled cubic-quintic nonlinear Schrödinger equations. Two relevant versions of the model, for the linear and circular polarizations, are analyzed in detail. In the former case, an important ingredient of the model are the four-wave-mixing terms, which give rise to a phase-sensitive nonlinear coupling between the two polarization components. Thresholds for the formation of both spinning and nonspinning 3D solitons are found. Instability growth rates of perturbation eigenmodes with different azimuthal indices are calculated as functions of the solitons’ propagation constant. As a result, stability domains in the model’s parameter plane are identified for solitons with the values of the spin of their components $s = 0$ and $s = 1$,

while all the solitons with $s \geq 2$ are unstable. The solitons with $s = 1$ are stable only if their energy exceeds a certain critical value, so that, in typical cases, their stability region occupies $\simeq 25\%$ of their existence domain. Direct simulations of the full nonlinear system produce results which are in perfect agreement with the linear-stability analysis: stable 3D spinning solitons readily self-trap from Gaussian initial pulses with embedded vorticity, and easily restore themselves after strong perturbations are imposed, while unstable spinning solitons split into a set of separating zero-spin fragments whose number is exactly equal to the azimuthal index of the strongest unstable perturbation eigenmode.

Published in: *Physical Review E*, v. 67, 056608 (2003)

Arresting wave collapse by wave self-rectification

L.C. Crasovan^{1,2}, J.P. Torres², D. Mihalache^{1,2}, L. Torner²

¹ Department of Theoretical Physics, Institute of Atomic Physics, National Institute of Physics and Nuclear Engineering, P.O. Box MG-6, Bucharest, Romania

² ICFO-Institut de Ciencies Fotoniques, and Department of Signal Theory and Communications, Universitat Politecnica de Catalunya, 08034 Barcelona, Spain.

We put forward a mechanism for tailoring, and even arresting, the collapse of wave packets in nonlinear media, whose dynamics is governed by nonlocal two-dimensional nonlinear Schrödinger-like equations. The key ingredient of the scheme is the self-generation

of nonlocal nonlinearities mediated by wave rectification.

Published in: *Physical Review Letters* , v. 91, 063904 (2003)

Spatial solitons in type II quasi-phasedmatched slab waveguides

N.C. Panoiu^{1,2}, D. Mihalache², H. Rao¹, R.M. Osgood¹

¹ Department of Applied Physics and Applied Mathematics, Columbia University, New York, New York 10027, USA

² Department of Theoretical Physics, Institute of Atomic Physics, P.O. Box MG-6, Bucharest, Romania

The existence and dynamics of one-dimensional spatial solitons formed upon propagation in quasi-phase-matched gratings, through three wave parametric interaction, is analyzed. We study the general case in which the grating exhibits a periodic modulation of both the refractive index and the second-order susceptibility. It is demonstrated that for negative effective

wave vector mismatch the induced third-order nonlinearities increase the domain of soliton instability. Finally, the dependence of the efficiency of the second harmonic generation process in the soliton regime, on the parameters of the grating, is discussed.

Published in: *Physical Review E*, v. 68, 065603(R) (2003)

Stable vortex dipoles in nonrotating Bose-Einstein condensates

L.C. Crasovan^{1,3}, V. Vekslerchik², V.M. Perez-Garcia², J.P. Torres¹, D. Mihalache^{1,3}, L. Torner²

¹ ICFO-Institut de Ciencies Fotoniques, and Department of Signal Theory and Communications, Universitat Politecnica de Catalunya, 08034 Barcelona, Spain.

² Departamento de Matemáticas, E.T.S.I. Industriales, Universidad de Castilla-La Mancha, 13071 Ciudad Real, Spain

³ Department of Theoretical Physics, Institute of Atomic Physics, National Institute of Physics and Nuclear Engineering, P.O. Box MG-6, Bucharest, Romania

We find stable families of vortex dipoles in nonrotating Bose-Einstein condensates. The vortex dipoles correspond to topological excited collective states of the condensed atoms. They exist and are dynamically and structurally stable for a broad range of parame-

ters. We show that they can be generated by phase-imprinting techniques on the ground state of condensates.

Published in: *Physical Review A* , v. 68, 063609 (2003)

Soliton "molecules": robust clusters of spatiotemporal optical solitons

L.C. Crasovan^{1,5}, Y.V. Kartashov^{1,2}, D. Mihalache^{1,5}, L. Torner¹, Yu.S. Kivshar³, V.M. Perez-Garcia⁴

¹ ICFO-Institut de Ciencies Fotoniques, and Department of Signal Theory and Communications, Universitat Politecnica de Catalunya, 08034 Barcelona, Spain.

² Physics Department, M. V. Lomonosov Moscow State University, 119899 Moscow, Russia

³ Nonlinear Physics Group, Research School of Physical Sciences and Engineering, The Australian National University, Canberra, Australia

⁴ Departamento de Matemáticas, E.T.S.I. Industriales, Universidad de Castilla-La Mancha, 13071 Ciudad Real, Spain

⁵ Department of Theoretical Physics, Institute of Atomic Physics, National Institute of Physics and Nuclear Engineering, P.O. Box MG-6, Bucharest, Romania

We show how to generate robust self-sustained clusters of soliton bullets-spatiotemporal (optical or matter-wave) solitons. The clusters carry an orbital angular momentum being supported by competing nonlinearities. The "atoms" forming the "molecule" are fully three-dimensional solitons linked via a staircase-like macroscopic phase. Recent progress in

generating atomic-molecular coherent mixing in Bose-Einstein condensates might open potential scenarios for the experimental generation of these soliton molecules with matter-waves.

Published in: *Physical Review E*, v. 67, 046610 (2003)

Robust soliton clusters in media with competing cubic and quintic nonlinearities

D. Mihalache^{1,3}, D. Mazilu¹, L.C. Crasovan^{1,4}, B.A. Malomed², F. Lederer³, L. Torner⁴

¹ Department of Theoretical Physics, Institute of Atomic Physics, P.O. Box MG-6, Bucharest, Romania

² Department of Interdisciplinary Studies, Faculty of Engineering, Tel Aviv University, Tel Aviv 69978, Israel

³ Institute of Solid State Theory and Theoretical Optics, Friedrich Schiller University Jena, Max-Wien-Platz 1, Jena, D-07743, Germany

⁴ ICFO-Institut de Ciencies Fotoniques, and Department of Signal Theory and Communications, Universitat Politecnica de Catalunya, 08034 Barcelona, Spain.

Systematic results are reported for dynamics of circular patterns ("necklaces"), composed of fundamental solitons and carrying angular momentum, in the two-dimensional model, which describes the propagation of light beams in bulk media combining self-focusing cubic and self-defocusing quintic nonlinearities. Semi-analytical predictions for the existence of quasi-stable necklace structures are obtained on the basis of an effective interaction potential. Then, direct simulations are run. In the case when the initial pattern is far from an equilibrium size predicted by the potential, it cannot maintain its shape. However, a necklace which was initially created close to a pre-

dicted equilibrium survive very long evolution, featuring persistent oscillations. The quasi-stable evolution is not essentially disturbed by a large noise component added to the initial condition. Basic conclusions concerning the necklace dynamics in this model are qualitatively the same as in a recently studied one which combines quadratic and self-defocusing cubic nonlinearities. Thus, we infer that a combination of competing self-focusing and self-defocusing nonlinearities stabilizes not only vortex solitons, but also vorticity-carrying necklace patterns.

Published in: *Physical Review E*, v. 68, 046612 (2003)

Microscopic analysis of the α -decay in heavy and superheavy nuclei

D.S. Delion¹, A. Săndulescu², W. Greiner³

¹ National Institute of Physics and Nuclear Engineering, POB MG-6, Bucharest-Magurele, Romania

² Center for Advanced Studies in Physics, Calea Victoriei 125, Bucharest, Romania

³ Institut für Theoretische Physik, J.W.v.-Goethe Universität, Robert-Mayer-Str. 8-10, 60325 Frankfurt am Main, Germany

We analyze α -decays along N-Z chains in heavy and superheavy nuclei. The α -particle preformation amplitude is estimated within the pairing model, while the penetration part by the deformed WKB approach. We show that for $N > 126$ the plateau condition is not fulfilled along any α -chain, namely the logarithmic derivative of the Coulomb function changes much faster in comparison with that of the preformation factor. Thus, the relative amount of the α -clustering cannot be described within the pairing approach and an additional mechanism is necessary. We correct this deficiency by considering an α -cluster factor in the

preformation amplitude, depending upon the Coulomb parameter. The plateau condition determines the Q-value, containing a shell model and a cluster component. It also allows us to analyze the relative α -clustering structure of the emitter. It turns out that the isotopes close to $N = 126$ and superheavy nuclei have a stronger clustering behaviour. For superheavy region an additional dependence upon the number of interacting α -particles indicates a clustering feature connected with a larger radial component. PACS number: 21.60.Gx, 23.60.+e

Extended quadrature rules for oscillatory integrands

KyungJoong Kim¹, R. Cools², L.Gr. Ixaru³

¹ School of Mathematical Science, Seoul National University, San 56-1 Shinrim-dong Kwanak-gu, Seoul 151 – 747, South Korea

² Department of Computer Science, Katholieke Universiteit Leuven, Celestijnenlaan 200A, B-3001 Heverlee, Belgium

³ Institute of Physics and Nuclear Engineering, Department of Theoretical Physics, POBox MG - 6, Bucharest, Romania

We consider the integral of a function $y(x)$, $I[y] = \int_{-1}^1 y(x)dx$ and its approximation by a quadrature rule of the form

$$\begin{aligned} Q_N[y] = & \sum_{k=1}^N (w_k^{(0)} y(x_k) + w_k^{(1)} y^{(1)}(x_k) + \\ & \dots + w_k^{(p)} y^{(p)}(x_k)) \end{aligned}$$

i.e., by a rule which uses the values of both y and its derivatives up to p -th order at the nodes of the

quadrature rule. We focus only on the case when the nodes are assumed known and present the procedure to calculate the weights. Two cases are actually examined: (i) $y(x)$ is a polynomial and (ii) $y(x)$ is an ω dependent function of the form $y(x) = f_1(x) \sin(\omega x) + f_2(x) \cos(\omega x)$ with smoothly varying f_1 and f_2 . For the latter case, the weights $w_k^{(j)}$ ($j = 0, 1, \dots, p$) are ω dependent. A series of properties for this case is established and a numerical illustration is given.

Appl. Numer. Math. **46**, 59 – 73, 2003

Exponentially fitted variable two-step BDF algorithm for first order ODEs

L.Gr. Ixaru¹, G. Vanden Berghe², H. De Meyer²

¹ Institute of Physics and Nuclear Engineering, Department of Theoretical Physics, POBox MG - 6, Bucharest, Romania

² Department of Applied Mathematics and Computer Science, Universiteit Gent, Krijgslaan 281-S9, B-9000 Gent, Belgium

We construct the exponential fitting extensions of the classical variable step-size two-step BDF algorithm and examine its properties. We give the expressions of the optimal value of the associated frequency and introduce a procedure for choosing the step widths in terms of the required accuracy. The order of the new

algorithm is three (that is by one unit higher than for the classical one). On three severe stiff cases we show that the new two-step algorithm behaves much better than its classical companion and that it is as good as the classical variable three-step algorithm.

Comput. Phys. Commun. **150**, 116 – 128, 2003

Reliability conditions in quadrature algorithms

Gh. Adam^{1,2}, S. Adam^{1,2}, N.M. Plakida²

¹ NIPNE-HH, Department of Theoretical Physics

² JINR Dubna, Bogolubov Laboratory of Theoretical Physics

The detection of ill-conditioned or insufficiently resolved integrand structures is critical for the reliability assessment of the quadrature rule outputs. We discuss a method of analysis of the *profile of the integrand at the quadrature knots* which allows inferences ap-

proaching the theoretical 100% rate of success, under error estimate sharpening.

The proposed procedure is of the highest interest for the solution of parametric integrals arising in complex physical models.

Published in Computer Physics Communications vol. 154 (no. 1) 49–64 (2003)
Also available at the LANL site <http://arXiv.org/abs/cs.NA/0303004>
and the Elsevier site <http://www.mathpreprints.com/math/Preprint/adamg/20030415/1>

Reliable software in computational physics

Gh. Adam¹, S. Adam¹

¹ NIPNE-HH, Department of Theoretical Physics

A bird's-eye-view of the approach offered by the computational physics to the solution of the problems of physics is given with emphasis on the key issue of

reliability.

Some meanings of the reliability are illustrated by specific examples.

Dedicated to the 70-th Anniversary of Marin Ivașcu, Romanian Reports in Physics, vol. 55, No. 4, (2003)

Exchange and spin-fluctuation mechanisms of superconductivity in cuprates

N.M. Plakida¹, L. Anton², S. Adam³, Gh. Adam³

¹ JINR Dubna, Bogoliubov Laboratory of Theoretical Physics

² INFIPR, Lab.22

³ NIPNE-HH, Department of Theoretical Physics

We propose a microscopical theory of superconductivity in CuO₂ layer within the effective two-band Hubbard model in the strong correlation limit. By applying a projection technique for the matrix Green function in terms of the Hubbard operators, the Dyson equation is derived. It is proved that in the mean-field approximation *d*-wave superconducting pairing mediated by the conventional exchange interaction occurs.

Allowing for the self-energy corrections due to kinematic interaction, a spin-fluctuation *d*-wave pairing is also obtained. T_c dependence on the hole concentration and \mathbf{k} -dependence of the gap function are derived. The results show that the exchange interaction (which stems from the interband hopping) prevails over the kinematic interaction (which stems from the intraband hopping).

*Original version published in Russian: ZhETF vol. 124 (no. 2) 367–378 (2003).
English translation: JETP vol. 97 (no. 2) 331–342 (2003)*

Localized and unlocalized structures in nonlinear lattices with fermions

A.S. Cârstea¹, D. Grecu¹, A. Vișinescu¹

¹ IFIN-HH, Department of Theoretical Physics; E-mail: dgrescu@theor1.theory.nipne.ro

We study the quasiclassical approximation for the equations of motion of a nonlinear chain of phonons and electrons having phonon mediated hopping. Describing the phonons and electrons as even and odd grassmannian functions and using the continuum limit we show that the equations of motion lead to a Zakharov-like system for bosonic and fermionic fields. Localized and nonlocalized solutions are discussed using Hirota bilinear formalism. Nonlocalized solutions turn out to appear naturally for any choice of wave parameters. The bosonic localized solution has a fermionic dressing while the fermionic one is the oscillatory localized field. They appear only if some constraints on the dispersion are imposed. In this case

the density of fermions is a strongly localized traveling wave. Also it is shown that in the multiple scales approach the emergent equation is linear. Only for the resonant case we get a nonlinear fermionic Yajima-Oikawa system. Physical implications are discussed.

References

- [1] F.A. Berezin, M.S. Marinov, Ann.Phys., **104**(1977) 336
- [2] A.S. Cârstea, Nonlinearity **13**, 1645 (2000)
- [3] R. Hirota, Phys.Rev.Lett., **27** 1192 (1971)

A holomorphic representation of coherent state Lie algebras of semi-direct product type

S. Berceanu¹, Al. Gheorghe¹

¹ NIPNE-HH, Department of Theoretical Physics

Let us consider the Heisenberg algebra generated by the creation and annihilation operators

$$\mathbf{h}_1 = \mathbf{g}_{HW} = \langle is1 + xa^+ - \bar{x}a \rangle_{s \in \mathbf{R}, x \in \mathbf{C}},$$

and the algebra

$$\mathbf{su}(1,1) = \langle 2i\theta K_0 + yK_+ - \bar{y}K_- \rangle_{\theta \in \mathbf{R}, y \in \mathbf{C}}.$$

Now we form the semi-direct product $\mathbf{g} = \mathbf{h}_1 \times \mathbf{su}(1,1)$ such that \mathbf{h}_1 is an ideal in \mathbf{g} , i.e. $[\mathbf{h}_1, \mathbf{g}] = \mathbf{h}_1$:

$$\left\{ \begin{array}{l} [a, a^+] = 1, \\ [K_0, K_{\pm}] = \pm K_{\pm}, \quad [K_-, K_+] = 2K_0, \\ [a, K_{\pm}] = a^+, \quad [K_-, a^+] = a, \\ [K_+, a^+] = [K_-, a] = 0, \\ [K_0, a^+] = \frac{1}{2}a^+, \quad [K_0, a] = -\frac{1}{2}a, \\ (a^+)^+ = a, \quad K_0^+ = K_0, \quad K_{\pm}^+ = K_{\mp}. \end{array} \right. \quad (1)$$

We introduce the coherent state vectors:

$$e_{z,w} := e^{za^+ + wK_+} e_0, \quad z \in \mathbf{C}, \quad |w| < 1,$$

$$\left\{ \begin{array}{l} ae_0 = 0, \quad K_- e_0 = 0; \\ K_0 e_0 = ke_0; \quad k > 0, 2k = 2, 3, \dots \end{array} \right. \quad (2)$$

To vectors in the Hilbert space we associate functions $f_{\psi}(z, w) = (e_{\bar{z}, \bar{w}}, \psi)$ and to elements of the Lie algebra we associate differential operators $\mathbf{g} \ni X \rightarrow \mathbf{X}$. We have proved that the differential action is given by the formulas

$$\left\{ \begin{array}{l} \mathbf{a} = \frac{\partial}{\partial z}; \quad \mathbf{a}^+ = z + w \frac{\partial}{\partial w}; \\ \mathbf{K}_- = \frac{\partial}{\partial \bar{w}}; \quad \mathbf{K}_0 = k + \frac{1}{2}z \frac{\partial}{\partial z} + w \frac{\partial}{\partial w}; \\ \mathbf{K}_+ = \frac{1}{2}z^2 + 2kw + zw \frac{\partial}{\partial z} + w^2 \frac{\partial}{\partial w}. \end{array} \right. \quad (3)$$

The reproducing kernel

$$K(\bar{z}, \bar{w}, z, w) := (e_0, e^{\bar{z}a + \bar{w}K_-} e^{za^+ + wK_+} e_0) \quad (4)$$

is

$$K(\bar{z}, \bar{w}, z, w) = (1 - w\bar{w})^{-2k} \exp \frac{2z\bar{z} + z^2\bar{w} + \bar{z}^2w}{2(1 - w\bar{w})}. \quad (5)$$

More generally, if $K(z, w; \bar{z}', \bar{w}') := (e_{\bar{z}, \bar{w}}, e_{\bar{z}', \bar{w}'})$, then

$$K(z, w; \bar{z}', \bar{w}') = (1 - w\bar{w}')^{-2k} \exp \frac{2\bar{z}'z + z^2\bar{w}' + \bar{z}'^2w}{2(1 - w\bar{w}')}$$

The coherent state vectors of the Lie algebra \mathbf{g} can be expressed in the base $|n\rangle$ of the algebra \mathbf{h}_1 and the base $e_{k,k+n}$ of the algebra $\mathbf{su}(1,1)$ as

$$\begin{aligned} e_{z,w} &= \sum_n \frac{i^{-n}}{(n!)^{1/2}} |n\rangle \times \\ &\quad \left(\frac{w}{2} \right)^n H_n \left(\frac{iz}{\sqrt{2w}} \right) \sum_m \frac{w^m}{m! a_{k'm}} e_{k', k'+m}, \end{aligned}$$

and the associated functions

$$f_{e_{|n>e_{k',k'+m}}} (z, w) = (e_{\bar{z}, \bar{w}}, |n> e_{k', k'+m})$$

are

$$\begin{aligned} f_{e_{|n>e_{k',k'+m}}} (z, w) &= (n!)^{-1/2} \left(\frac{i}{\sqrt{2}} \right)^n \sqrt{\frac{\Gamma(m+2k')}{m! \Gamma(2k')}} \times \\ &\quad w^{m+\frac{n}{2}} H_n \left(\frac{-iz}{\sqrt{2w}} \right). \end{aligned}$$

The scalar product is

$$\begin{aligned} (\phi, \psi) &= \Lambda \int_{z \in \mathbf{C}; |w| < 1} \bar{f}_{\phi}(z, w) f_{\psi}(z, w) (1 - w\bar{w})^{2k} \times \\ &\quad \exp - \frac{|z|^2}{1 - w\bar{w}} \exp - \frac{z^2\bar{w} + \bar{z}^2w}{2(1 - w\bar{w})} d\nu \\ d\nu &= \frac{d\Re w d\Im w}{(1 - w\bar{w})^3} d\Re z d\Im z; \quad \Lambda = \frac{4k - 3}{2\pi^2}. \end{aligned}$$

The two-form ω and the volume form are:

$$\begin{aligned} f &:= \log K, \\ f &= \frac{2z\bar{z} + z^2\bar{w} + \bar{z}^2w}{2(1 - w\bar{w})} - 2k \log(1 - w\bar{w}), \\ \omega \wedge \omega &= 4k(1 - w\bar{w})^{-3} 4\Re z \Im z \Re w \Im w. \end{aligned}$$

References

- [1] S. Berceanu and A. Gheorghe, *J. Math. Phys.* **33** (1992), 998-1007; S. Berceanu and L. Boutet de Monvel, *J. Math. Phys.* **34** (1993), 2353-2371
- [2] S. Berceanu and A. Gheorghe, *Rom. J. Phys.* **45** (2000), 285-288
- [3] S. Berceanu and A. Gheorghe, *Analele Universității din Timișoara, seria matematică - informatică*, **XXXIX** (2001), 31-56
- [4] S. Berceanu and A. Gheorghe, *Differential operators on orbits of coherent states*, DG/0211054
- [5] S. Berceanu *Realization of coherent state algebras by differential operators*, 2nd Operator Algebras and Mathematical Physics Conference, Sinaia, June 26-July 04, 2003 (submitted)
- [6] K.-H. Neeb, *Holomorphy and Convexity in Lie Theory*, de Walter de Gruyter, Berlin-New York, 2000

Selection rules for jumps between resonant states induced by potential strength variation

N. Grama¹, C. Grama¹, I. Zamfirescu¹¹IFIN-HH

The jump phenomenon between two S-matrix poles induced by a small potential strength variation is studied for the scattering by a central square potential $gV(r)$, $g \in \mathbf{C}$. Let $R_g^{(l)}$ denote the Riemann surface over the complex g -plane, on which the pole function $k = k^{(l)}(g)$ is single valued and analytic. By associating a sheet $\Sigma_n^{(l)}$ of $R_g^{(l)}$ and its k -plane image $\Sigma'_n^{(l)}$ to a state with the quantum numbers (l, n) the jump between the states (l, n) and (l, m) , induced by the potential strength variation, is understood as the jump between the sheet images $\Sigma'_n^{(l)}$ and $\Sigma'_m^{(l)}$. The rules for the jumps $(l, n) \iff (l, m)$ as a consequence of a small potential strength variation are deduced. The junctions between various Riemann sheets at the branch points with $\operatorname{Re} k(g_{s,s'}^{l,\pm}) > 0$ are governed by the following rules:

Let $r = (l-1)/2$, $t = 1$ for odd l , and $r = l/2$, $t = 2$ for even $l > 0$. Then

- (1) At the branch points $g_{s,p}^{l,-}$ ($p = t, t+1, \dots, r$) the sheet $\Sigma_{s+p-2}^{(l)}$ is joined to the sheet $\Sigma_{s+p-1}^{(l)}$,
- (2) At the branch points $g_{s,p}^{l,+}$ ($p = t, t+1, \dots, r+1$) the sheet $\Sigma_{p-1}^{(l)}$ is joined to the sheet $\Sigma_{s+p-1}^{(l)}$.

where $s = 1, 2, \dots$. The rules (1) and (2) for the junction of the sheets $\Sigma_n^{(l)}$ and $\Sigma_m^{(l)}$ at a branch point $g_{s,s'}^{l,\pm}$ are valid provided that the pole corresponding to the potential strength value $g_{s,s'}^{l,\pm}$ is not an exotic resonant state pole on both sheet images $\Sigma'_n^{(l)}$ and $\Sigma'_m^{(l)}$.

A special case is that of the branch points $g_{s,1}^{l,\pm}$ for even l , having the images on the negative imaginary k -axis. For even l at the branch points $g_{s,1}^{l,\pm}$ the junctions between the sheets with k -plane images in the half-plane $\operatorname{Re} k \leq 0$ and the sheets with the images in the half-plane $\operatorname{Re} k \geq 0$ occur. Due to this in the case of even l the junctions at the branch points $g_{s,1}^{l,\pm}$ are governed by rules that differ from the rules (1) and (2).

In the case $l = 0$ there is a single set of branch points, namely $g_{s,1}^{0,+}$, whose image in the k -plane are

situated on the imaginary k -axis at $k = \kappa_s^{0,+} = -i$. The analysis of the Riemann surface $R_g^{(0)}$ shows that at $g_{s,1}^{0,+}$ the sheet $\Sigma_0^{(0)}$ cannot be joined to any other sheet of $R_g^{(0)}$. This means that the potential strength variation does not induce any jump between the ground state $(0, 0)$ and the other states $(0, n)$ of the system. At $g_{s,1}^{0,+}$ the sheets $\Sigma_s^{(0)}$ and $\Sigma_{-s}^{(0)}$ with $s > 0$ are joined. In the case $l = 0$ the following rules for the junctions of the Riemann sheets at the branch points can be extracted:

- (3) For $l = 0$ the sheet $\Sigma_0^{(0)}$ is not joined to any other sheet,
- (4) For $l = 0$ at the branch points $g_{s,1}^{0,+}$ the sheet $\Sigma_s^{(0)}$ is joined to the sheet $\Sigma_{-s}^{(0)}$.

By the analysis of the Riemann surfaces $R_g^{(l)}$ with even $l > 0$ the rules for the junctions at $g_{s,1}^{l,\pm}$ have been deduced. It results that there are two pairs of sheets that are joined at each branch point $g_{s,1}^{l,\pm}$:

- (5) For even $l > 0$ at the branch points $g_{s,1}^{l,\pm}$ the sheet $\Sigma_0^{(l)}$ is joined to the sheet $\Sigma_{l/2-1+s}^{(l)}$ and the sheet $\Sigma_1^{(l)}$ is joined to the sheet $\Sigma_{-l/2+2-s}^{(l)}$.

The rules (1-5) given above for the junction of various sheets define some selection rules for the jump from one sheet of the Riemann surface $R_g^{(l)}$ to some other sheet of the same surface.

There are some sheets $\Sigma_n^{(l)}$ that are not joined to any other sheet at some $g_{s,s'}^{l,\pm}$, i.e. $g = g_{s,s'}^{l,\pm}$ is not a branch point for $\Sigma_n^{(l)}$. In this case the jump from $\Sigma_n^{(l)}$ to other sheet $\Sigma_m^{(l)}$ when the potential strength varies around $g_{s,s'}^{l,\pm}$ is forbidden.

- [1] C. Grama, N. Grama and I. Zamfirescu, Phys. Rev. A **61** (2000) 032716.
- [2] C. Grama, N. Grama and I. Zamfirescu, Phys. Rev. A **68** (2003) 032723.

Finite-level systems, hermitean operators, isometries, and a novel parameterisation of Stiefel and Grassmann manifolds

P. Dita¹

¹ NIPNE-HH, Department of Theoretical Physics

The paper provide an explicit parameterisation of arbitrary n -dimensional Hermitean operators on the Hilbert space \mathbf{C}^n , operators that may be considered either as Hamiltonians, or density matrices for finite-level quantum systems. This description give a complete solution to the over parameterisation problem. It is shown that all the spectral multiplicities are en-

coded in a flag unitary matrix obtained as an ordered product of special unitary matrices, each one generated by a complex $n - k$ -dimensional unit vector, $k = 0, 1, \dots, n - 2$. As a byproduct, an alternative and simple parameterisation of Stiefel and Grassmann manifolds is obtained.

Preprint quant-ph/0305156

New results on the parameterisation of complex Hadamard matrices

P. Dita¹

¹ NIPNE-HH, Department of Theoretical Physics

In the paper one provides an analytical procedure which leads to a system of $(n - 2)^2$ polynomial equations whose solutions give the parameterisation of the complex $n \times n$ Hadamard matrices. The key ingredient is a new factorisation of unitary matrices in terms of n diagonal phase matrices interlaced with $n - 1$ orthogonal matrices each one generated by a real vector. It is shown that in general the Hadamard matrices depend

on a number of arbitrary phases and a lower bound for this number is given. The moduli equations define interesting geometrical objects whose study may shed light not only on the parameterisation of Hadamard matrices, but also on the rationally connected varieties.

Preprint quant-ph/0212036 v.2

Extended supersymmetries in the causal approach

D.R. Grigore¹

¹ NIPNE-HH, Department of Theoretical Physics

The scattering matrix is formal series of operator valued distributions $T(W_1(x_1), \dots, W_n(x_n))$ which act in the Fock space of some collection of free fields; they are called *chronological products* and verify Bogoliubov axioms expressing the following properties: the initial condition, skew-symmetry in all arguments, Poincaré invariance, causality and unitarity. The expressions W_j are arbitrary Wick monomials. The existence of solutions is rigorously established in [1] using a recursive procedure based on the causality axiom. Sometimes it is possible to supplement these axioms by other invariance properties. In this way supersymmetric invariance can be treated also in this formalism [2], [4].

A quantum **extended** supersymmetric theory is a collection of quantum relativistic free fields b_j (resp. f_A) which are bosonic (resp. fermionic) acting in the Hilbert space \mathcal{H} together with the operators Q_{aj}, Z_{jk} (here $a = 1, 2, \dots, N$) such that the following properties are valid:

$$\begin{aligned} Q_{aj}\Omega &= 0, & \bar{Q}_{\bar{a}j}\Omega &= 0, & Z_{jk}\Omega &= 0 \\ \{Q_{aj}, Q_{bk}\} &= 0 & \{Q_{aj}, \bar{Q}_{\bar{b}k}\} &= 2\delta_{jk}\sigma_{ab}^\mu P_\mu \\ [Q_{aj}, P_\mu] &= 0 & U_{a,A}^{-1}Q_{bj}U_{a,A} &= A_b{}^c Q_{cj} \\ V_U^{-1}Q_{ja}V_U &= \rho(U)_{jk}Q_{ka}, & \forall U \in G \\ i[Q_{aj}, b] &= f, & \{Q_{aj}, f\} &= b; \end{aligned} \quad (1)$$

here $P_\mu = -i \partial_\mu$ are the infinitesimal generators of the translation group, σ^μ are the usual Pauli matrices and $\bar{Q}_{bj} \equiv (Q_{bj})^\dagger$. We have denote generically by b (resp. f) arbitrary linear combinations of the Bose (resp. Fermi) fields and their partial derivatives. These relations express the tensor properties of the fields with respect to (infinitesimal) supersymmetry transformations and the definition of a supersymmetric algebra with *central charges* Z_{jk} ; by definition, they commute with all other SUSY generators and $U \mapsto \rho(U)$ is N -dimensional a representation of the group G . We will consider only the case $\rho = Id$.

If these conditions are true we say that Q_{aj} are *super-charges* and b_j, f_A are forming a *quantum (extended) supersymmetric multiplet*.

Then supersymmetric invariance of the model can be expressed in an infinitesimal form analogue with gauge invariance [3]:

$$[Q_{aj}, T(x_1, \dots, x_n)] = i \sum_{l=1}^n \frac{\partial}{\partial x_l^\mu} T_{a;l}^\mu(x_1, \dots, x_n) \quad (2)$$

for some chronological products $T(X)$, $T_{a;l}^\mu(X)$.

One can establish by a direct analysis that the chronological products can be normalized such that these identities are true in all orders for toy models as it is Wess-Zumino model [4].

One can introduce *superfields* for extended supersymmetric theories as in the more simple case of $N = 1$ (without central charges) and one can generalize the Bogoliubov axioms in the supersymmetric context [5].

From the analysis of the irreducible representations of the supersymmetric algebra it is known that there

are only five multiplets describing irreducible representations with particles of spin $s \leq 1$ namely: for $N = 1$ the chiral multiplet and the vector multiplet [6]; for $N = 2$ the hyper-multiplet and a vector multiplet; for $N = 4$ a vector multiplet. In [7] we show that the starting point of the analysis is not trivial. The construction of the corresponding quantum multiplet with extended supersymmetry is a non-trivial task because of the condition of positivity of the scalar product. This condition is not imposed in the standard literature where it is assumed that it follows automatically from the path-integral quantization procedure.

References

- [1] H. Epstein, V. Glaser, Ann. Inst. H. Poincaré **19 A** (1973) 211-295
- [2] F. Constantinescu, M. Gut, G. Scharf, Ann. Phys. (Leipzig) **11** (2002) 335-356
- [3] M. Dütsch, T. Hurth, F. Krahe, G. Scharf, Il Nuovo Cimento **A 106** (1993) 1029-1041
- [4] D. R. Grigore, European Phys. Journ. **C 21** (Particles and Fields) (2001) 732-734
- [5] D. R. Grigore, G. Scharf, hep-th/0204105, Annalen der Physik **12** (2003) 5-36
- [6] D. R. Grigore, G. Scharf, hep-th/0212026, Annalen der Physik **12** (2003) 643-683
- [7] D. R. Grigore, G. Scharf, hep-th/0303176, to appear in Annalen der Physik

Quantum dynamics of deformed open systems

A. Isar¹, A. Săndulescu¹, W. Scheid²

¹ NIPNE-HH, Department of Theoretical Physics

² Institut of Theoretical Physics, University of Giessen, Germany

In the framework of the Lindblad theory for open quantum systems, a master equation for the quantum harmonic oscillator interacting with a dissipative environment, in particular with a thermal bath, is derived for the case when the interaction is based on deformed algebra. The equations of motion for observables strongly depend on the deformation func-

tion. The expectation values of the number operator and squared number operator are calculated in the limit of a small deformation parameter for the case of zero temperature of the thermal bath. The steady state solution of the equation for the density matrix in the number representation is obtained and its independence of the deformation is shown.

The induced representation of the isometry group of the euclidean Taub-NUT space and new spherical harmonics

I.I. Cotăescu¹, M. Vișinescu²

¹ West University of Timișoara, 1900-Timișoara, Romania; E-mail: cota@physics.uvt.ro

² IFIN-HH, Department of Theoretical Physics; E-mail: mvisin@theor1.theory.nipne.ro

The Euclidean Taub-Newman-Unti - Tamburino (Taub-NUT) metric is involved in many modern studies in physics. One of the first examples given of a gravitational instanton was the self-dual Taub-NUT solution. Much attention has been paid to the Euclidean Taub-NUT metric since in the long-distance limit the relative motion of two monopoles is described approximately by its geodesics. On the other hand this metric is just the space part of the metric of the celebrated Kaluza-Klein monopole of Gross and Perry and of Sorkin.

The Taub-NUT space is also of interest since beside isometries there are hidden symmetries giving rise to conserved quantities associated to Stäckel-Killing tensors. There is a conserved vector, analogous to the Runge-Lenz vector of the Kepler type problem, whose existence is rather surprising in view of the complexity of the equations of motion. These hidden symmetries are related to the existence of special objects arising in this geometry, i.e. four Killing-Yano tensors gener-

ating the Stäckel-Killing ones.

The quantum theory in the Euclidean Taub-NUT background has also interesting specific features in the case of the scalar fields as well as for Dirac fields of spin $\frac{1}{2}$ fermions. In both cases there exist large algebras of conserved observables including the components of the angular momentum and three components of the Runge-Lenz operator that complete a six-dimensional dynamical algebra. Remarkably, the orbital angular momentum has a special unusual form that generates new harmonics called $SO(3) \otimes U(1)$ -harmonics. What is the explanation of this fact?

In our opinion the form of the angular momentum operator is determined by the specific type of isometries of the Euclidean Taub-NUT space which combine linear representations with induced ones. The purpose of this article is to prove this showing that the fourth Cartesian (or spherical) coordinate transforms under rotations according to a representation of the $SO(3)$ isometry group induced by one of its $SO(2)$ subgroups.

Symmetries of the Dirac operators associated with covariantly constant Killing-Yano tensors

I.I. Cotăescu¹, M. Vișinescu²

¹ West University of Timișoara, 1900-Timișoara, Romania; E-mail: cota@physics.uvt.ro

² IFIN-HH, Department of Theoretical Physics; E-mail: mvisin@theor1.theory.nipne.ro

The (skew-symmetric) Killing-Yano (K-Y) tensors, that were first introduced by Yano from purely mathematical reasons, are profoundly connected to the supersymmetric classical and quantum mechanics on curved manifolds where such tensors do exist. The K-Y tensors play an important role in theories with spin and especially in the Dirac theory on curved space-times where they produce first order differential operators, called Dirac-type operators, which anticommute with the standard Dirac one, D . Another virtue of the K-Y tensors is that they enter as square roots in the structure of several second rank Stäckel-Killing tensors that generate conserved quantities in classical mechanics or conserved operators which commute with D . The construction of Carter and McLenaghan de-

pended upon the remarkable fact that the (symmetric) Stäckel-Killing tensor $K_{\mu\nu}$ involved in the constant of motion quadratic in the four-momentum p_μ

$$Z = \frac{1}{2} K^{\mu\nu} p_\mu p_\nu \quad (1)$$

has a certain square root in terms of K-Y tensors $f_{\mu\nu}$:

$$K_{\mu\nu} = f_{\mu\lambda} f_{\nu}^{\lambda}. \quad (2)$$

The K-Y tensor here is a 2-form $f_{\mu\nu} = -f_{\nu\mu}$ which satisfies the equation $f_{\mu\nu;\lambda} + f_{\mu\lambda;\nu} = 0$.

These attributes of the K-Y tensors lead to an efficient mechanism of supersymmetry especially when the Stäckel-Killing tensor $K_{\mu\nu}$ in Eq. (1) is proportional with the metric tensor $g_{\mu\nu}$ and the corresponding K-Y tensors in Eq. (2) are covariantly constant.

Then each tensor of this type, f^i , gives rise to a Dirac-type operator, D^i , representing a supercharge of the superalgebra $\{D^i, D^j\} \propto D^2 \delta_{ij}$.

The typical example is the Euclidean Taub-NUT space which is a hyper-Kähler manifold possessing three covariantly constant K-Y tensors with real-valued components which constitute a hypercomplex structure generating a $N = 4$ superalgebra at the level of the Dirac theory. Moreover, each involved K-Y tensor is a root of the metric tensor as it results from the definition of the Kählerian geometries (given in Appendix A). It is worth pointing out that the Euclidean Taub-NUT space has, in addition, a non-covariantly constant K-Y tensor related to its specific hidden symmetry showed off by the existence of a conserved Runge-Lenz operator that can be constructed with the help of the Dirac-type operators produced by all the four K-Y tensors of this space.

In what concerns the superalgebras of Dirac-type operators, the inverse problem is to find the suitable conjectures allowing the construction of Dirac-type operators D' which should satisfy the condition $(D')^2 \propto D^2$. It was shown that these can be produced by covariantly constant K-Y tensors having not only real-valued components but also complex ones. This extension seems to be productive since it permits to construct superalgebras in the Dirac theory in Minkowski spacetime which is not Kählerian, having only complex-valued covariantly constant K-Y tensors. For this reason, in what follows we shall consider such more general tensors, called *roots* (instead of complex structures) since all of them are, up to constants, roots of the metric tensor. We note that the complex struc-

tures defining Kählerian geometries are particular automorphisms of the tangent bundle while the roots we use here are automorphisms of the *complexified* tangent bundle.

It is known that in four-dimensional manifolds the standard Dirac operator and the Dirac-type ones can be related among themselves through continuous or discrete transformations. It is interesting that there are only two possibilities, namely either transformations of the $U(1)$ group associated with the discrete group Z_4 or $SU(2)$ transformations and discrete ones of the quaternionic group Q .

Our main purpose is to investigate the specific symmetries of the Dirac operators constructed using roots in geometries of arbitrary dimensions. We start with the observation that any root give rise simultaneously to a Dirac-type operator and a generator of the one-parameter Lie group relating this operator to the standard Dirac one. In fact the group generator is the main piece of the theory since it is able to produce itself the Dirac-type operator through a simple commutation with the standard Dirac operator. Exploiting this mechanism we study the continuous and discrete symmetries of the Dirac-type operators showing that, as in the case of the Kählerian geometries, there exists only two types of continuous symmetries, $U(1)$ and $SU(2)$, and the corresponding discrete symmetries, Z_4 and Q respectively. One of our important results is the concrete form of the $SU(2)$ transformations in the general case of any $4n$ -dimensional manifold equipped with sets of roots having similar algebraic properties as the quaternion units.

Harmonic oscillator inertia

D.N. Poenaru¹, R.A. Gherghescu¹, W. Greiner²

¹ NIPNE, Department of Nuclear Physics

² Frankfurt Institute for Advanced Studies, Frankfurt am Main University, Germany

The tensor of inertial coefficients [1], B_{ij} , is needed to describe fission dynamics. It is computed either phenomenologically (irrotational [2] or Werner-Wheeler approximation [3]) or microscopically with the cranking model [1, 4]. As an intermediate stage, allowing to test complex computer codes one should develop in a realistic approach, we present a simplified case of a spheroidal harmonic oscillator without spin-orbit interaction, for which an analytical result may be obtained. There is one deformation parameter expressed as $\varepsilon = 3(c - a)/(2c + a)$ in terms of semiaxes a, c .

The eigenvalues [5], in units of $\hbar\omega_0^0 = 41A^{-1/3}$ MeV, and the eigenfunctions [4] of the spheroidal harmonic

oscillator are given by:

$$\epsilon_i = [N + 3/2 + \varepsilon(n_\perp - 2N/3)][1 - \varepsilon^2(1/3 + 2\varepsilon/27)]^{-1/3} \quad (1)$$

$$|n_r m n_z\rangle = \frac{\sqrt{2}}{\alpha_\perp} \psi_{n_r}^m(\eta) \frac{1}{\sqrt{2\pi}} e^{im\varphi} \frac{1}{\sqrt{\alpha_z}} \psi_{n_z}(\xi) \quad (2)$$

where the quantum numbers n_z , $n_r = 0, 1, 2, \dots n_\perp$, $m = n_\perp - 2n_r$, $N = n_\perp + n_z$. The wave functions $\psi_{n_r}^m(\eta)$ and $\psi_{n_z}(\xi)$ are expressed in terms of associated Laguerre polynomials and Hermite polynomials, respectively. The undimensional variables are defined by: $\eta = \rho^2/\alpha_\perp^2$ and $\xi = z/\alpha_z$ with $\alpha_\perp = \sqrt{\hbar/(M\omega_\perp)}$ and $\alpha_z = \sqrt{\hbar/(M\omega_z)}$. The potential $V(\eta, \xi; \varepsilon) =$

$(\hbar\omega_{\perp}\eta + \hbar\omega_z\xi^2)/2$ derivative is given by

$$\frac{1}{\hbar\omega_0^0} \frac{dV}{d\varepsilon} = \frac{3}{2} [f_1(\varepsilon)\eta + f_2(\varepsilon)\xi^2] \quad (3)$$

where

$$f_1 = \frac{\varepsilon(\varepsilon+6)+9}{[27-\varepsilon^2(9+2\varepsilon)]^{4/3}}; f_2 = 2\frac{\varepsilon(2\varepsilon+3)-9}{[27-\varepsilon^2(9+2\varepsilon)]^{4/3}} \quad (4)$$

For a single deformation parameter the cranking inertia tensor becomes a scalar:

$$B_{\varepsilon} = 2\hbar^2 \sum_{\nu\mu} \frac{\langle\nu|\partial V/\partial\varepsilon|\mu\rangle\langle\mu|\partial V/\partial\varepsilon|\nu\rangle}{(E_{\nu}+E_{\mu})^3} (u_{\nu}v_{\mu}+u_{\mu}v_{\nu})^2 \quad (5)$$

where E_{ν} , v_{ν} , u_{ν} are the BCS quasiparticle energies and occupation probabilities for quasiparticles and holes, and the summation is performed over the whole number of states ν , μ around the Fermi level, which are considered in pairing interactions. The contribution of the neutron level scheme is added to that of proton levels.

Finally, in order to obtain B_{ε} in units of \hbar^2/MeV , one has to add $b_{\varepsilon} = b_{\varepsilon 1} + b_{\varepsilon 2} + b_{\varepsilon 3}$ by multiplying each term with $\delta_{n'_r n_r} \delta_{m' m} 9/4$ and the result should be divided by $\hbar\omega_0^0$.

$$b_{\varepsilon 1} = \sum_{\nu=k_i}^{k_f} [f_1(2n_r + |m| + 1) + f_2(n_z + 1/2)]^2 \frac{(u_{\nu}v_{\nu})^2}{E_{\nu}^3} \quad (6)$$

$$b_{\varepsilon 2} = \frac{f_2^2}{2} \sum_{\nu \neq \mu} (n_z + 1)(n_z + 2) \frac{(u_{\nu}v_{\mu} + u_{\mu}v_{\nu})^2}{(E_{\nu} + E_{\mu})^3} \delta_{n'_z n_{z+2}} \quad (7)$$

$$b_{\varepsilon 3} = \frac{f_2^2}{2} \sum_{\nu \neq \mu} (n_z - 1)n_z \frac{(u_{\nu}v_{\mu} + u_{\mu}v_{\nu})^2}{(E_{\nu} + E_{\mu})^3} \delta_{n'_z n_{z-2}} \quad (8)$$

Results for ^{252}Cf are presented in figure 1.

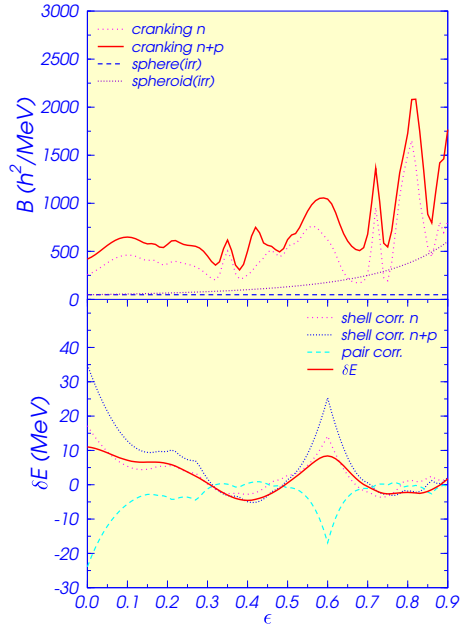


Figure 1: Top: nuclear inertia (in units of \hbar^2/MeV) calculated microscopically for the proton and neutron level scheme, only for neutrons, the irrotational value and that of a spherical shape. Bottom: shell and pairing corrections. Nucleus ^{252}Cf .

References

- [1] M. Brack, J. Damgaard, A. Jensen, H.C. Pauli, V.M. Strutinsky, G.Y. Wong, *Rev. Mod. Phys.* **67** (1972) 320.
- [2] A. Sobiczewski, *E.Ch.A.Ya.* **10** (1979) 1170.
- [3] R.A. Gherghescu, D.N. Poenaru, W. Greiner, *Phys. Rev. C* **52** (1995) 2636; *Z. Phys. A* **354** (1996) 367.
- [4] J. Damgaard, H.C. Pauli, V.V. Pashkevich, V.M. Strutinski, *Nucl. Phys. A* **135** (1969) 432.
- [5] D.N. Poenaru, W. Greiner (Eds) *Nuclear Decay Modes*, (IOP Publishing, Bristol, 1996).

Further candidates for experiments on cluster radioactivities

D.N. Poenaru¹, R.A. Gherghescu¹, W. Greiner²

¹ NIPNE, Department of Nuclear Physics

² Frankfurt Institute for Advanced Studies, Frankfurt am Main University, Germany

Cluster radioactivities have been predicted in 1980, four years before the first experimental confirmation of ^{14}C radioactivity of ^{223}Ra was reported. The obtained until now data on half-lives and branching ratios relative to α -decay of ^{14}C , $^{18,20}\text{O}$, ^{23}F , $^{22,24-26}\text{Ne}$, $^{28,30}\text{Mg}$ and $^{32,34}\text{Si}$ radioactivities are in good agreement with

predicted values within the analytical supersymmetric fission (ASAF) model. The unified approach of cold binary fission, cluster radioactivity, and α -decay was extended to cold ternary fission and to multicluster fission including the quaternary one. The cluster emitters ^{221}Fr , $^{221-224,226}\text{Ra}$, ^{225}Ac , $^{228,230}\text{Th}$, ^{231}Pa ,

$^{230,232-236}\text{U}$, $^{236,238}\text{Pu}$, and ^{242}Cm are either β -stable or not far from stability nuclei.

Experimental difficulties are mainly related to the low yield in the presence of a strong background of alpha-particles. Sometimes the experimental sensitivity is not high enough to achieve a positive result, hence only an upper limit can be established. The longest upper limit determined up to now is $T \geq 10^{29.2}$ s for the $^{24,26}\text{Ne}$ radioactivity of ^{232}Th , and the smallest branching ratio $b_\alpha = 10^{-15.87}$ for ^{34}Si decay of ^{242}Cm . On the other side, the most favourable values are $T = 10^{11.01}$ s for ^{14}C radioactivity of ^{222}Ra ,

and $b_\alpha = 10^{-8.88}$ for ^{14}C decay of ^{223}Ra . Spontaneous fission starts to be important in the region of heavy cluster emitters with $10^{14} < T_f < 10^{29}$. For Pa, U, Np, Am, and Pu isotopes the branching ratio $b_f = T_f/T \equiv b_{fc} = 1/b_{cf}$ is in the range $(10^{-7}, 10^2)$, but for ^{242}Cm it approaches 10^{-9} , making very difficult the measurement of ^{34}Si radioactivity.

We presented (Phys. Rev. **C** **65** (2002) 054308) a systematics of experimental results compared to calculations, clearly showing other possible candidates for future experiments, given in Table 1. The universal curves may be used to estimate the expected half-lives.

Table 1: New candidates for experimental searches of cluster radioactivities. Half-lives are predicted within ASAF model. Alpha decay life time is either measured (m) or estimated (es). T_t is the total half-life.

Effect of target deformation in superheavy nuclei synthesis

R.A. Gherghescu¹, G. Münzenberg², D.N. Poenaru¹, W. Greiner³

¹NIPNE, Department of Nuclear Physics

²G.S.I., Darmstadt, Germany

³Frankfurt Institute for Advanced Studies, Frankfurt am Main University, Germany

Effects of target and projectile deformation on the shell corrections are calculated within the deformed two-center shell model [1, 2]. The deformed two center oscillator potential which assures equipotentiality on the surface of the two intersected nuclei reads:

$$V^{(r)}(\rho, z) = \begin{cases} V_1 &= \frac{1}{2}m_0\omega_{\rho_1}^2\rho^2 + \\ &+ \frac{1}{2}m_0\omega_{z_1}^2(z+z_1)^2 &, v_1 \\ V_2 &= \frac{1}{2}m_0\omega_{\rho_2}^2\rho^2 + \\ &+ \frac{1}{2}m_0\omega_{z_2}^2(z-z_2)^2 &, v_2 \end{cases} \quad (1)$$

where v_1 and v_2 are the space regions where the two potentials are acting. The frequencies are shape dependent, thus one obtains from volume conservation and mass dependency of ω the relations:

$$\begin{aligned} m_0\omega_{\rho_i}^2 &= (a_i/b_i)^{2/3} \cdot m_0\omega_{0i}^2 = (a_i/b_i)^{2/3} \cdot 54.5/R_i^2 \\ m_0\omega_{z_i}^2 &= (b_i/a_i)^{4/3} \cdot m_0\omega_{0i}^2 = (b_i/a_i)^{4/3} \cdot 54.5/R_i^2 \end{aligned} \quad (2)$$

In this way the two center oscillator potential for fusion like shapes follows the changes of the two spheroidal partner deformations.

In order to find out each of the space regions v_1 and v_2 , we rely on the assumption that the pass from

V_1 to V_2 must be smooth; hence no abrupt cusp in the potential value has to exist between v_1 and v_2 . If the two regions comply to this condition, they have to be bordered by the same surface. Such a surface is the solution of the following matching condition between $V_1(\rho, z)$ and $V_2(\rho, z)$:

$$V_1(\rho, z) = V_2(\rho, z) \quad (3)$$

Eq. (3) describes an ellipsoidal surface. On any of its points the two potentials, V_1 and V_2 , match each other.

The total Hamiltonian of the system is:

$$H = -\frac{\hbar^2}{2m_0}\Delta + V^{(r)}(\rho, z) + V_{\Omega s} + V_{\Omega^2} \quad (4)$$

where $V_{\Omega s}$ and V_{Ω^2} are the spin-orbit and the squared angular momentum interaction potentials.

The spin-orbit operator is calculated as usual using creation and annihilation components:

$$\Omega s = \frac{1}{2}(\Omega^+ s^- + \Omega^- s^+) + \Omega_z s_z \quad (5)$$

where:

$$\begin{aligned} \Omega^+ &= -e^{i\varphi} \left[\frac{\partial \mathbf{V}^r(\rho, \mathbf{z})}{\partial \rho} \frac{\partial}{\partial \mathbf{z}} - \frac{\partial \mathbf{V}^r(\rho, \mathbf{z})}{\partial \mathbf{z}} \frac{\partial}{\partial \rho} - \frac{i}{\rho} \frac{\partial \mathbf{V}^r(\rho, \mathbf{z})}{\partial \mathbf{z}} \frac{\partial}{\partial \varphi} \right] \\ \Omega^- &= e^{-i\varphi} \left[\frac{\partial \mathbf{V}^r(\rho, \mathbf{z})}{\partial \rho} \frac{\partial}{\partial \mathbf{z}} - \frac{\partial \mathbf{V}^r(\rho, \mathbf{z})}{\partial \mathbf{z}} \frac{\partial}{\partial \rho} + \frac{i}{\rho} \frac{\partial \mathbf{V}^r(\rho, \mathbf{z})}{\partial \mathbf{z}} \frac{\partial}{\partial \varphi} \right] \\ \Omega_z &= -\frac{i}{\rho} \frac{\partial \mathbf{V}^r}{\partial \rho} \frac{\partial}{\partial \varphi} \end{aligned} \quad (6)$$

In this way the angular momentum dependent operators are also shape-dependent. Details of calculation and matrix element formulae are given in [1, 3].

The superheavy synthesis reaction $U + {}^{48}Ca \rightarrow {}^{112}$ has been analyzed for different isotopes of uranium spanning continuously the spheroidal target deformation. In Fig. 1 the level schemes (upper plot) and the shell effects for protons $E_{shell}^{(p)}$ and total E_{shell} are drawn. Differences are visible for the higher energy levels. Until the last part of the overlapping almost no difference exists within the proton shell cor-

rection. Divergence in the curve behaviour appears at the end of the fusion process. The two branches in E_{shell} correspond to the two proton level scheme deformations of $Z=112$ (where the ratio of spheroid semi-axes is $\chi = 0.89$ and $\chi = 1$). The total shell correction E_{shell} follows the same behaviour slightly lowering the ${}^{232}U$ reaction shell correction in the first part of the process. Shell correction values less than those corresponding to sphere suggest a more deformed ground state for 112 isotopes than those taken into account here.

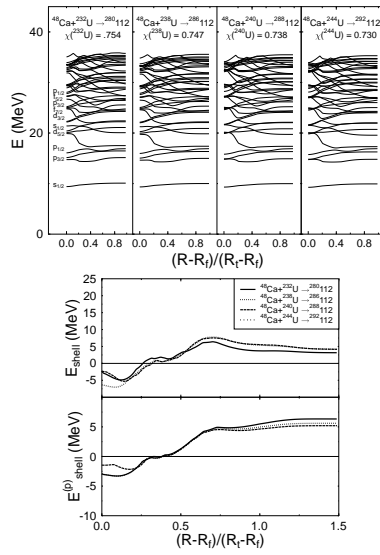


Figure 1: Target deformation effects on the level scheme (upper plot) and on the proton and total shell correction for four isotopic reactions in the synthesis of Z=112.

References

- [1] R. A. Gherghescu, *Phys. Rev. C* **67**, 014309 (2003).
- [2] R. A. Gherghescu, D. N. Poenaru and W. Greiner, in *Fission and Properties of Neutron-Rich Nuclei* Eds. J. H. Hamilton, A. V. Ramayya and H. K. Carter (World Sci., Singapore, 2003) p. 177.
- [3] R. A. Gherghescu, W. Greiner and G. Münzenberg, *Phys. Rev. C* **68**, 054314 (2003).

Electromagnetic radiation in quantum tunneling

S. Mișicu^{1,2}, M. Rizea¹, W. Greiner²

¹ National Institute of Physics and Nuclear Engineering, Department of Theoretical Physics, PO Box MG - 6, Bucharest, Romania

² Institut für Theoretische Physik, J.W. Goethe Universität, Frankfurt am Main, Germany

Quantum particles undergoing tunneling are not moving uniformly across the barrier but with varying velocity. In the case when these particles are carrying an electric charge it is natural to expect that the non-uniform motion gives rise to electromagnetic radiation. A possible candidate is provided by the electrons moving in the periodic potential of a crystal or by the α or β decay of a heavy nucleus. After reviewing the state-of-the-art we study the electromagnetic radiation (bremsstrahlung) emitted by an α particle when crossing the barrier formed by the Coulomb + nuclear potential in a time-dependent quantum formalism. The dynamical characteristics of the α parti-

cle such as position, velocity and acceleration are computed by taking average values of the position and momentum operators, and next the bremsstahlung emission is determined by resorting to the classical formula for the radiation power. The contribution of the α particle intra-barrier motion to the total bremsstrahlung yield is evaluated and some hints are given for the case when one consider the α decay from the ground state.

Proceedings of the International Symposium on **Channeling - Bent Crystals - Radiation Processes**, Frankfurt am Main, Germany, 5-6 June 2003, p. 105 - 114

Efficient numerical solution of the time - dependent Schrödinger equation for deep tunneling

N. Carjan¹, M. Rizea², D. Strottman³

¹ Centre d'Études Nucléaires de Bordeaux - Gradignan, BP 120 Le Haut Vigneau, 33175 Gradignan Cedex, France

² National Institute of Physics and Nuclear Engineering, Department of Theoretical Physics, PO Box MG - 6, Bucharest, Romania

³ Los Alamos National Laboratory, Theoretical Division, Los Alamos, NM 87544, USA

The numerical challenge associated with the time-dependent approach to the general problem of the decay of a metastable state by quantum - tunneling is discussed and methods towards its application to concrete problems are presented. In particular, Crank - Nicolson, multiple step differencing and Chebyshev methods are described emphasizing their main features. Also, different artificial boundary conditions

(transparent, absorbing and discrete transparent) were implemented in order to reduce the reflections of the wave packet at the numerical boundaries. They are illustrated and optimized for the deep - tunneling case of ground - state proton decay.

Romanian Reports in Physics, vol. 55 no. 4, p. 555 - 579, 2003

Numerical methods for solving some boundary problems associated to the Schrödinger equation

M. Rizea¹

¹ National Institute of Physics and Nuclear Engineering, Department of Theoretical Physics, PO Box MG - 6, Bucharest, Romania

The Schrödinger equation is the basic equation of nonrelativistic quantum mechanics. From mathematical point of view this is a partial differential equation of parabolic type, containing a temporal variable and one or more space variables. By separating the temporal part one arrives to the stationary equation, which is a partial differential equation of elliptic type. In some conditions, this equation can be transformed in a system of ordinary differential equations with boundary conditions specific to the problem. The natural domain of definition is unbound. For the numerical solution one should restrict to a finite domain. The adequate treatment of boundary conditions on this computational domain is decisive for the accuracy of the results.

Concerning the stationary equation, of interest is the radial equation which is obtained by separating the angular part from the radial one. The interval of the independent variable r (which from physical point of view is $[0, \infty)$) is truncated to a segment whose first end is in the vicinity of the origin (r_{min}), and the second in the asymptotic region (r_{as}). The influence of the two excluded subintervals $[0, r_{min}]$ and $[r_{as}, \infty)$, should be carefully taken into account. Mathemati-

cally, the essential peculiarity is that the first interval is a singular zone, while the second is an asymptotic zone and thus the numerical solution in these regions should be constructed by considering these features. The thesis presents a systematic approach to the numerical solution of the Schrödinger equation in the two extreme zones. Our aim was to obtain stable and rapid algorithms, and also, with controlled accuracy. The used procedures have been: perturbative, exponential fitting, convergence acceleration and summation methods. The case of systems of coupled equations has been also discussed.

In the case of the time dependent equation, the limitation to a finite spatial domain leads to reflexions which affect the propagated wavefunction and to errors in the calculation of the physical quantities. To eliminate or at least to reduce the reflexions one uses special procedures which allow reasonable large mesh sizes. They have the generic name of "artificial boundary conditions" and we have presented three kinds of such procedures, namely: "transparent", "absorbing" and "discrete transparent" boundary conditions. Together with an appropriate numerical method (like Crank-Nicolson) for propagation they were success-

fully applied to the study of the proton decay in a time - dependent formalism. The cases of one spatial coordinate and of two spatial coordinates have been considered.

The final purpose of the thesis has been to de-

velop efficient methods and a robust software for numerical solving the boundary problems associated to the Schrödinger equation, with a large applicability to physics research.

Doctoral thesis, Defended in June 2003

Nuclear effects on neutrino emissivities from nucleon-nucleon bremsstrahlung

S. Stoica¹, V.P. Paun², A.G. Negoita³

¹ IFIN-HH, Department of Theoretical Physics; E-mail: stoica@theor1.theory.nipne.ro

² Physics Department, Politehnica University, 77206-Bucharest, Romania

³ IFIN-HH, Department of Theoretical Physics; E-mail: negoita@theor1.theory.nipne.ro

The rates of neutrino pair emission by nucleon-nucleon (NN) bremsstrahlung are calculated with the inclusion of the full contribution from a nuclear one pion exchange potential (OPEP). We computed the contributions from the neutron-neutron (nn), proton-proton (pp) and neutron-proton (np) processes for physical conditions encountered in supernovae and neutron stars, both in the degenerate (D) and non-degenerate (ND) limits. We found a significant reduction of these rates, especially for the nn and pp processes, in comparison with the case when the whole nuclear contribution was replaced by constants, representing the high-momentum limits of the expression of the nuclear potential. Further, we also performed the calculations by including contributions due to the ρ meson exchange between nucleons, in the expression of the OPEP. This may be relevant for processes produced in the inner cores of NS, where the density can exceed several times the standard nuclear density and the short-range part of the NN interaction should be taken into account. These corrections lead to an additional suppression of the neutrino emission rates between (8 - 36) %, depending on the process (nn (pp) or np) and physical conditions (temperature and degeneracy of the nucleons).

For a quantitatively understanding of the competition between different neutrino emission processes determining the evolution and properties of the neutron stars (NS) accurate calculations of the corresponding neutrino production rates are very required. A detailed description of these processes and the recent achievements in this domain are presented in many good reviews. We kindly ask the reader to refer, for instance, to [1]- [2] and the references therein. At present, there is a qualitatively understanding of the importance of these processes according to specific density-temperature ranges. For example, within a smooth composition model of ground state matter, the

main contribution to neutrino emission from deep layers of the crust of an NS comes from plasmon decay at very high temperatures and from neutrino-pair bremsstrahlung and Cooper pairing of neutrons at $T \leq 10^9$ K. For other density temperature ranges ($T \leq 10^{10}$ K, $\rho \leq 10^{10}$ g cm⁻³), the electron-positron pair annihilation and the photoneutrino emission may produce comparable emission rates. In non-superfluid NS cores there are many neutrino reactions that can be classified as follows: (I) baryon direct URCA processes, (II) baryon modified URCA processes, (III) baryon bremsstrahlung processes, (IV) lepton modified URCA processes and (V) Coulomb bremsstrahlung processes. The neutrino emissivities of many reactions are reliably calculated being only slightly dependent on a particular microscopic model of strong interactions. However, other reactions are dependent on the adopted model of NN interaction and for these there is still room for improvements for calculation of the emission rates. Particularly, we refer to the neutrino pair emission from NN bremsstrahlung (NNB) processes:

$$\begin{aligned} n + n &\rightarrow n + n + \nu + \bar{\nu}; \quad p + p \rightarrow p + p + \nu + \bar{\nu} \\ n + p &\rightarrow n + p + \nu + \bar{\nu} \end{aligned} \quad (1)$$

In the early nineties Suzuki's calculations [3] showed that these bremsstrahlung processes play, besides the modified baryon URCA processes, a significant role in the cooling mechanisms of the NS [4]- [5]. Contrary to the modified URCA processes, the reactions (1) have no threshold and, for certain temperature-density ranges, they may be more important for the neutrino pair production than the formers.

The main difficulty in calculation of their emission rates is the appropriate treatment of the strong NN interaction which is responsible for the ν production together with the weak interactions. In the early calculations this interaction has been treated either by

computing the overlap integrals associated with the initial and final nucleon wave function [4] or through the use of a Fermi liquid parametrization [6]. Later on, several authors have deduced an NN potential based on the one pion exchange (OPE) approximation [7]-[8] and used it in calculations of the neutrino emissivities of the modified URCA processes and NNB.

However, for an accurate computation of the neutrino pair emissivities from these processes an accurate treatment of the nuclear potential is certainly required. For that, in a recent work [10] a method was developed for treating explicitly the momentum dependence of the OPEP. The authors showed that in particular physical conditions, characterized by temperatures $T \leq m_\pi^2/m \sim 20\text{MeV}$, the integral over the nuclear matrix elements (NME) collapses, in a good approximation, to an integral which is independent of angles. The remaining part of the nuclear contribution, which depends only on the nucleon and neutrino energies, can be easily integrated numerically. As a first application, this method was used to the computation of the neutrino emission rates for the like-nucleon bremsstrahlung processes in the (D) and (ND) regimes. The aim was just to compare (for $T=6$) their results with the results obtained by the authors of ref. [9] where the whole nuclear contribution was reduced to a constant factor ζ . Both in the (D) and (ND) limits there was found that the inclusion of the full contribution of an NN OPE potential produces neutrino emissivities which are about two times larger than the case when the NN interaction is reduced to a constant $\zeta = 1$.

In this brief review we extend the method developed in ref. [10] to calculate the neutrino emission rates from the (nn), (pp) and (np) bremsstrahlung processes taking into account the full contribution from a nuclear OPEP. The calculations are performed for several temperatures and are relevant for physical conditions encountered in supernovae and NS, both in the degenerate (D) and non-degenerate (ND) limits. Further, we also include in the calculation the short-range part of the NN interaction by adding the contribution of ρ mesons in the expression of the OPEP. The

general effect of these nuclear contributions is a suppression of the corresponding neutrino emission rates which depends on the specific process and the physical conditions (temperature and degeneracy).

References

- [1] D.G. Yakovlev, A.D. Kaminker, O.Y. Gnedin and P. Haensel, astro-ph/0012122.
- [2] A. Burrows and T.A. Thomson, astro-ph/0211404.
- [3] H. Suzuki, *um. Astrophys. Japan*, **2**, 267 (1991); Proc. International Symp. on Neutrino Astrophys. Frontiers of Neutrino Astrophysics, ed. Y. Suzuki and K. Nakamura, (Tokyo: Universal Academic Press).
- [4] J. N. Bahcall and R. A. Wolf, Phys. Rev. B **140**, 1452 (1965).
- [5] C. Hanhart, D. R. Phillips and S. Reddy, astro-ph/0003445.
- [6] E. G. Flowers, P. G. Sutherland and J. R. Bond, Phys. Rev. D **12**, 2 (1975).
- [7] B. L. Friman and O. V. Maxwell, *Astrophys. J.*, **232**, 541 (1979).
- [8] S. Hannestad and G. Rafelt, *Astrophys. J.* **507**, 339 (1998).
- [9] T. A. Thomson, A. Burrows, J. Horvath, Phys. Rev. C **62**, 035802 (2000).
- [10] S. Stoica, J. Horvath, Phys. Rev. C **65**, 028801 (2002).
- [11] R. P. Brikmann and M. Turner, Phys. Rev. D **38**, 2338 (1988).
- [12] T. Ericson and J.F. Mathiot, Phys. Lett B **219**, 507 (1989).

Spatiotemporal discrete multicolor solitons

Z. Xu¹, Y.V. Kartashov¹, L.C. Crasovan^{1,2}, D. Mihalache^{1,2}, L. Torner¹

¹ ICFO-Institut de Ciencies Fotoniques, and Department of Signal Theory and Communications, Universitat Politècnica de Catalunya, 08034 Barcelona, Spain

² Department of Theoretical Physics, National Institute of Physics and Nuclear Engineering, P.O. Box MG-6, Bucharest, Romania

We have found various families of 2D spatiotemporal solitons in quadratically nonlinear waveguide arrays. The families of unstaggered odd, even, and twisted stationary solutions are thoroughly characterized and their stability against perturbations is in-

vestigated. We show that the twisted and even solitons display instability, while most of the odd solitons show remarkable stability upon evolution. Published in: *Physical Review E*, v. 70, 066618 (2004).

Nonlinear optics of a few-cycle optical pulse: slow-envelope approximation revisited

I.V. Melnikov¹, H. Leblond², F. Sanchez², D. Mihalache³

¹ E. S. Rogers Sr. Department of Electrical and Computer Engineering, University of Toronto, Toronto, ON M5S 3G4, Canada

² Laboratoire Propriétés Optiques des Matériaux et Applications, Unité Mixte de Recherche 6136 de Centre National de la Recherche Scientifique, 49045 Angers Cedex 01, France

³ Department of Theoretical Physics, National Institute of Physics and Nuclear Engineering, P.O. Box MG-6, Bucharest, Romania

Using Maxwell-Bloch equations, we analyze the response of an ensemble of two-level atoms driven by a femtosecond optical pulse beyond the traditional approach of slowly varying amplitudes and phases. For

optical pulses of a given duration, we show that the off-resonance optical field can evolve into a stable (spatio-) temporal soliton. Published in: *IEEE J. Sel. Top. Quantum Electron.*, v. 10, 870-875 (2004).

Spatiotemporal optical solitons: an overview

D. Mihalache¹

¹ Department of Theoretical Physics, National Institute of Physics and Nuclear Engineering, P.O. Box MG-6, Bucharest, Romania

A new topic in both theoretical and experimental studies of optical solitons is provided by the possibility of existence of spatiotemporal optical solitons, sometimes called "light bullets" or "superspikes", which are completely localized pulses of light. These fully localized spatiotemporal physical objects result from the simultaneous balance of diffraction and dispersion by nonlinear phase modulation. They hold promise for potential applications in ultrafast all-optical process-

ing devices, where each spatiotemporal soliton may represent an elementary bit of information, provided that stable "light bullets" can be formed from pulses at reasonable energy levels in available optical materials. A brief up-to-date survey of recent theoretical and experimental studies in the field of spatiotemporal solitons in optical media is given. Published in: *Proceedings of SPIE*, vol. 5581, pp. 564-570 (2004).

Stable vortex solitons supported by competing quadratic and cubic nonlinearities

D. Mihalache^{1,3}, D. Mazilu¹, B.A. Malomed², F. Lederer³

¹ Department of Theoretical Physics, National Institute of Physics and Nuclear Engineering, P.O. Box MG-6, Bucharest, Romania

² Department of Interdisciplinary Studies, Faculty of Engineering, Tel Aviv University, Tel Aviv 69978, Israel

³ Institute of Solid State Theory and Theoretical Optics, Friedrich Schiller University Jena, Max-Wien-Platz 1, Jena, D-07743, Germany

We address the stability problem for vortex solitons in 2D media combining quadratic and self-defocusing cubic nonlinearities. We consider the propagation of spatial beams with intrinsic vorticity S in such bulk optical media. It was earlier found that the $S = 1$ and $S = 2$ solitons can be stable, provided that their power (i.e., transverse size) is large enough, and it was conjectured that all the higher-order vortices with $S > 3$ are always unstable. On the other hand, it was recently shown that vortex solitons with $S > 2$ and very large transverse size may be stable in media combining cubic self-focusing and quintic self-defocusing nonlinearities. Here, we demonstrate that the same is true in the model, the vortices with $S = 3$ and $S = 4$ being stable in regions occupying, respectively, 3% and

1.5% of their existence domain. The vortex solitons with $S > 4$ are also stable in tiny regions. The results are obtained through computation of stability eigenvalues, and are then checked in direct simulations, with a conclusion that the stable vortices are truly robust ones, easily self-trapping from initial beams with embedded vorticity. The dependence of the stability region on the phase-mismatch parameter is specially investigated. We thus conclude that the stability of higher-order two-dimensional vortex solitons in narrow regions is a generic feature of optical media featuring the competition between self-focusing and self-defocusing nonlinearities. A qualitative analytical explanation to this feature is proposed. Published in: *Physical Review E*, v. 69, 066614 (2004).

Three-dimensional parallel vortex rings in Bose-Einstein condensates

L.C. Crasovan^{1,4}, V.M. Perez-Garcia², I. Danaila³, D. Mihalache^{1,4}, L. Torner¹

¹ ICFO-Institut de Ciencies Fotoniques, and Department of Signal Theory and Communications, Universitat Politècnica de Catalunya, 08034 Barcelona, Spain.

² Departamento de Matemáticas, E.T.S.I. Industriales, Universidad de Castilla-La Mancha, 13071 Ciudad Real, Spain

³ Laboratoire Jacques-Louis Lions, Université Paris 6, 175 Rue du Chevaleret, 75013 Paris, France

⁴ Department of Theoretical Physics, National Institute of Physics and Nuclear Engineering, P.O. Box MG-6, Bucharest, Romania

We construct three-dimensional structures of topological defects hosted in trapped wave fields, in the form of vortex stars, vortex cages, parallel vortex lines, perpendicular vortex rings, and parallel vortex rings, and we show that the latter exist as robust stationary, collective states of nonrotating Bose-Einstein con-

densates. We discuss the stability properties of excited states containing several parallel vortex rings hosted by the condensate, including their dynamical and structural stability. Published in: *Physical Review A* v.70, 033605 (2004).

Stable three-dimensional spatiotemporal solitons in a two-dimensional photonic lattice

D. Mihalache^{1,2,3}, D. Mazilu^{2,3}, F. Lederer³, Y.V. Kartashov¹, L.C. Crasovan^{1,2}, L. Torner¹

¹ ICFO-Institut de Ciencies Fotoniques, and Department of Signal Theory and Communications, Universitat Politecnica de Catalunya, 08034 Barcelona, Spain

² Department of Theoretical Physics, National Institute of Physics and Nuclear Engineering, P.O. Box MG-6, Bucharest, Romania

³ Institute of Solid State Theory and Theoretical Optics, Friedrich-Schiller University Jena, Max-Wien-Platz 1, D-077743 Jena, Germany

We investigate the existence and stability of 3D spatiotemporal solitons in self-focusing cubic Kerr-type optical media with an imprinted 2D harmonic transverse modulation of the refractive index. We demonstrate that two-dimensional photonic Kerr-type nonlinear lattices can support stable one-parameter

families of 3D spatiotemporal solitons provided that their energy is within a certain interval and the strength of the lattice potential, which is proportional to the refractive index modulation depth, is above a certain threshold value. Published in: *Physical Review E*, v. 70, 055603(R) (2004).

Soliton clusters in three-dimensional media with competing cubic and quintic nonlinearities

D. Mihalache^{1,2,3}, D. Mazilu^{2,3}, L.C. Crasovan^{1,2}, B.A. Malomed⁴, F. Lederer³, L. Torner¹

¹ ICFO-Institut de Ciencies Fotoniques, and Department of Signal Theory and Communications, Universitat Politecnica de Catalunya, 08034 Barcelona, Spain

² Department of Theoretical Physics, National Institute of Physics and Nuclear Engineering, P.O. Box MG-6, Bucharest, Romania

³ Institute of Solid State Theory and Theoretical Optics, Friedrich-Schiller University Jena, Max-Wien-Platz 1, D-077743 Jena, Germany

⁴ Department of Interdisciplinary Studies, Faculty of Engineering, Tel Aviv University, Tel Aviv 69978, Israel

We introduce a class of robust soliton clusters composed of N fundamental solitons in three-dimensional media combining the self-focusing cubic and self-defocusing quintic nonlinearities. The angular momentum is lent to the initial cluster through staircase or continuous ramp-like phase distribution. Formation of these clusters is predicted analytically, by calculating an effective interaction Hamiltonian H_{int} . If a minimum of H_{int} is found, direct three-dimensional simulations demonstrate that, when the initial pattern is close to the predicted equilibrium size, a very robust rotating cluster does indeed exist, featuring persistent oscillations around the equilibrium configuration (clusters composed of $N = 4, 5$, and 6 fundamental solitons are investigated in detail). If a strong random noise is added to the initial configuration, the clus-

ter eventually develops instability, either splitting into several fundamental solitons or fusing into a nearly axisymmetric vortex torus. These outcomes match the stability or instability of the three-dimensional vortex solitons with the same energy and spin; in particular, the number of the fragments in the case of the breakup is different from the number of solitons in the original cluster, being instead determined by the dominant mode of the azimuthal instability of the corresponding vortex soliton. The initial form of the phase distribution is important too: under the action of the noise, the cluster with the built-in staircase-like phase profile features azimuthal instability, while the one with the continuous distribution fuses into a vortex torus. Published in: *J. Opt. B: Quantum Semiclass. Opt.*, v. 6, S333 (2004).

Stable vortex solitons in a vectorial cubic-quintic model

D. Mihalache^{1,2}, D. Mazilu^{1,2}, B.A. Malomed³, F. Lederer²

¹ Department of Theoretical Physics, National Institute of Physics and Nuclear Engineering, P.O. Box MG-6, Bucharest, Romania

² Institute of Solid State Theory and Theoretical Optics, Friedrich-Schiller University Jena, Max-Wien-Platz 1, D-077743 Jena, Germany

³ Department of Interdisciplinary Studies, Faculty of Engineering, Tel Aviv University, Tel Aviv 69978, Israel

We investigate the stability of vectorial (two-component) vortex solitons of two types. Their stationary shapes are identical, but their stability (which is the most important issue for spinning solitons) is drastically different. These are solitons with vorticities (S, S) and $(S, -S)$ in the two components. The analysis is performed in a vectorial cubicquintic model, with the two components nonlinearly coupled by the incoherent cross-phase-modulation interaction, but we expect that the results are quite generic. The stability was investigated by means of computing eigenvalues of perturbations around the stationary solitons, as well as in direct simulations. We also report new analytical results for the well-known problem of the description of the stationary form of scalar solitons in media of this type. The analytical results explain the shape of the spinning solitons, and the strong dependence of their

norm (power) on the vorticity, in both the 2D and 3D cases. In this paper we also give the first estimate of the physical characteristics (power and radius) of the stable solitons with different values of S , making use of recently measured values of the necessary nonlinear parameters. All the two-component solitons of type $(S, -S)$ are unstable. In contrast, those of type (S, S) have their stability regions, the size of which strongly depends on S . An unstable soliton always splits into a set of separating zero-spin ones, in precise compliance with the azimuthal index of the most unstable perturbation eigenmode. Direct simulations demonstrate that stable solitons readily self-trap from arbitrary initial pulses which belong to their topological class. Published in: *J. Opt. B: Quantum Semiclass. Opt.*, v. 6, S341-S350 (2004).

Dynamics of dual-frequency solitons under the influence of frequency-sliding filters, third-order dispersion, and intrapulse Raman scattering

N.C. Panoiu^{1,2}, D. Mihalache^{2,3}, D. Mazilu^{2,3}, I.V. Melnikov⁴, J.S. Aitchison⁴, F. Lederer³, R.M. Osgood¹

¹ Department of Applied Physics and Applied Mathematics, Columbia University, New York, NY 10027, USA

² Department of Theoretical Physics, National Institute of Physics and Nuclear Engineering, P.O. Box MG-6, Bucharest, Romania

³ Institute of Solid State Theory and Theoretical Optics, Friedrich-Schiller University Jena, Max-Wien-Platz 1, D-077743 Jena, Germany

⁴ E. S. Rogers Sr. Department of Electrical and Computer Engineering, University of Toronto, Toronto, ON M5S 3G4, Canada

We analyze the structure of the optical field emerging from a superposition of two soliton-like pulses with different frequencies and arbitrary phase-shift between them, and show that the optical output contains either symmetric or antisymmetric twosoliton states. Furthermore, we study numerically the dynamics of

these emerging two-soliton states under the influence of perturbative effects that are important for optical communications systems: frequency-sliding filters, third-order dispersion, and intrapulse Raman scattering. Published in: *IEEE J. Sel. Top. Quantum Electron.*, v. 10, 885-892 (2004).

Vectorial spatial solitons in bulk periodic quadratically nonlinear media

N.C. Panoiu^{1,2}, D. Mihalache^{2,3}, D. Mazilu^{2,3}, F. Lederer³, R.M. Osgood¹

¹ Department of Applied Physics and Applied Mathematics, Columbia University, New York, NY 10027, USA

² Department of Theoretical Physics, National Institute of Physics and Nuclear Engineering, P.O. Box MG-6, Bucharest, Romania

³ Institute of Solid State Theory and Theoretical Optics, Friedrich-Schiller University Jena, Max-Wien-Platz 1, D-077743 Jena, Germany

We present a comprehensive analysis of the generation, propagation and characteristic properties of two-dimensional spatial solitons formed in quasi-phase-matched gratings through type-II vectorial interaction. By employing an averaging approach based on asymptotic expansion theory, we show that the dynamics of

soliton propagation in the grating and their stability properties are strongly influenced by induced Kerr-like nonlinearities. Finally, through extensive numerical simulations, we verify the validity of our theoretical predictions. Published in: *J. Opt. B: Quantum Semiclass. Opt.*, v. 6, S351-S360 (2004).

Solitary waves in a 2-D "zig-zag" model of coupled chains

A. Vișinescu¹, D. Grecu¹

¹ IFIN-HH, Department of Theoretical Physics; E-mail: dgrecu@theor1.theory.nipne.ro

The "zig-zag" model proposed several years ago by Zolotaryuk et al. [1] as a 2-D approximation for the DNA structure is studied in the continuum limit. In the linear approximation the dispersion relations for the acoustic and optical modes are determined. A functional relation in the acoustic sector between model's variables is assumed. In the linear case this reproduces the dispersion relation of the acoustic mode in the long wave length limit. The equations of motion are analyzed using the multiple scales method and the same KdV equation is obtained from both equations. This self-consistent analysis completely determines the coefficients in the functional relation assumed between the field variables.

The "zig-zag" model (Z-Z model) consists of two parallel chains of identical points of mass M , their motion being restricted to the plane determined by the two chains. The Z-Z model mimics the helical structure of DNA, the molecules being able to move and rotate in the 2-D plane [1]-[4]. The x - and y -axis are taken along the chain and in the perpendicular direction respectively. The molecules on the lower chain are labeled by the index $n = 0, \pm 2, \pm 4, \dots$ while those on the upper one by $n = \pm 1, \pm 3, \dots$ The

equilibrium distance between two neighboring atoms along the chain is denoted by l , and the distance between chains is bl , where $b = \sqrt{h^2 + \frac{1}{4}}$. It deserves to observe the different orientation of the y variable for molecules belonging to the two chains. We assume to have N molecules on each chain (N even), and we impose periodic boundary conditions. In consequence the allowed values of the wave vector k are restricted to the first Brillouin zone $(-\frac{\pi}{l}, \frac{\pi}{l})$, and are given by $k_\nu = \frac{2\pi}{L}\nu$, $L = Nl$ and ν an integer number. The instantaneous position of the n -th molecule is given by the pair (x_n, y_n) .

The Z-Z model is described by the Hamiltonian

$$H = \sum_n \left[\frac{1}{2}M(\dot{x}_n^2 + \dot{y}_n^2) + Kl^2(U(r_n) + V(q_n)) \right] \quad (1)$$

where M is the mass of the molecule, K is a characteristic stiffness constant, and the dimensionless interaction potentials $U(r_n), V(q_n)$ are assumed to depend only on the dimensionless displacements lengths r_n and q_n between two nearest neighbors on different chains and on the same chain, respectively; they are given by

$$\begin{aligned} r_n &= \sqrt{\left(\frac{1}{2} + \frac{x_{n+1} - x_n}{l}\right)^2 + \left(h - \frac{y_n + y_{n+1}}{l}\right)^2} - b \\ q_n &= \sqrt{\left(1 + \frac{x_{n+1} - x_{n-1}}{l}\right)^2 + \left(\frac{y_{n+1} - y_{n-1}}{l}\right)^2} - 1. \end{aligned} \quad (2)$$

The corresponding Euler Lagrange equations of motion are

$$\begin{aligned} M\ddot{x}_n &= -Kl^2 \frac{\partial}{\partial x_n} W_n \\ M\ddot{y}_n &= -Kl^2 \frac{\partial}{\partial y_n} W_n \end{aligned} \quad (3)$$

where

$$W_n = U(r_{n-1}) + U(r_n) + V(q_{n-1}) + V(q_{n+1}) \quad (4)$$

It is useful to introduce the dimensionless time $\tau = \omega_0 t$, where $\omega_0^2 = \frac{K}{M}$, to re-scale the lattice fields $u_n = \frac{x_n}{l}$, $v_n = \frac{y_n}{l}$ and to introduce the relative displacements

$$\rho_n = u_{n+1} - u_n, \quad \eta_n = v_n + v_{n+1}. \quad (5)$$

With these new variables we have

$$\begin{aligned} r_n &= \sqrt{\left(\frac{1}{2} + \rho_n\right)^2 + (h - \eta_n)^2} - b \\ q_n &= \sqrt{(1 + \rho_{n-1} + \rho_n)^2 + (\eta_n - \eta_{n-1})^2} - 1 \end{aligned} \quad (6)$$

The nonlinear terms in the equations of motion have two distinct sources. One is from the anharmonic character of the interaction potentials U and V . Assuming weak nonlinearity we shall consider

$$\begin{aligned} U(r) &= k_1 \left(\frac{1}{2} r^2 - \frac{1}{3} \alpha r^3 \right) \\ V(r) &= k_2 \left(\frac{1}{2} q^2 - \frac{1}{3} \beta q^3 \right), \end{aligned} \quad (7)$$

with k_1, k_2 dimensionless stiffness constants and α, β parameters describing cubic nonlinearity. But even if we remain in the harmonic approximation for the interaction potentials ($\alpha, \beta = 0$) anharmonic terms can appear from the development of the square roots in (6) in higher order. This is usually known as "geometrical nonlinearity", [1].

Introducing the abbreviations

$$\begin{aligned} P_n &= \frac{\partial}{\partial \rho_n} U(r_n) & Q_n &= \frac{\partial}{\partial \rho_n} V(q_n) \\ S_n &= \frac{\partial}{\partial \eta_n} U(r_n) & T_n &= \frac{\partial}{\partial \eta_n} V(q_n) \end{aligned} \quad (8)$$

it is easily shown that the equations of motion (3) becomes

$$\frac{d^2 \rho_n}{d\tau^2} = P_{n+1} - 2P_n + P_{n-1} + Q_{n+2} - Q_{n+1} - Q_n + Q_{n-1} \quad (9)$$

$$\frac{d^2 \eta_n}{d\tau^2} = -(S_{n-1} + 2S_n + S_{n+1}) + T_{n+2} + T_{n+1} - T_n - T_{n-1}$$

which represents the starting point of our analysis.

In the followings we shall consider the continuum limit of eqs.(9). We introduce the continuum variable x ($n \rightarrow x$) and the displacement operator

$$f_{n+p} \rightarrow e^{p \frac{\partial}{\partial n}} f_n \rightarrow e^{p \frac{\partial}{\partial x}} f(x).$$

Separating in P_n, \dots, T_n the linear terms from the nonlinear ones, using the variable z_n , and the new time variable $t = \Omega_0 \tau$, the equations of motion (9) write

$$\begin{aligned} \frac{\partial^2 \rho}{\partial t^2} &= \frac{1}{16h^2} \left(1 + \frac{1}{12} \frac{\partial^2}{\partial x^2} \right) \frac{\partial^2 z}{\partial x^2} + c \left(1 + \frac{1}{3} \frac{\partial^2}{\partial x^2} \right) \frac{\partial^2 \rho}{\partial x^2} \\ &+ \frac{1}{16h^2} \left(1 + \frac{1}{12} \frac{\partial^2}{\partial x^2} \right) \frac{\partial^2 \bar{P}}{\partial X^2} + \\ &+ c \left(1 + \frac{1}{2} \frac{\partial}{\partial x} + \frac{1}{3} \frac{\partial^2}{\partial x^2} \right) \frac{\partial^2 \bar{Q}}{\partial x^2} \\ \frac{\partial^2 \rho}{\partial t^2} - \frac{\partial^2 z}{\partial t^2} &= \left(1 + \frac{1}{4} \frac{\partial^2}{\partial x^2} + \frac{1}{48} \frac{\partial^4}{\partial x^4} \right) z + \\ &+ \left(1 + \frac{1}{4} \frac{\partial^2}{\partial x^2} \right) \bar{S} + c \left(1 + \frac{1}{2} \frac{\partial}{\partial x} + \frac{5}{12} \frac{\partial^2}{\partial x^2} \right) \frac{\partial \bar{T}}{\partial x} \end{aligned} \quad (10)$$

The effect of a small nonlinearity, at least in the continuum limit is a cumulative effect which manifests at long space and time scales. A correct mathematical description of this effect is based on the asymptotic method of multiple scales (MS) analysis [5]. Restricting ourselves to the discussion of the acoustical sector in the long wave length limit, we shall concentrate our attention to the first equation (10), as in this approximation the acoustic mode is almost longitudinal, being described by the ρ -variable.

It is well known that Korteweg-de Vries equation (KdV) is the relevant equation resulting from a MS analysis of a nonlinear problem with weak dispersion and small nonlinearity. We introduce the slow variables (stretched variables) [5]

$$\xi = \epsilon(x - vt), \quad t_2 = \epsilon^2 t, \dots \quad (11)$$

with the velocity v to be determined later, and expand ρ in a Taylor series

$$\rho = \sum_{j=1} \epsilon^{2j} A_j(\xi, t_2, \dots) \quad (12)$$

the amplitudes A_j depending only on the slow variables. Then

$$\frac{\partial}{\partial x} \rightarrow \epsilon \frac{\partial}{\partial \xi} \quad (13)$$

$$\frac{\partial^2}{\partial t^2} \rightarrow \epsilon^2 v^2 \frac{\partial^2}{\partial \xi^2} - \epsilon^4 2v \frac{\partial^4}{\partial \xi^2 \partial t_2^2}$$

and taking $v = \sqrt{c}$ the following KdV equation is found in ϵ^6 order

$$\begin{aligned} \frac{\partial A_1}{\partial t_2} + & \frac{\sqrt{c}}{2} \left(\frac{1}{3} + \frac{1}{16h^2} \right) \frac{\partial^3 A_1}{\partial \xi^3} + \\ & + \frac{1}{\sqrt{c}} \left[\frac{1}{16h^2} \left(1 + \frac{1}{4h^2} + a_1 \right) - 2\beta c \right] \rho \frac{\partial \rho}{\partial x} = 0. \end{aligned} \quad (14)$$

Then the KdV equation resulting from the MS analysis of the equations of motion (10) in the acoustical sector is

$$\frac{\partial A_1}{\partial t_2} + \frac{\sqrt{c}}{2} \left(\frac{1}{3} + \frac{1}{16h^2} \right) \frac{\partial^3 A_1}{\partial \xi^3} - 2\beta c A_1 \frac{\partial A_1}{\partial \xi} = 0. \quad (15)$$

With the scaling

$$\begin{aligned} t_2 \rightarrow T, \quad \xi = & \left[\frac{\sqrt{c}}{2} \left(\frac{1}{3} + \frac{1}{16h^2} \right) \right]^{\frac{1}{3}} X \quad (16) \\ A_1 = & -\frac{3}{\beta c} \left[\frac{\sqrt{c}}{2} \left(\frac{1}{3} + \frac{1}{16h^2} \right) \right]^{\frac{1}{3}} \Psi \end{aligned}$$

the equation (15) is transformed into

$$\frac{\partial \Psi}{\partial T} + \frac{\partial^3 \Psi}{\partial X^3} + 6\Psi \frac{\partial \Psi}{\partial X} = 0 \quad (17)$$

which is the usual form of the KdV equation. One soliton solution of (17) is given by

$$\Psi(X, T) = 2\eta^2 \frac{1}{\cosh^2 \eta(X - X_0 - 4\eta^2 t)}. \quad (18)$$

The procedure used is much simpler than that used in [1], but the results are similar.

For the optical sector the problem becomes more complicated by the necessity to consider the dependence of the solution on fast variables also (at least on the fast time variable), not only on the slow variables as in the acoustic case. Work in this direction is in progress.

References

- [1] A.V. Zolotaryuk, P.L. Christiansen, A.V. Savin, Phys.Rev. E **54**, 3881(1996)
- [2] S.W. Englander, N.R. Kallenbach, A.J. Heegor, J.A. Krumhansl, A. Litvin, Proc.Natl.Acad.Sci.USA **77**, 7222(1980)
- [3] L.V. Yakushevich, "Nonlinear Science at the Dawn of 21-th Century", p. 373 (Eds. P.L Christiansen, M.P. Sorensen, A.C. Scott; Springer, 2000)
- [4] A.S. Davydov, "Solitons in Molecular Systems", (Kluwer, Dordrecht, 1991)
- [5] T. Taniuti, Suppl.Prog.Theor.Phys. **55**,1(1974)

Limits and degeneracies of discrete Painleve equations: a sequel

A.S. Cărstea¹, A. Ramani¹, R. Willox¹, B. Grammaticos¹, J. Satsuma¹

¹ IFIN-HH, Department of Theoretical Physics; E-mail: acarst@theor1.theory.nipne.ro

We present the discrete integrable systems which result from the q-discrete Painleve equation $q-P_{VI}$ and difference Painleve equation $d-P_V$ associated to the affine Weyl group $E_7^{(1)}$. Two different procedures (limits and degeneracies) will be used. The various equations will be classified in two broad classes. Discrete and q-Painleve equations and linearisable mappings. For the first we shall use a discrete integrability criterion (such as singularity confinement or algebraic entropy). It is expected that the number of parameters will be equal or superior with the case of Painleve VI. In the case of linearisable mappings several transformations will be implemented to construct effective

linearisations.

References

- [1] A. S. Cărstea, A. Ramani, B. Grammaticos, R. Willox, J. Phys. A; Math. Gen, 36 (2003), 8419
- [2] A. Ramani, A.S. Cărstea, B. Grammaticos, Y. Ohta, Physica A 305, (2002), 437
- [3] K. M. Tamizhmani, B. Grammaticos, A. S. Cărstea, A. Ramani, Reg. Chaot. Dyn. 2, (2004),13

Statistical approach on modulational instability in nonlinear discrete systems

D. Grecu¹, A. Vișinescu¹

¹ IFIN-HH, Department of Theoretical Physics; E-mail: dgrecu@theor1.theory.nipne.ro

The modulational instability (Benjamin-Feir instability) in several nonlinear discrete systems (discrete NLS, Ablowitz-Ladik, discrete deformable NLS equation) is investigated using a statistical approach. A kinetic equation for a 2-point correlation function is obtained, and using a Wigner-Moyal transformation it is written in a mixed space-wave number representation. A linear stability analysis of the resulting equation is performed, and the obtained integral stability equation is discussed using several forms of the initial unperturbed spectrum (δ -spectrum, Lorentzian). The results are compared with the continuum limit (NLS equation) and previous results.

Ten years ago Kivshar and Salerno [1] have discussed the problem of modulational instability in a "deformable nonlinear Schrödinger equation" (dNLS),

$$i \frac{d\Psi_n}{dt} + D(\Psi_{n+1} - 2\Psi_n + \Psi_{n-1}) + \gamma|\Psi_n|^2\Psi_n + \lambda|\Psi_n|^2(\Psi_{n+1} + \Psi_{n-1}) = 0. \quad (1)$$

It arises naturally from an evolution equation

$$i \frac{d\Psi_n}{dt} + \omega_n \Psi_n + J_n(\Psi_{n+1} + \Psi_{n-1}) = 0$$

in which the local mode frequency ω_n and the local inter-site coupling constant J_n are dependent on the local deformation

$$\begin{aligned} \omega_n &= \omega_0 + \omega_1 |\Psi_n|^2 \\ J_n &= J_0 + J_1 |\Psi_n|^2 \end{aligned}$$

The model is suitable to investigate the effect of the interplay between the nonlinear on-site and inter-site interactions on the modulational instability. For $\lambda = 0$ it becomes the discrete nonlinear Schrödinger equation (or discrete self-trapping equation) which is non-integrable, while for $\gamma = 0$ it becomes the integrable Ablowitz-Ladik equation. The problem of modulational instability is discussed in [1] from a deterministic point of view; a linear stability of a small modulated plane wave is investigated. Besides the usual instability in the long wave length region, an instability in the short wave region is found, and this is the effect of the interplay mentioned above ($\gamma < 2\lambda$).

If the deterministic approach of the modulational instability (DAMI) phenomenon is well known (for a recent review see [2]), the complementary statistical approach (SAMI) is less used [3]-[5].

In this approach a kinetic equation for a two-point correlation function is written down and a linear stability analysis of it is performed. The aim is to investigate the influence of the statistical properties of the medium on the instability development. This can have important consequences (in hydrodynamics and plasma physics) and indeed the influence is significant. The main result can be formulated in the following way: if the space correlation in the initial state is of too short range the instability is suppressed.

Recently we applied this approach to discrete systems [6], [7], like the discrete self-trapping and Ablowitz-Ladik equations. It is the aim of the present paper to discuss SAMI for dNLS equation (1) and to see the effect of the interplay between on-site and inter-site interactions on the development of MI.

Let us briefly review the DAMI for dNLS eq. (1). We consider a plane wave solution of (1) $\Psi_n = ae^{i(kn-\omega t)}$, with a constant amplitude, but with an amplitude dependent dispersion relation $\omega = 4D \sin^2 \frac{k}{2} - \gamma|a|^2 - 2\lambda|a|^2 \cos k$ (a Stokes wave). Next we consider a slowly modulated solution

$$\Psi_n(t) = a(1 + \epsilon b_n(t))e^{i(kn-\omega t)}$$

Keeping only linear terms in ϵ the equation of motion for b_n writes

$$\begin{aligned} i \frac{db_n}{dt} + D(e^{ik}b_{n+1} + e^{-ik}b_{n-1} - 2 \cos kb_n) + \gamma|a|^2(b_n + b_n^*) + \\ + \lambda|a|^2(e^{ik}b_{n+1} + e^{-ik}b_{n-1} + 2 \cos kb_n^*) = 0 \end{aligned}$$

Looking for plane wave solutions

$$b_n = \alpha e^{i(Qn-\Omega t)} + \beta e^{-i(Qn-\Omega^* t)}$$

a system of two homogeneous linear equations in α and β^* is obtained, and the compatibility conditions gives

$$\Omega = 2(D + \lambda|a|^2) \sin k \sin Q +$$

$$+ i2\sqrt{2}|\cos k| \sin \frac{Q}{2}(D + \lambda|a|^2)$$

$$\sqrt{\cos Q - \frac{1}{D + \lambda|a|^2} \left(D - \lambda|a|^2 - \frac{\gamma|a|^2}{\cos k} \right)}$$

Here both k and Q are restricted to the first Brillouin zone $(-\pi, \pi)$. The instability appears if $Im\Omega > 0$, i.e.

$$\cos Q > \frac{1}{1 + \frac{\lambda}{D}|a|^2} \left(1 - \frac{\lambda}{D}|a|^2 - \frac{\gamma}{D}|a|^2 \frac{1}{\cos k} \right)$$

As $|a|^2 \ll 1$ this relation can be written

$$\sin \frac{Q}{2} < |a| \sqrt{\frac{\lambda}{D} + \frac{\gamma}{2D} \frac{1}{\cos k}}$$

The picture of instability regions is more complex (compared with the NLS case) and depends on the signs of D, λ, γ and the value of k . If D, λ, γ have the same sign an instability is possible also in the short wave limit ($k \rightarrow \pi$) if $\gamma < 2\lambda$. We don't insist any more on this problem, as being carefully discussed in [1].

The deformable nonlinear Schrödinger model discussed by Kivshar and Salerno is well suited to see the effect of the interplay between on-site and inter-site nonlinearity on the modulational instability phenomenon. This problem was studied in the present paper both in a deterministic and statistical approach. In both approaches a new instability region is found, when k , the wave vector of the carrying wave, is near the boundary of the Brillouin zone ($k \simeq \pi$). This new instability region is a direct consequence of the interplay mentioned above.

A complete treatment of MI from a statistical approach is done. An integral stability equation was obtained and it was solved for several initial spectral functions (δ -spectrum centered on $k = 0$ and $k = \pm\pi$, a Lorentzian spectrum). In the case of Lorentzian spectrum the increment of the instability (the imaginary part of the frequency of the slow modulation) was calculated for the discrete NLS equation. The result, eq. (??), emphasizes the strong influence of the statistical properties of the medium on the development of MI, namely the instability is possible only if a certain long range correlation exists between the parti-

cles in the initial state. If it is too short the instability is suppressed. The same conclusion is obtained also in other situations and seems to be generally valid [3]-[7].

References

- [1] Y.S. Kivshar, M. Salerno - *Phys.Rev.E* **49**, 3543 (1994)
- [2] F.Kh. Abdulaev, S.A. Darmanyan, J. Garnier - in "Progress in Optics" vol. **44**, 303 (2002)
- [3] I.E. Alber - *Proc.Roy. Soc. London A*, **363**, 525 (1978)
- [4] R. Fedele, P.K. Shukla, M. Onorato, D. Anderson, M. Lisak - *Phys. Lett.A* **303**, 61 (2002)
- [5] M. Onorato, A. Osborne, R. Fedele, M. Serio - *Phys.Rev.E* **67**, 046305 (2003)
- [6] Anca Visinescu, D. Grecu - *Eur. Phys. J. B* **34**, 225-229 (2003)
- [7] D. Grecu, Anca Visinescu - Proc. NATO ARW "Nonlinear Waves - Classical and Quantum Aspects" NATO Sciences Series, II. Mathematics, Physics and Chemistry - vol. 153, Edited by F.Kh. Abdulaev, V.V. Konotop, 151-156 (2004)
- [8] D. Grecu, Anca Visinescu - Proc.IWGA-Cankaya, Turkey , *AIP Conf. Proc.* **729**, p. 389 (2004), Editors: K. Tas, D. Baleanu, D. Krupka, O. Krupkova (New York, 2004).

Nuclear & Particle Physics

Romanian contributions to the ATLAS experiment

C. Alexa¹, E. Bădescu¹, V. Boldea¹, I. Caprini¹, M. Caprini¹, S. Constantinescu¹, P. Dită¹, S. Dită¹, L. Micu¹, D. Pantea¹, T. Preda¹, G. Popescu²

¹ IFIN-HH, Bucharest-Magurele

² ITIM-Cluj

The ATLAS experiment of the LHC programme at CERN entered the phase of commissioning and integration, in view of the first data taking in 2007. A group of physicists and engineers from IFIN-HH and ITIM-Cluj is actively involved since 1993 in the design, construction, tests and simulation of the ATLAS detector, as well as in the investigation of several physical processes at LHC. We first make a brief overview of the Romanian contributions and prospects of future work for the hadronic calorimeter with scintillating tiles (TILECAL), the Online Software component of the ATLAS Trigger/DAQ/DCS system and the development of a testbed GRID facility allowing to take part in the ATLAS distributed computing environment based on the LCG software. We present then in more detail recent results on the analysis of the TILECAL response to pions and protons and the investigation of the ATLAS potential for the discovery of heavy charged leptons. We show that the data yielded by the 2002 beam tests with final modules confirm the

different response and performances of the calorimeter to pions and protons. The simulation code GEANT4 is consistent with the experimental results concerning the ratio between the pion and proton response and the linearity and resolution of pions and protons only if the physics library LHEP3.6 is used. This is a very important result in the present phase, when the validation of the physics implemented in GEANT4 is a priority of ATLAS. We finally discuss the production at LHC of exotic charged heavy leptons predicted by various models with an extended gauge sector. Both Drell-Yan and gluon-gluon production processes are considered. We present the ATLAS discovery potential, for the decay channel with lepton and dijets in the final state, as a function of the heavy lepton and Z' masses. We also show that the inclusion of QCD radiative corrections to lepton production by gluon fusion reduces the unphysical dependence of the production rate on the renormalization and factorization scales.

Portal monitor incorporating smart probes

D. Bartoş¹, F. Constantin¹, T. Gută¹

¹ "Horia Hulubei" National Institute of Physics and Nuclear Engineering, Bucharest-Magurele

Purpose intent

Portal monitors are intended for detection of radioactive and special nuclear materials in vehicles, pedestrians, luggage, as well as for prevention of illegal traffic of radioactive sources. Monitors provide audio and visual alarms when radioactive and/or special nuclear materials are detected. They can be recommended to officers of customs, border guard and emergency services, civil defense, fire brigades, police and military departments or nuclear research or energetic facilities. Technical description.

The portal monitor developed by us consists in a portal frame, which sustains five intelligent probes having long plastic scintillator (0.5 liters each). The probes communicate, by serial transmission, with a Central Unit constructed around the 80552 microcontroller.

This one manages the handshake, calculates the background, establishes the measuring time, starts and stops each measurement and makes all the other decisions. Sound signals and an infrared sensor drive the passing through the portal and the measuring procedure.

For each measure act the result is displayed on an LCD device contaminated/uncontaminated; for the contaminated case a loud and long sound signal is also issued. An RS 232 serial interface is provided in order to further developments or custom made devices.

Performances.

As a result, the portal monitor detects 1 μCi ^{137}Cs , spread all over a human body, in a $20\mu\text{R}/\text{h}$ gamma background for a measuring time of 1, 5 or 10 seconds giving a 99% confidence factor.

Spectroscopy of the heaviest nuclei with $N \approx Z$

D. Bucurescu¹

¹ "Horia Hulubei" Institute of Physics and Nuclear Engineering, Bucharest

The results of a program of investigation of the nuclei with $N=Z$ and $N=Z+1$ from the mass region $A \approx 80-100$ with the gamma-ray array GASP (Italian Gamma-ray SPHERE) are presented. Eight such nuclei, between Zr-81 and Ag-95, have been spectroscopically investigated for the first time. The special techniques that allowed the study of such nuclei, which are populated with very small cross sections in the reactions available today, are briefly illustrated. This nuclear region stands out through unique phenomena, such as rapid structure changes (particle alignments, shape changes and shape coexistence)

with both mass number and angular momentum, as well as the possibility to search for the experimental signal of enhanced neutron-proton (np) correlations, especially in the pairing channel (both $T=1$ and $T=0$ modes). Experimental evidence for such phenomena are presented. This nuclear region remains interesting for future studies with new, more efficient gamma-spectroscopy arrays, and radioactive beams. Such detailed studies will address not only the problem of the np pairing, but other interesting topics as well, such as nuclei at critical points, and unusual (tetrahedral) nuclear shapes.

A statistical approach of the distribution of elements in universe

Al. Calboreanu¹

¹ "Horia Hulubei" National Institute of Physics and Nuclear Engineering, Bucharest-Magurele,
calbo@ifin.nipne.ro

Cluster formation is a common feature of a large number of physical phenomena in molecular physics, atomic and nuclear physics, astrophysics, condensed matter and biophysics. Common to all these is the large number of degrees of freedom, thus justifying a statistical approach. The distribution of elements in universe can be regarded as a clustering of nuclear matter in early stages of the present universe formation. This hypothesis is discussed in terms of

Boltzmann-Gibbs equilibrium thermodynamics and in the frame of the non-extensive statistical formalism, recently introduced by Tsallis. The results suggest that the primordial nucleo-synthesis of elements might have produced a larger amount of heavy nuclei than expected from Boltzmann-Gibbs distribution. A non extensivity parameter $q=1.13$ is characteristic to cluster formation in hot nuclear matter.

Perspectives for positron emission tomography with RPCs

F. Constantin¹, C. Nicorescu¹, I. Cruceru¹, I. Manea¹

¹ NIPNE-HH, Applied Nuclear Physics Department

The basis of PET consists on the administration of a radioactive isotope attached to a tracer that permits to reveal its molecular pathways in a human body. A 3-D Complete-Body-Scan is desired in order to minimize the radiation dosage to the patient and to sensitive increase of the axial field of view (FOV). A major candidate for gamma pair detection in 3-D Complete-

Body-Scan are the RPCs (Resistive Plate Counters). They consist in a longitudinal microstrip grid 1.5 mm thick, spaced at 1 mm; the grid is placed between a large electric resistive glass anode and an aluminum cathode; the gap, around 300 μm is filled with a special gas and is polarized at around 6 kV. Every microstrip is equipped with high-speed preamplifier at

both ends, allowing time of flight measurements. The RPC are solely tracking devices enjoying a large density of detection units. By construction they are able to provide an extremely large transverse resolution, the collecting leads being some 2.5 mm spaced. The longitudinal resolution is less sensitive, depending on the speed of the time of flight electronics; at this moment we estimate a 20 mm resolution. The RPCs present two main features: large longitudinal dimension and large transversal resolution which made them ideal for complete-body-scan devices; these peculiar features are the keys of a RPCs tomographic device. The evaluation of RPCs for 3-D Complete-Body-Scan followed two steps: the simulation of data acquisition and the image reconstruction. We choose the detecting base unit like a RPC, 2 meters long and 0.5 meters wide. According to previous assumptions this plate has a transverse resolution of 256 detection units and a longitudinal resolution of 100. (The transversal step is around 2 mm and the longitudinal step about 20 mm). Several base units are assembled to form different detecting structures; two plates form an open detection structure like a sandwich; four and six plates are arranged like a parallelepiped box respectively a hexagonal box. Also, we consider an ideal case of a cylindrical structure, which is technological unrealistic. Inside this detection structure we placed a transverse 256 x 256 pixels bidimensional picture simulating the examined cross section. In a rectangular coordinate axis every pixel of the picture emits a number of positrons proportional to its value (from 0, black, to 255, white); the annihilation gamma pair rays direction (the polar angles theta and phi) is random generated. The two

gamma rays hit the detection structure and the acquisition device records every coincident event. The amount of data is considerable; we select only a few coincident events and built up a matrix for the easiest case: the parallel projection. As we know from the "classical" image reconstruction method, the parallel projection is most lucrative and intuitive. For this reason we selected only the coincident events involving the detector units from a transverse belt; of course the detector unit belt could be taken on various angles with the longitudinal axis of the detector structure. As we already mentioned, the method used in the image reconstruction was the Filtered Backprojection. On the image reconstruction, the FB advantage of speed is added to the advantages of the proposed detection structure (the large number of detector units on the cross section belt, the projection rays number and the number of rotations are the same or multiples thus eliminating the artifacts). The FB algorithm along with the simulation was implemented on a PC type computer, in Visual C/C++ language. In conclusion:

- The four and six plates detecting structures are excellent candidates for 3D Complete-body-Scan.
- The classical algorithm of Filtered Backprojection gives excellent results due to the large number of detector units in the belt.
- Further improvements will focus on multiple human body cross sections reconstruction and 3D internal body view.

Studies on romanian archaeological objects using atomic methods: the cases of Pietroasa hoard and Cucuteni ceramics

B. Constantinescu¹, V. Cojocaru¹, R. Bugoi¹, D.E. Dumitriu¹, D. Grambole², F. Herrmann², D. Seicleman³, M. Popovici³

¹ National Institute for Physics and Nuclear Engineering "Horia Hulubei", Bucharest-Magurele, Romania

² Institute for Ion Beam Physics and Materials Research - Rossendorf, Germany

³ National Museum of Romania's History, Bucharest

The study of trace-elements in archaeological metallic objects can provide important clues about the metal provenance and the involved manufacturing procedures, leading to important conclusions regarding the commercial, cultural and religious exchanges between the antique populations. Ancient metallic materials are usually inhomogeneous on a scale of 20 microns or less: they contain remains of imperfect smelting, segregated phases in alloys, inclusions. Due to their exceptional chemical stability, gold artifacts remain es-

sentially unchanged during weathering and aging processes. Several fragments of ancient gold objects coming from an Eneolithical treasury and from Pietroasa "Closca cu Puii de Aur" ("The Golden Brood Hen with Its Chickens") hoard, unearthed on Romanian territory and two Romanian native gold nuggets samples were analyzed using micro-PIXE technique at the Rossendorf TANDEMTRON microbeam facility. The purpose of the study was to clarify the metal provenance, establishing if the hypothesis of local gold

holds. To reach this goal, trace elements (Cu, Te, Sn, Pb, Hg, As, Zr, Sb) and PGE (Platinum Group Elements) concentrations were determined. The presence of inclusions (micrometeric size areas of composition different from the surroundings) was also checked. We found some Si, Ca, Fe ones on two Eneolithic samples, and a Ta-Cr one on a sample from Pietroasa hoard. The measurements led to conclusions regarding the alluvial origin of the gold for the Eneolithic samples and gave some indications for the possible gold ore sources of Pietroasa treasury - Urals mountains and North-Eastern Turkey, confirming the heterogeneity of this treasury (the two analyzed pieces belonged to different stylistic and compositional groups).

Synchrotron Radiation X-Ray Powder Diffraction was used at MAXLAB synchrotron (Lund, Sweden) to distinguish different clays and mineral pigments of various neolithic pottery-producing centres on Romanian territory. As main results we can mention:

- identification of black pigment composition from Cucuteni (Northern Moldova) and Arius (South-Eastern Transylvania) type pottery (VI - IV Millenia B. Chr.) as various combinations of goethite (αFeOOH), hausmannite ($MnMn_2O_4$) and bixbyite ($Mn, Fe)_2O_3$ - for high-temperatures (more than 600°C) fired pottery (the advanced Cucuteni ceramics types A and B) and psilomelane ($MnO + MnO_2 + H_2O$ in variable proportions) for low temperatures (less than 400°C) fired pottery (the primitive pre-Cucuteni type C) - all

these minerals originary from North Moldova mineral deposits of Iacobeni (neolithic trade routes put in evidence in this way - approx 500 km crossing Carpathian Mountains along Bistritza river);

- no evidence of pyrolusite (MnO_2) and manganite [$MnO(OH)$] - main components of Ukrainian Nikopol manganese deposit (used as black pigment source by contemporary Tripolye Neolithic culture) was found;
- identification of magnetite (iron oxide $Fe_2 + Fe_3 + O_3$) as main component for black pigments of Central Transylvania Petresti culture (4200 - 3500 B. Chr.)
- identification of graphite as black pigment for Oltenia Starcevo-Cris culture - VI - V Millenia B. Chr.-ceramics (probably from Northern Bulgaria graphite deposits);
- identification of organic origin (bones or wood) carbon-based pigments for few Cucuteni sherds from North-Eastern Moldavia;
- identification of white pigment composition as calcite ($CaCO_3$) for Cucuteni culture and as calcium silicates mixed with illite (K, H_2) $Al_2[(H_2O, OH)_2]AlSi_3O_{10}$ for Petresti culture (Transsylvania) and their minerals provenance areas;
- identification of hematite (iron oxide Fe_2O_3) as main component for red pigments for all examined sherds;
- identification of all examined sherds as having local provenance for the clay.

Pre-emission of correlated neutrons in the fusion of ^{11}Li halo nuclei with Si targets

M. Petrascu¹, A. Constantinescu¹, I. Cruceru¹, I. Tanihata², T. Kobayashi², K. Morimoto²

¹ Horia Hulubei-National Institute for physics and Nuclear Engineering ,P.O.Box MG 6,Bucharest, Romania

² RIKEN, Hirosawa, 2-1, Wako, Saitama 351-0198, Japan

The neutron halo nuclei are characterized by very large matter radii, small separation energies, and small internal momenta of valence neutrons. Recently it was predicted [1] that, due to the very large dimension of ^{11}Li , one may expect that in a fusion process on a light target the valence neutrons may not be absorbed together with the ^9Li core, but may be emitted in the early stage of the reaction. Indeed, the experimental investigation of neutron pre-emission in the fusion of ^{11}Li halo nuclei with Si targets [3, 4] have shown that a fair amount of fusions ($40 \pm 12\%$) are preceded by one or two halo neutron pre-emission. Therefor it was decided to perform a new experiment aiming to investigate the neutron pair pre-emission in conditions of much higher statictics, by means of a neutron array detector. This experiment has been performed at

the RIKEN-RIPS facility. The coincidences between adjacent detectors are denoted as "first order coincidences". Coincidences between two detectors separated by one detector are denoted as "second order coincidences" and so on. With a proper trigger one could investigate inclusively the $^{9,11}\text{Li}+\text{Si}$ fusion. The measurement were performed with 13A MeV ^{11}Li and ^9Li beams. The energy range corresponding to the neutron pre-emission process was established between 8 and 15.5 MeV [5]. The criterion for selecting the true coincidences against cross-talk(c.t.) was adopted. Cross-talk is a spurious effect in which the same neutron is registered by two or more detectors. A coincidence between two detectors is rejected whenever the following condition is fulfilled:

$$E1 > E_{min} = \frac{1}{2} \frac{d^2_{min}}{t_2 - t_1}$$

As a result of rejection by d_{min} , a sample of 204 true coincidences, including also the order ones was obtained. The significance of the obtained data was additionally tested through a complete simulation of the array detector performances by using MENATE. We have investigated in this way the c.t. distribution as a function of $t = t_2 - t_1$ for different coincidence (1 to 4) orders. The simulation was performed by firing the central detector 1 by neutrons of given energy and by extracting the cross-talk events corresponding to 2-9 detectors (first order), to 10-25 detectors (second order) and so on. We obtained that $\sigma_{t1}=0.53$ ns, 0.59 ns, 0.63 ns for, respectively, 15 MeV, 11MeV and 8 MeV neutron energy. We consider that at present a challenging task is to try to distinguish between the r_0 predicted by COSMA1 and by COSMA11 models [4]. An answer to this question will be an experiment aiming to determine the intrinsic correlation function by using ^{11}Li and ^{11}Be halo nuclei. The ^{11}Be nucleus will be an ideal uncorrelated background source, since be done by using a ^{12}C instead a Si target. A sharp cutoff estimation [8] has indicated that the n-n correlation peak will be about two times higher in the case of ^{12}C than in the case of the Si target. The experimentaly

observed signature of residual correlation could be of use in the identification of new halo nuclei [9].

References

- [1] M. Petrascu et al., Balkan Phys. Lett. 3(4),214 (1995)
- [2] M. Petrascu et al., Phys. Lett. B 405, 224 (1997)
- [3] M. Petrascu et al., Rom . J. Phys. 44, 83 (1999).
- [4] M. V. Zhukov et al., Phys. Rep. 231, 151 (1993)
- [5] M. Petrascu, Proceedings of International Symposium on Exotic Nuclei, Baikal-Lake, Russia, 2001 (World Scientific, Singapore, 2001), p. 256
- [6] N. Colonna et al., Phys. Rev. Lett. 75, 4190 (1995).
- [7] R. Getti et al., Nucl.Instrum. Methods Phys. Research A 421 , 542 (1999)
- [8] M. Petrascu et al., (unpublished)
- [9] M. Petrascu et al., (unpublished)

The measure techniques and devices for TLA and UTLa on wear/corrosion measurements developed in NIPNE Bucharest

P.M. Racolta¹, L. Crăciun¹, D. Plostinaru¹, D. Voiculescu¹, Em. Cincu¹

¹"Horia Hulubei" National Institute of Physics and Nuclear Engineering, Bucharest-Magurele

Thin Layer Activation (TLA) and Ultra Thin Layer Activation (UTLA) methods are frequently used to follow real time wear, corrosion and/or erosion of different surfaces, engine parts, mechanical constructions, structural material, surface loss of sculptures etc. The principle of these nondestructive techniques involves activation/incorporation of a suitable radionuclide over a certain thickness of the sample part followed by continuous measurement of the radioactivity of the radionuclide during the wear, corrosion and/or erosion process. The material removed

from the surface by wear, corrosion or erosion process should be separated from the remaining bulk activity completely in order to be able to measure the change of the activity. A calibration curve between the thickness of the layer removed and the residual activity is generated before the investigation.

The paper describes the general features of these methods and applications on biomaterials, and presents also the conclusions of the exchanged experience with partners from JRC IHCP Ispra Italy and CNRS-CERI Orleans France.

In - beam study of excited states in ^{69}As

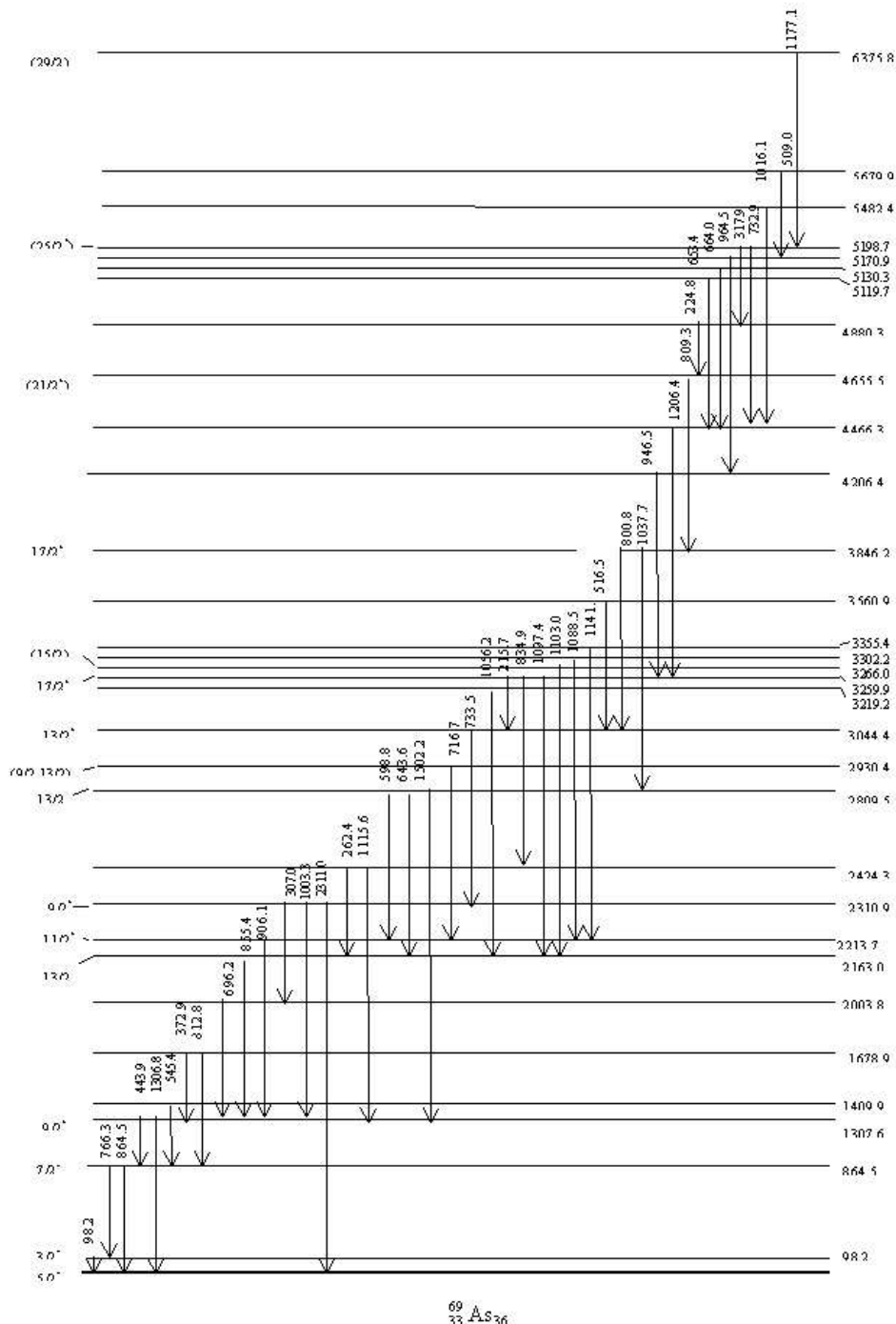
T. Badica¹, I.V. Popescu^{1,2}, A. Olariu¹, V. Cojocaru¹, I. Stefanescu¹, M. Petre¹

¹ IFIN-HH, Department of Nuclear Physics

² Valahia University of Târgoviste

Excited states of the odd nucleus ^{69}As have been studied via the ^{58}Ni ($^1\text{4N}, 2pn$) reaction. On the basis of the neutron - γ and neutron - $\gamma\gamma$ coincidences a new, more complete scheme has been established up

to 6.3 MeV. Gamma angular distribution and linear polarization were used to extract information on spins and parities of the levels of this nucleus.



An integrate system for radioactivity monitoring

Al. Rusu¹, D. Bartoș¹, F. Constantin¹, D. Stanga¹, Gh. Giolu¹, R. Calin¹, T. Gută¹, A. Stochioiu¹, A. Lupu¹

¹"Horia Hulubei" National Institute of Physics and Nuclear Engineering, Bucharest-Magurele

This is one of the projects included in NIPNE's nucleus programme "Nuclear Physics Advanced Researches and Applied Nuclear Techniques".

A new instrument generation for measuring or monitoring the environmental radioactivity is to be developed, based on nowadays components, technology and data processing methods.

The additional results should be:

- the instrument and related procedures to certify the national etalon for neutron dosimetry;

- the operational simplicity and higher confidence in the new portable instruments for radioprotection;
- the instruments and methods for gase's absolute volume activity measuring laboratory;
- a transportable stand to measure the efficiency of the aerosol's filtering systems;
- a PC based technique to reconstruct the radiometric map of an area supervised by an intelligent gamma probe array.

The lecture is a review of the activities to be done.

SIG XX - a generation of intelligent gamma ray probes

Al. Rusu¹, D. Bartoș¹, F. Constantin¹, Gh. Caragheopol¹, I. Cruceru¹, A. Lupu¹, L. Serbina¹

¹"Horia Hulubei" National Institute of Physics and Nuclear Engineering, Bucharest-Magurele

Nowadays, the radioprotection activities are governed by the ALARA principle. To comply with, we have decided to use scintillators, due to their large efficiency.

The surface mounted devices allow the design of the entire gross gamma ray measuring system into a volume of about 0.5 liters. So it is done.

The microcontrollers having an EPROM of 4k bytes offer the opportunity to run resident programmes dedicated to: data acquisition, local processing, data communication, system supervising. Such an intelligence is embeded into SIG XX probes.

By designing an array of such probes, one can easely obtain a portal monitor, an area monitor and so on, each of them under the control of a PC.

A few modifications may transform an intelligent probe into a portable instrument for radioprotection. In such a case, to make the probe shorter, replacing the photomultiplier by a photodiode, is an attractive goal. To reach it, a dedicated charge preamplifier has to be developed.

The works and results on SIG XX probes and charge preamplifier are reported.

The potential of external IBA and LA-ICP-MS for obsidian elemental characterization

R. Bugoi¹, B. Constantinescu¹, C. Neelmeijer², F. Constantin¹

¹National Institute for Physics and Nuclear Engineering, PO BOX MG-6, Bucharest-Magurele, Romania
²Research Center Rossendorf Inc., Institute for Ion Beam Physics and Materials Research, PO BOX 510119, D-01314 Dresden, Germany

The application of Ion Beam Analysis (IBA) to the study of cultural heritage led to the development of the external beam set-up, which allows to analyze artefacts at atmospheric pressure, avoiding sampling or the harmful effects of vacuum irradiation. Combined external Ion Beam Analysis (IBA) measurements, consisting of Proton Induced X-ray Emission, Proton Induced Gamma-ray Emission, Rutherford Back-Scattering (PIXE - PIGE - RBS) have been performed on several obsidian fragments with archaeological significance at the Rossendorf Tandem accelerator using a 3.85 MeV proton beam.

Obsidian raw materials and end-products were valuable commodities in Neolithic period, being traded over appreciable distances during those prehistoric times. Since obsidian is found in a limited number of volcanic districts, it is an ideal material for source and trade routes identification. The very few archaeological obsidian artefacts found in Transylvania are a particularly intriguing case for Romanian historians as there is no obsidian source in the Romanian Carpathian Mountains. In this experiment, an archaeological obsidian sample coming from the Oradea region was analyzed in order to establish its provenance. IBA measurements were also performed on two geological obsidian fragments, one from Tolcsva (the Hungarian Tokay Mountains) and another from Vinicki (the Slovakian Tokay Mountains), previously analyzed by LA-ICP-MS at IRAMAT, Centre de Recherches Ernest Babelon, Orleans, France with a VG Plasma Quad PQXS (an inductively coupled plasma mass spectrometer) and a VG UV Laser (a probe laser ablation sampling device).

The Rossendorf external beam set-up simultaneously detected the PIXE, PIGE, and RBS signals emit-

ted by the proton-bombarded object. The focused proton beam (approx. 1 mm in diameter and 3.85 MeV in energy) was provided by the 5 MV Tandem accelerator of the Rossendorf Research Centre. Proton irradiation was performed using low beam currents (500 pA), and computer-controlled exposures (10 minutes). The set-up comprised two X-ray detectors - one for low X-ray energies (PIXE1) and another for higher X-ray energies (PIXE2), a high efficiency HPGe detector for PIGE and a PIPS detector for RBS. The RBS detector can help determine the presence and possibly the depth profile of the near-surface elements, checking in this way the potential surface abrasion and/or surface contamination, while PIXE and PIGE results can provide an almost complete compositional recipe of the obsidian. The simultaneously measured spectra of X-rays, particles, and gamma-rays were stored and evaluated by special software. The PIXE spectra were analyzed using the GUPIX software package in thick target option, whereas the RBS spectra were simulated by means of a modified version of RUMP code.

A good agreement between the results of LA-ICP-MS and the ones obtained using external PIXE-PIGE when analyzing the geological obsidian samples was obtained. A good correlation ($R^2=0.99$) between the concentrations of all determined elements for the archaeological obsidian found in Oradea region and that from the Slovakian Tokay Mountains, leading in this way to the attribution of the archaeological obsidian to this source. The RBS spectrum for the archaeological sample revealed no Ca or P contamination on the surface, a possible conclusion being that the archaeological obsidian was used as a weapon and not as a cutting tool.

Molecular dynamics in triglycine sulphate by cold neutron spectroscopy

V. Tripăduș¹, J. Pieper², A. Buchsteiner², A. Serban¹

¹ National Institute for Physics and Nuclear Engineering, Bucharest, Romania

² "Hahn-Meitner Institut", Berlin, Germany

The preliminary incoherent neutron scattering on TGS polycrystalline sample were carried out at NEAT BENSC -HMI. The inelastic scattering part of the spectra remains practically unchanged on going through the critical point. The quasielastic peak is described by the sum of the EISF and two Lorentzians with different widths: 0.1meV and 0.61 meV respec-

tively. For a fixed Q the both widths change dramatically on going through T_c . From the analysis of the EISF as a function of momentum transfer Q we concluded that the mobile protons are moving on the surface of two spheres of different radius: 0.16 Å and 3.1 Å respectively.

The study of diffusive motion in bitumen compounds by quasielastic neutron scattering

V. Tripăduș¹, M. Popovici², M. Peticila³, L. Crăciun¹, O. Mureșan¹

¹ National Institute of Physics and Nuclear Engineering, Bucharest

² Missouri University Research Reactor, Columbia MO, USA

³ LCPC, Centre Nantes, France, CESTRIN - Bucharest, Romania

The paper presents the results of quasielastic neutron scattering experiments on two bitumen samples. Using the triple axis spectrometer from Missouri University Research Reactor we have obtained the spectra of quasielastic scattered neutrons at five momentum transfers between 0.5 and 2.3 Å-1, and for five temperature values between 22°C and 140°C. The width

of the resolution function was comprised between 0.018 meV and 0.0196 meV. Applying the most suited diffusion models for such bounded media, we obtained the dimensions of the restricted volume, the diffusion constants as a function of temperature, as well as the residence times introduced by these models.

Spectroscopy around N=20 shell closure: β -n- γ decay studies of ^{33}Mg and ^{35}Al isotopes

C. Timiș^{1,2}, J.C. Angélique², A. Buță¹, N. Achouri², D. Baiborodin⁶, P. Baumann³, C. Borcea¹, S. Courtin³, P. Dessagne³, Z. Dlouhy⁶, J.M. Daugas, S. Grévy², D. Guillemaud-Mueller⁷, A. Knipper³, F.R. Lecolley², J.L. Lecouey², M. Lewitowicz⁴, E. Lienard², S.M. Lukyanov⁵, F.M. Marqués², C. Miehé³, J. Mrazek⁶, F. Negoita¹, N.A. Orr², J. Péter², S. Pietri², Yu.E. Penionzhkevich⁵, E. Poirier³, M. Stănoiu⁴, G. Walter³

¹ National Institute for Physics and Nuclear Engineering, P.O. Box MG-6, Bucharest, Romania

² LPC, ISMRA-Université de Caen, Boulevard Maréchal Juin, 14050 Caen, France

³ IReS, IN2P3-CNRS, Louis Pasteur University, BP 20 F-67037 Strasbourg, France

⁴ GANIL, Boulevard Henri Becquerel, 14021 Caen, France

⁵ FLNR, JINR, Dubna, Russia

⁶ NPI, Rez, Czech Republic

⁷ Institut de Physique Nucléaire, F-91406 Orsay, France

⁸ IKS, KU Leuven, Celestijnenlaan 200D, 3001 Leuven, Belgium

The delayed neutron detector array TONNERRE was used, coupled with high efficiency γ -detectors, for a spectroscopic investigation of some neutron rich Mg and Al isotopes around the shell closure $N = 20$. The delayed neutron and γ spectra, following the β -decay of ^{33}Mg and ^{35}Al have been measured. A detailed analysis of such spectra allowed one to construct for the first time the level schemes of their daughters, $^{32,33}\text{Al}$ and $^{34,35}\text{Si}$.

The experiment was done at GANIL. The neutron-rich ^{33}Mg and ^{35}Al have been produced using the projectile fragmentation of a high energy (78 MeV/nucleon) ^{36}S beam. The ions of interest were selected by the double achromatic LISE3 spectrometer. At the end of LISE3, the beams were focused onto a detector telescope which provided for ion identification, collection and β -detection, located at the centre of the TONNERRE array [1].

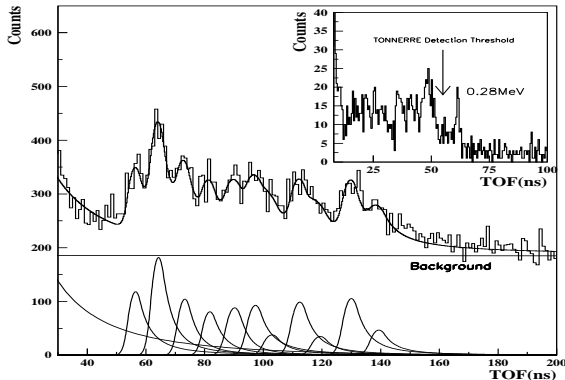


Figure 1: TOF spectrum measured with TONNERRE array, and low threshold counters for β - n neutrons from ^{33}Mg

The TOF spectrum for β -delayed neutrons from ^{33}Mg is shown in Fig. 1 for the TONNERRE array and in inset the TOF spectrum from low threshold neutron counters. In Fig. 2 we show the proposed decay scheme of ^{35}Al nucleus.

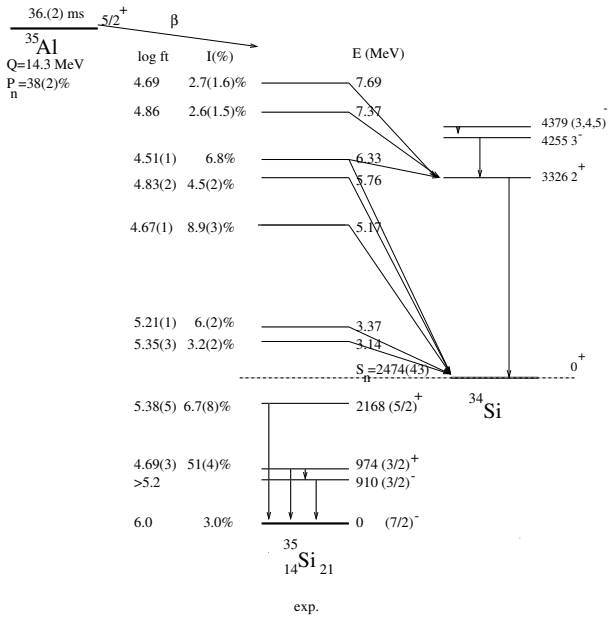


Figure 2: The proposed decay scheme of ^{35}Al

References

- [1] A. Buță *et al.*, Nucl. Instr. Meth. Phys. Res. **A455** (2000) 412

On the physics of high charge state ion production in ECR ion sources

L. Schachter¹, S. Dobrescu¹, K.E. Stiebing², J.D. Meyer²

¹ Institute of Physics and Nuclear Engineering (IFIN-HH), P.O.Box MG-6, Bucharest- Romania

² Institut fr Kernphysik(IKF) der Johann Wolfgang Goethe - Universitt, August Euler Strasse 6, D-60486 Frankfurt/Main, Germany

In a previous research we have demonstrated that metal-dielectric (MD) structures have high capabilities of to enhance the high-charge-state ion production in ECR Ion Sources [1, 2]. In order to explain this effect, dedicated experiments have been performed, in which changes of main plasma parameters in the presence of a MD structure have been observed and an explanation for the mechanism of "MD-effect" was given [3].

In this contribution we present a new experiment [4], where we have concentrated on the question whether the effect of the high-charge-state enhancement by the MD structures is due to the presence of just a dielectric layer in the plasma chamber (e.g. working simply as a breaking of the non ambipolar wall currents) or whether details of the structure of the MD-layer play an essential role. By comparing ion charge state distributions (CSD) and bremsstrahlung spectra for two MD cylinders, of drastically different layer thicknesses, the importance of the MD effect, and hence of the detailed structure of this type of layer for the production of very highly charged ions is demon-

strated.

The effect of the two different MD cylinders on the charge state distributions (CSD) of extracted argon ion is given in fig. 1. It is obvious that both cylinders influence the CSD in a totally different manner. Whereas the thin MD-liner serves to strongly enhance the currents of ions with charge states higher than 9+, the thick MD-liner acted in the opposite way, i.e. enhancing the lower charge states.

The experiments reported here demonstrate the role of the MD physics for obtaining an enhanced high charge state ion production in ECRIS. Following established scaling laws, the observed shift of the mean charge state in this experiment is equivalent to a frequency upgrade of an ECRIS from e.g. 14GHZ to 18GHz. It has also been demonstrated that than the simple fact of restoring ambipolarity by breaking the Simon short circuits cannot explain this effect. Therefore, the method may serve as a standard tool to significantly enhance the performance of ECRIS.

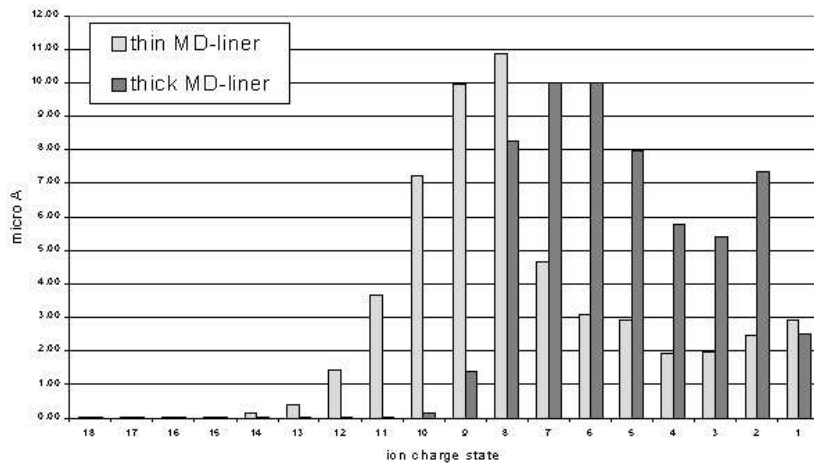


Figure 1:

References

- [1] L.Schachter, K.E.Stiebing, S.Dobrescu, Al.I.Badescu-Singureanu, S.Runkel, O.Hohn, L.Schmidt, A.Schempp, and H.Schmidt-Bocking, Rev. Sci. Instrum. 71, 918(2000)
- [2] L. Schachter, S. Dobrescu, G. Rodrigues, A. G. Drentje, Rev. Sci. Instrum. 73, 570, 2002
- [3] L. Schachter, S. Dobrescu, K.E.Stiebing, Rev. Sci. Instrum. 73, 4172 (2002)
- [4] L. Schachter, S. Dobrescu, K. E. Stiebing, J. D. Meyer, Rev. Sci. Instrum. 75, 2004 (in print)

DIRAC: a high resolution spectrometer for pionium detection

M. Penția¹, DIRAC Collaboration

¹ IFIN-HH, Nuclear Physics Department

Pionium atom is a metastable electromagnetic bound-state system of a π^+ and a π^- , produced by Coulomb interaction of the components and decaying into $\pi^0\pi^0$ ($\simeq 99.6\%$) via strong interaction.

In the last time the width of pionium (ground state) $\Gamma_{2\pi}$ has been calculated by considering the isospin breaking effects using the effective Lagrangian framework, i.e. *Chiral Perturbation Theory* (ChPT) [1, 2, 3].

$$\Gamma_{2\pi^0} = \frac{2}{9}\alpha^3 p_{\pi^0}^* \mathcal{A}^2 (1 + \mathcal{K}) \quad (1)$$

\mathcal{A} is the $\pi^+\pi^- \rightarrow \pi^0\pi^0$ scattering amplitude at threshold, which has been evaluated from relevant Feynman diagrams. In the isospin symmetry limit ($\alpha = 0$ and $m_u = m_d$),

$$\mathcal{A} = a_0^0 - a_0^2 \quad (2)$$

where a_0^0 and a_0^2 are the strong $\pi\pi$ scattering lengths evaluated in QCD in the isospin symmetry limit $e = 0, m_u = m_d$. The quark masses are tuned such that the pion mass in the isospin symmetry world coincides with the charged pion mass $m_\pi = m_{\pi^+}$.

Evaluating \mathcal{K} (exact, without chiral expansion) [3, 4, 5, 6],

$$\mathcal{K} = (1.15 \pm 0.03) \cdot 10^{-2} \quad (3)$$

Using the procedure described above, DIRAC [7] will be in the position to provide from the experimental width $\Gamma_{2\pi^0}$ a value for $|a_0^0 - a_0^2|$.

DIRAC - a double-arm spectrometer (see Fig. 1) has been built and installed at CERN with the pur-

pose of detecting the signal of pionium ($\pi^+\pi^-$) atom breakup produced by 24 GeV/c high intensity proton beam collisions on thin-foil targets.

The spectrometer achieves a resolution of 0.6 MeV/c (0.4 MeV/c) in the longitudinal (transverse) components of the relative momentum of the $\pi^+\pi^-$ pairs in their center-of-mass frame. It is capable to handle a large particle fluence, corresponding to a 1.2×10^{10} primary protons impinging on the target within a 400-500 ms burst.

The main spectrometer components are the tracking detectors (drift chambers and upstream trackers, both with single-detector space resolution better than $90\mu m$), two threshold Cherenkov counters and pre-shower detectors which provide jointly a e/π ratio better than 10^{-4} , and the triggering and time-of-flight hodoscope system, with 110 ps single-counter resolution. The spectrometer has the additional capability to identify very small opening angle pairs by measuring the double-ionisation produced in dedicated hodoscope layers upstream the dipole magnet.

The trigger system achieves selection of pion pairs with relative center-of-mass momentum less than approximately 30 MeV/c, suitable to study the Coulomb region where pionium production takes place as a narrow state. Accidental pairs within a time gate of 40 ns are recorded by the data acquisition system, along with prompt pairs, in order to facilitate Coulomb interaction analysis.

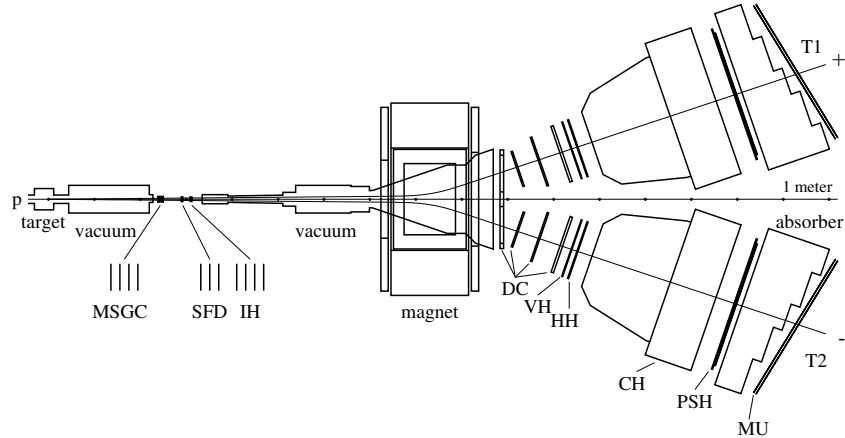


Figure 1: Schematic top view of the DIRAC spectrometer. Moving from the target station towards the magnet there are 4 planes of microstrip gas chambers (GEM/MSGC), 3 planes of scintillating fibre detectors (SFD) and 4 planes of ionisation hodoscope (IH). Downstream the dipole magnet, on each arm of the spectrometer, there are 4 stations of drift chambers (DC), vertical and horizontal scintillation hodoscopes (VH, HH), gas Cherenkov counter (CH), preshower detector (PSH) and, behind the iron absorber, muon detector (MU).

References

- [1] A.Gall, J.Gasser, V.E.Lyubovitskij and A.Rusetsky, Phys.Lett. B462, (1999), 335.
- [2] H.Sazdjian, hep-ph/9911520.
- [3] J.Gasser, V.E.Lyubovitskij, A.Rusetsky, A.Gall, Phys.Rev. D64, (2001), 016008.
- [4] A.Rusetsky, Proc. Chiral Dynamics 2000, Newport News (USA), July 17-20, 2000.
- [5] G.Colangelo, J.Gasser and H.Leutwyler, hep-ph/0007112.
- [6] A.Gasser, V.E.Lyubovitskij and A.G.Rusetsky, hep-ph/9910524.
- [7] B.Adeva et al. - DIRAC Group, Proposal to the SPSLC, *Lifetime measurement of $\pi^+\pi^-$ atoms to test low energy QCD prediction*, CERN/SPSLC 95-1, SPSLC/P 284 (1995)

RBS and ERDA characterisation of PZT ferroelectric layers

D. Pantelică¹, F. Vasiliu², F. Negoita¹, P. Ionescu¹, N. Scintee¹

¹ National Institute for Physics and Nuclear Engineering

² National Institute for Materials Physics

PZT layers ($\text{Pb}(\text{Zr},\text{Ti})\text{O}_3$) have been largely investigated for their ferroelectric properties. This properties offer several advantages for non-volatile memory applications. The PZT layers were deposited on Pt/Ti/SiO₂/Si electrodes [1] using the sol-gel method.

RBS (Rutherford Backscattering Spectrometry) and ERDA (Elastic Recoil Detection Analisys) techniques were used for the characterisation of the PZT layers. The RBS measurements were carried out at the Aramis Van den Graaf Tandem accelerator at CSNSM-Orsay (Fance). The sample surface was perpendicular to the beam and the detector was placed at 165° with respect to the beam. He ions at 3.065 MeV were used. The energy spectrum of the backscattered ions

is shown in fig. 1. The simulation of the energy spectrum plotted on the same graph was conducted using the code RUMP [2]. The energy chosen for the He ions is close to a nuclear resonance energy of helium on oxygen. The resonance peak can be seen at channel 160.

RBS and ERDA measurements were conducted at the Van den Graaf Tandem accelerator of NIPNE using ¹⁰B at 8 MeV for RBS and ²⁸Si beam at 50 MeV for ERDA. For the ERDA measurement a $\Delta E(\text{gas})-\text{E}(\text{Si})$ telescope was placed at 30° with respect to the beam. The total energy spectrum of O is shown in fig. 2. The analysis of the spectra has been performed using our code SURFAN [3] (the simulation is plotted on the

same graph). Oxygen is coming from the PZT layer and from the SiO_2 sublayer. The atomic ratio of the elements in the PZT layer is $\text{Pb}_{0.96}\text{Zr}_{0.33}\text{Ti}_{0.60}\text{O}_3$. These result is in good agreement with the RBS measurements.

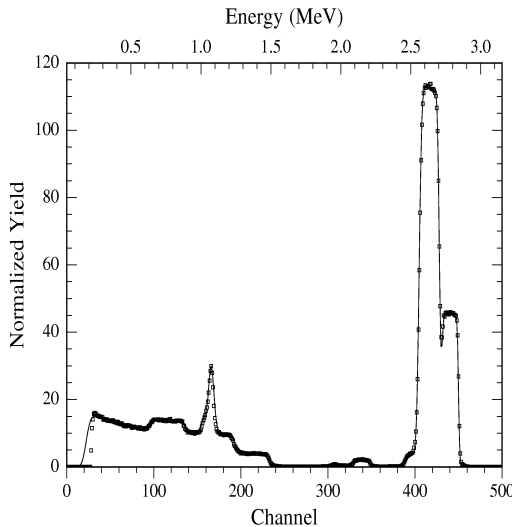


Figure 1: RBS spectrum of PZT layer deposited on Pt/Ti/ SiO_2 /Si. Simulation with RUMP is presented with points.

References

- [1] B. Vilquin, G. Poullain, R. Bouregba, H. Murray, *Thin Solid Films*, 436 (2003), 157-161
- [2] L. R. Doolittle, *Nucl. Instrum. Meth.* B15 (1986)227
- [3] F. Negoita, Cristina Borcan, D. Pantelica, NIPNE Scientific Report 1996, p120

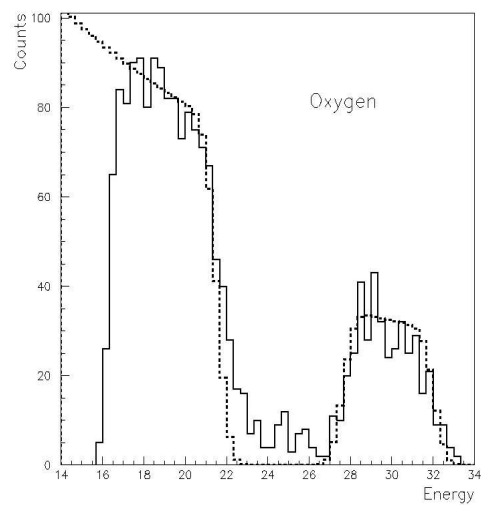


Figure 2: Total energy spectrum of oxygen. Simulation with SURFAN is drawn with dashed line.

Ion-beam characterisation of He implanted into nuclear matrices

D. Pantelică¹, L. Thome², S.E. Enescu², F. Negoită¹, P. Ionescu¹, I. Stefan¹, A. Gentils²

¹ National Institute for Physics and Nuclear Engineering

² Centre de Spectrometrie Nucléaire et SPECTROMETRIE de Masse, 91405 Orsay, France

The behaviour of helium produced by the disintegration of actinides is a very important issue in the management of radioactive waste arising from nuclear reactors [1]. The experimental techniques generally used to determine He profiles, based on standard nuclear reaction analysis [2] are either time consuming or lacking in accuracy. Elastic Recoil Detection Analysis (ERDA) with high energy heavy ions [3] offers the possibility to extract helium profiles in a more simple way. Aluminate spinel (MgAl_2O_4) single crystals were implanted with 30 keV He ions at several fluences providing different He concentrations (2 and 5 at.% re-

spectively). ERDA measurements were carried out at the 8.5 MeV Van de Graaf tandem accelerator of the National Institute for Physics and Nuclear Engineering at Bucharest. A ^{63}Cu beam was used. The detection of the elastically scattered recoil atoms was made by using a ΔE -E telescope consisting of a ΔE pulse ionisation chamber and a residual energy silicon detector placed inside the ionisation chamber. The telescope and samples were fixed at 30° and 15° respectively, with respect to the beam direction. The ΔE -E spectrum of the spinel sample implanted at a fluence of $2 \times 10^{16} \text{ cm}^{-2}$ is presented in fig. 1. The simulation of

the energy spectra for the He recoils was done using the code SURFAN [4] considering a gaussian profile for the He depth distribution. The energy spectrum and the simulation are presented in fig. 2.

References

- [1] Scientific Basis for Nuclear Waste Management XIX, ed. W. M. Murphy and D. A. Knecht, Mater. Res. Soc. Symp. Proc. 412(1996) 15
- [2] Handbook of Modern Ion Beam Materials Analysis, ed. J. R. Tesmer and M. Nastasi, Materials Research Society (1995)
- [3] J. A. Davies, J. S. Forster, S. R. Walker, Nucl. Instrum. Meth. B 136-138, 594(1998)
- [4] D. Pantelica, M. Petrascu, F. Negoita, N. Scintee, H. Petrascu, A. Isbasescu, Report WP8, IDRANAP 10-01(2001)

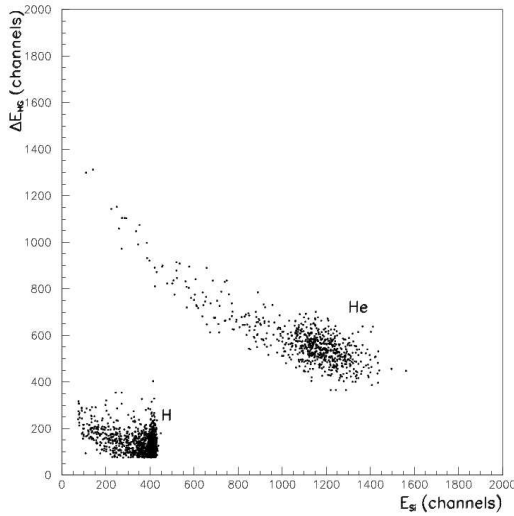


Figure 1: ΔE - E spectrum of the spinel sample implanted at a fluence $2 \times 10^{16} \text{ cm}^{-2}$.

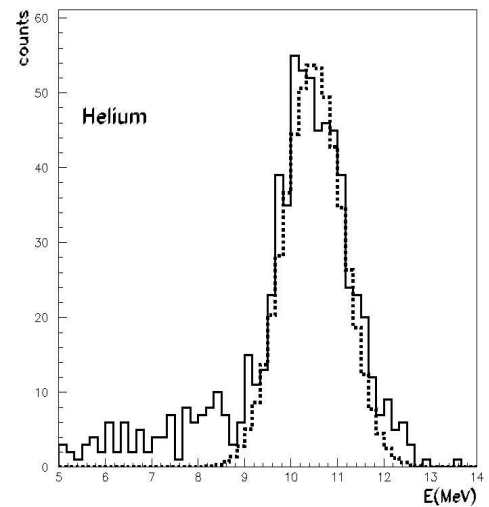


Figure 2: Total energy spectrum of helium implanted in spinel. Simulation with SURFAN is drawn with dashed line.

Preliminary studies of lateral particle density at KASCADE-Grande distances

G. Toma¹, B. Mitrica¹, I.M. Brancus¹, H. Rebel⁴, O. Sima³, A. Haungs², A.F. Badea^{1,2}, J. Oehlschlaeger²

¹ NIPNE-HH, Department of Nuclear Physics

² Forschungszentrum Karlsruhe, Institut für Kernphysik

³ NIPNE-HH, University of Bucharest

⁴ University of Heidelberg, Faculty for Physics and Astronomy

The lateral particle density has been investigated for simulated (using CORSIKA) EAS events at KASCADE-Grande distances (up to 1000m). The lateral density distributions of particles in the shower core has been approximated with a modified Linsley distribution with three parameters(1):

$$\Delta = \frac{N}{R_0^2} C(\alpha, \eta) \left(\frac{R}{R_0} \right)^{-\alpha} \left(1 + \frac{R}{R_0} \right)^{-(\eta-\alpha)} \quad (1)$$

where

$$C = \Gamma(\eta - \alpha) [2\pi\Gamma(2 - \alpha)\Gamma(\eta - 2)]^{-1}$$

and

Δ - the particle density at a distance R from the shower axis

N - the shower size (in our case the total number of electrons and muons)

R_0 - Molliere radius; R_0 has been given a value of 92m

for this study

R - radius and α, η - two parameters

When fitting the lateral density distribution(Fig.1), there appears a dependence of η parameter with mass of the primary particle(Fig.2).

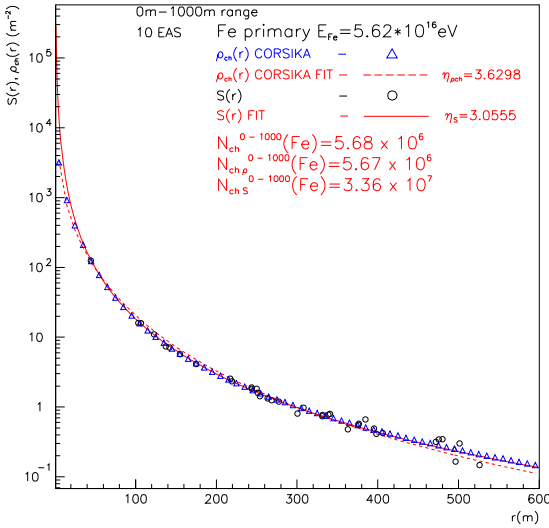


Figure 1: Fig.1: Lateral distribution of particle density and reconstructed lateral density, with fits.

As the study was done for a total of 150 simulated events (all being initiated by three types of primaries p, C, Fe with the same energy $E_0 = 10^{16}$ eV), it proves the possibility of using η in a multiparametric study of the EAS phenomena along with other suitably chosen parameters. In the case of this parametrisation, the α

parameter shows no relevant sensitivity to the mass of the primary.

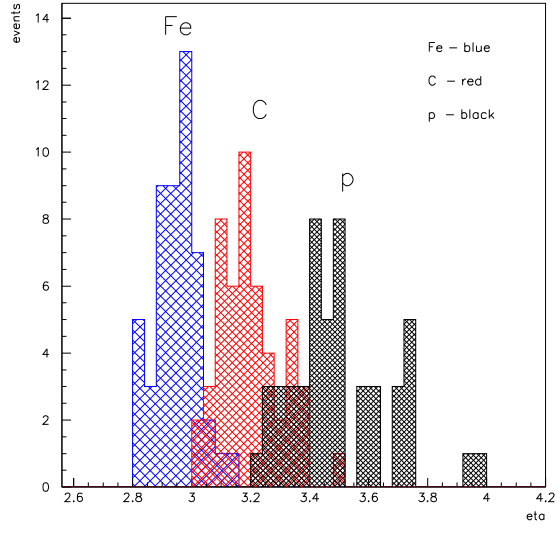


Figure 2: Fig.2: The η fit parameter shows sensitivity to a change in the mass of the primary particle.

References

- [1] J. Linsley, L. Scarsi, B. Rossi, Energy Spectrum and Structure of Large Air Showers, Journal of the Physical Society of Japan, Vol.17, Supplement A-III, 1962

Energy dependence of muon charge ratio for incident momentum range $< 1\text{GeV}/c$

B. Mitrica¹, I.M. Brancus¹, J. Wentz², A. Bercuci¹, M. Petcu³, G. Toma¹, H. Rebel^{2,4}, M. Duma¹, C. Aiftimiei¹

¹ NIPNE-HH, Department of Nuclear Physics

² Forschungszentrum Karlsruhe, Institut für Kernphysik

³ NIPNE-HH, Department of Applied Nuclear Physics

⁴ University of Heidelberg, Faculty for Physics and Astronomy

1 The problem

The charge ratio of the atmospheric muons is a quantity sensitive to hadronic interactions of cosmic rays and to the influence of the geomagnetic field. Experimental information is of current interest for tuning

models used for the calculation of atmospheric neutrino fluxes [1]. We are performing measurements of the charge ratio based on the observation of the lifetime of the muons stopped in the absorber layers (aluminum support) of the detector WILLI, mounted in a rotatable frame and installed in IFIN-HH Bucharest

(vertical geomagnetic cut-off rigidity of 5.6 GV) [2, 3].

2 The results

Our method to determine the muon charge ratio by measuring the lifetime of muons stopped in the matter, overcomes the uncertainties appearing in measurements based on magnetic spectrometers, which are affected by systematic effects at low muon energies, due to problems in the particle and trajectory identification. The results obtained with the rotatable WILLI detector, inclined at 45° [4, 5] (i.e. a mean zenith angle of detected muons of 35°), relevant to the atmospheric neutrino anomaly [6], show a pronounced east-west effect. The energy dependence of the muon charge ratio indicates an increasing asymmetry of the muon charge ratio with decreasing incident energy.

References

- [1] J.Wentz et al, J.Phys. G 27(2001)1699
- [2] B.Vulpescu , Nucl. Instr. Meth. A 414(1998)205
- [3] B.Vulpescu et al, J. Phys. G 27(2001) 977

- [4] B.Mitrica, Diploma thesis (2002)
- [5] Brancus I.M., Report WP17 IDRANAP(2002)18-02
- [6] Futagami T., Phys. Rev. Lett. 82,(1999)5194

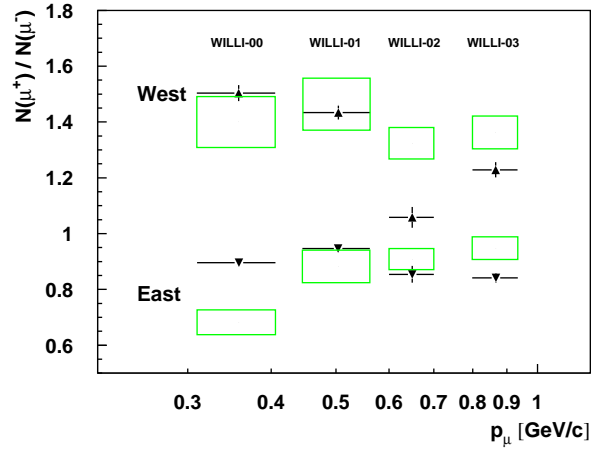


Figure 1: The energy dependence of muon charge ratio measured with WILLI

Fast neutron fluency measurements at the cyclotron facility by the fission track method

A. Danis¹, I. Vata¹, D. Dudu¹

¹ NIPNE-HH,Cyclotron

In order to establish the optimal conditions for neutron fluency measurements, during neutron irradiations, at Cyclotron facility, NIPNE, (IFIN-HH) Bucharest, two methods were utilized: the radioactivation method using ^{58}Ni as radioactive indicator by $^{58}Ni(n,p)^{58}Co$ reaction, and the fission track method using the neutron induced fission of the ^{238}Th and the track registration of its fission fragments in the muscovite-mica track detector. The measurable size, the track density [tracks.cm^{-2}], was studied by optical microscopy using a calibrated Zeiss-Jena binocular microscope. The plastic foil calibrated in ^{238}Th was prepared using a proper homologated procedure. The ^{58}Co gamma activity was measured with a HPGe gamma spectrometer. The ^{58}Co gamma is direct proportional with neutron fluency. Fast neutron fluency measurements ranging from $10^{10} \text{ neutrons.cm}^{-2}$ up to $10^{13} \text{ neutrons.cm}^{-2}$ were performed for different

work conditions of the Cyclotron. The obtained experimental results, using both the fission track method and ^{58}Ni radioactivation method, are given. The advantages and disadvantages of the fission track method and radioactivation method were put into evidence.

For methodological reasons, neutron fluency was measured in different position relatively to Beryllium target. In fig. 1 a typical neutron fluency distribution is presented.

The paper was presented at 22–nd International Conference on Nuclear Tracks in Solids, Barcelona, Spain, 23–27 August 2004.

References

- [1] High neutron fluence measurements using simultaneously mica-muscovite both as track detectors and as material with low Uranium content. Danis

A., Onicescu M. Nucl. Instrum. and Methods. 173, 143-146 (1980)

- [2] Energy spectrum of neutrons produced by deuterons on thick Be target. F. Tancu at all. Rev.Roum. Phys, Tome 28, no:10 p 857-865 (1983)
- [3] Fleischer R. L., Price P.B. and Walker R. M. (1975) Nuclear Tracks in Solids, Univ. California Press, NY.
- [4] Danis A. (2003) Procedure for the preparation of plastic foils calibrated in U and/or Th with the homogeneous distributions of their atoms in the elemental matrix. CS nr.1118/NIPNE-2003 (IFIN-HH, Bucharest), (Romanian language).

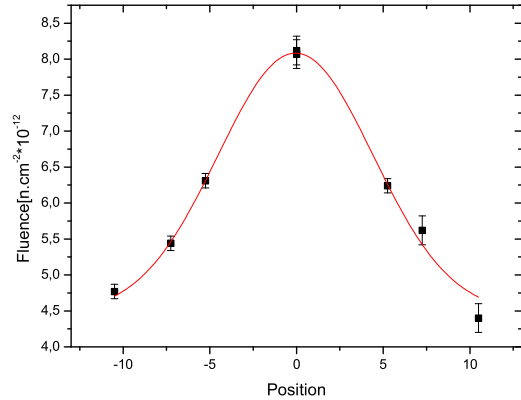


Figure 1: Neutron fluency distribution at 30 cm distance from Be target perpendicular on symmetry axis

RBS characterization of nanometric ZrN/TiN and ZrNC/TiNC multilayers used as reflectors for X-ray water window

D. Dudu¹, D. Plostinaru¹, D. Catana¹, M. Balaceanu², V. Braic², M. Braic², A. Kiss²

¹ NIPNE-HH,Cyclotron

² INCD OPTOELECTRONICA, Magurele

Multilayer nitride coatings, or so called super lattice hard ceramic coatings are well recognized as reflectors for X-ray water windows or as high performance coating structures [1,2]. Typically multilayers have periods (i.e. thickness of two adjacent layers) in the range of 1 to 50nm and the composition of the individual layers and their relative thickness play an important role in their performances. In the frame of a cooperative research project (NIPNE-HH and OPTOELECTRONICA), was started the preparation and characterization of different nanostructured multilayers. In this contribution we present first results obtained. TiN/ZrN and TiCN/ZrCN alternate multilayer coatings, with bilayer periods ranging from 30 to 250 nm, were deposited on Si and steel substrates by the cathodic arc method. The experimental set-up was equipped with two cathodes made of Ti and Zr, the reactive atmosphere consisting of nitrogen or nitrogen and a rich carbon gas. The multilayer structures were obtained by alternatively supplying the two cathodes. The characterization of such structures is performed using Rutherford Backscattering Spectroscopy (RBS), conventional X-ray diffraction (XRD) and glancing angle XRD (GAXRD) techniques which allow nondestructive determination of layer structure and compo-

sition. Rutherford Backscattering Spectroscopy using 2.7 MeV Helium and 9.8 MeV Nitrogen beams has been applied to investigate the elemental composition and bilayer periodicity since the diffraction patterns for such structures is strongly dependent of bilayer period and no data about the composition is provided. The experimental data given by RBS investigation of a five TiN/ZrN bilayers sample with 30nm periodicity as well as simulations performed for depth profiling of elemental composition using SIMNRA program are shown in fig.1 for 2.7 MeV helium beam and fig.2 for 9.8 MeV nitrogen beam..

It is worthwhile to mention that even at the limit of layer discrimination, He beams can be still used for characterization of elemental composition of layers in the range of 10nm, data obtained in this case being corrected using N beams with no more than 10 percent for thickness and 20 percent for composition. Further improvement are possible by using lower energy (3-5 MeV) N or Ne beams for better layer discrimination (in the range of 1-5nm) and combined NRA/RBS analysis using deuteron for better determination of light element (C, N, O) content

References

- [1] Interfacial roughness of multilayered TiN/ZrN coatings. C.J.Tavares and all. Nucl. Instr. & Meth in Physi. Res. B 136 -138 (1998)278

- [2] Multilayer nitride coatings by closed field unbalanced magnetron sputter ion plating. K.E.Cooke and all in Surf. & Coatings Technology 162 (2003) 276-287

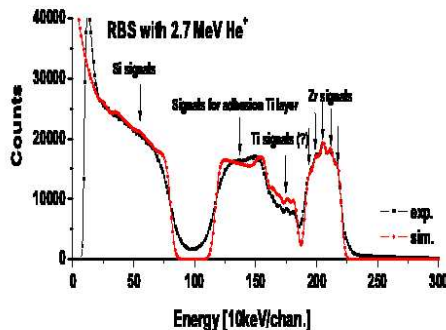


Figure 1: Experimental/simulated RBS data and corresponding depth profiling of elemental composition using 2.7 MeV α particle

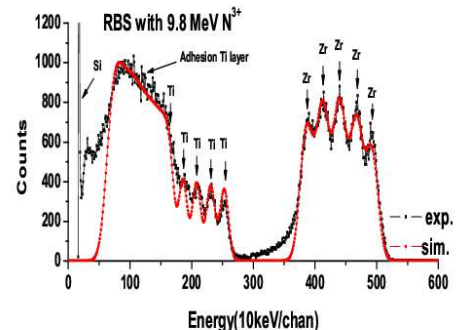


Figure 2: Experimental/simulated RBS data and corresponding depth profiling of elemental composition using 9.8 MeV N^{3+} ions

Combined nuclear reaction (NR) and back scattering (BS) spectroscopy for light elements (C, N, O) analysis with deuterons at the cyclotron accelerator

E.A. Ivanov^{1,2}, I. Vata¹, D. Plostinaru¹, D. Catana¹, D. Dudu¹

¹ NIPNE-HH,Cyclotron

² Center of Advanced Studies in Physics of Romanian Academy

High sensitivity analysis of light elements (C,N,O) by (d,p) and (d, α) exoenergetic nuclear reactions at low bombarding energy (1-2 MeV) of deuterons at the Bucharest Cyclotron have been well documented earlier [1]. Further advances have became possible at our Cyclotron under following circumstances:

1. Oil free vacuum (turbo-pumping) in the reaction chamber reducing substantially the carbon uptake on the probe during the measurement;
2. Precise empirical data are available for (d,p) and (d, α) nuclear reactions cross sections at selected geometries for the particle spectrometer; the measurements have to be done according to

the required geometrical arrangement for consistent data processing in quantitative analysis and depth profiling of light elements;

3. Deuteron elastic scattering on heavy elements has a (known) rather monotonic behavior against bombarding energy and detector angle. Heavy elements are often present either in the bulk of the probe (merely as major component) or below thin layer deposit to be analyzed. By a simultaneous spectroscopic registration of back scattered deuterons and exoenergetic reaction charge particles (p, and/or α) one should be able to measure relative atomic concentrations in-

cluding depth profiles, without any other standard probe. Spectra with selected degrading foils are generally used to remove interferences (different $\Delta E / \Delta x$ for p, d and α);

4. The SIMNRA [2] program has been implemented for data processing.

The elemental concentrations depth profils are obtained by Monte-Carlo simulation method based on nuclear and elastic Rutherford cross sections. In fig. 1 examples are shown to illustrate typical spectra measured for analysis of Re thin layers deposited by evaporation. High sensitivity of the analysis is demonstrated by relatively low concentration of Cu and C (technological contaminants during the Re deposition process).

References

- [1] Simultaneous Microanalysis of Oxygen and Nitrogen on Silicon using NRA with a Cyclotron E. Ivanov, D. Plostinaru, G. Niculescu and A. Ivan Nucl. Instrum. Meth. in Phys. Res. B85 (1994) 293
- [2] M. Mayer, SIMNRA User's Guide, Report IPP 9/113, Max-Planck-Institut für Plasmaphysik, Garching, Germany, 1997

Magnetic interaction of positronium atoms measured by perturbed angular distribution in 3 gamma annihilation decay

E.A. Ivanov^{1,2}, I. Vata¹, D. Plostinaru¹, D. Catana¹, D. Dudu¹

¹ NIPNE-HH,Cyclotron

² Center of Advanced Studies in Physics of Romanian Academy

When long lived Positronium atoms are produced, by polarized positrons (**P**), in a perpendicular magnetic field **B** (**B** \perp **P**), quantum interference beats occur [1,2]. Particularly, the emission of 3γ annihilation quanta initially isotropic (at zero age of Positronium), develops in time an oscillatory anisotropic pattern which can be observed by a Time Differential method commonly used in positron life-time spectroscopy, in muonium spin-rotation (μSR) or nuclear Larmor precession experiment in Perturbed Angular Correlation (PAC) [3]. Quantum beats in positronium 3γ have been predicted theoretically by Baryshevski [1,2] and

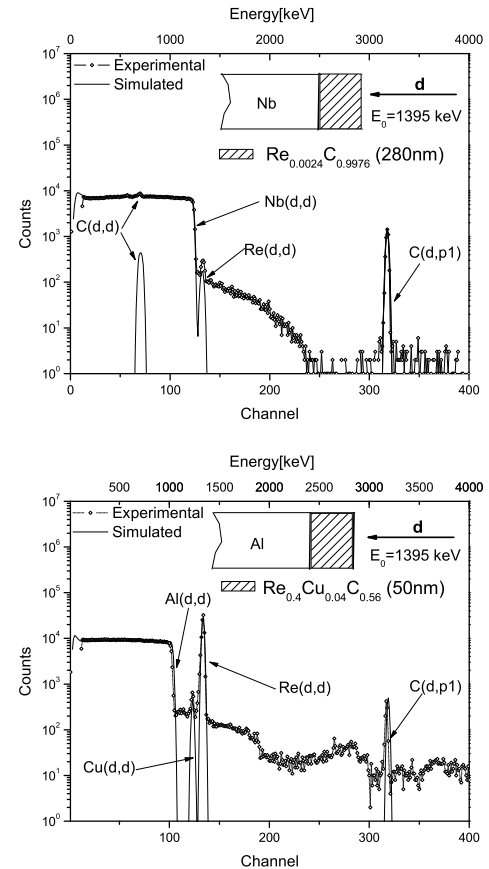


Figure 1: RBS and NRA spectra for Rhenium deposited on Niobium and Aluminium. (Note the log scale of the vertical axis)

demonstrated experimentally in other two laboratories [4,5]. In this contribution we report our experimental results in an attempt to consolidate this new method for further applications of positron spectroscopy. The polarized Postronium atoms were formed in porous SiO_2 powder with positrons emitted from ^{22}Na source ($\simeq 1\mu\text{Ci}$). The source probe geometry as well as the detector geometry are similar to those described in [6].

As seen from figure, in our experiment, "quantum beat" spin oscillations could satisfactorily be observed immediately after the creation of ortho Positronium (5 ns from the prompt annihilation events) against about

50 ns in former experiments [3,4]. The oscillation amplitude remains rather constant at positronium ages as long as 260 ns pointing to relatively long relaxation time ($\tau_{rel} \geq 1000$ ns). This result is in agreement with other methods to investigate positronium thermalization [7].

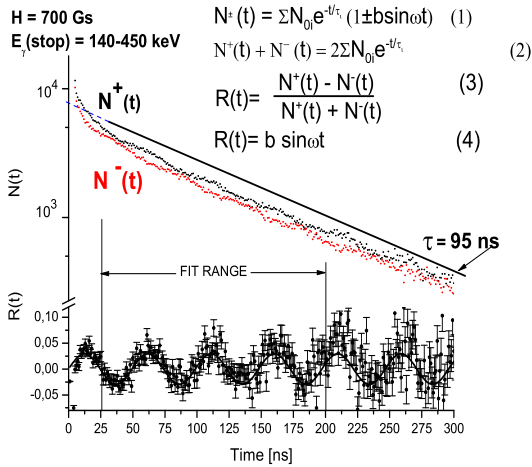


Figure 1: Age dependent perturbed angular distribution (ADPAD) spectra for 3γ decay of Positronium in an external magnetic field. The coincidence count rates $N^+(t)$ and $N^-(t)$ (1), for opposite polarization \mathbf{P} and fixed detector angles are shown in the upper part of the figure. The count rate ratio $R(t)$ (the quantum beats oscillation spectrum) is shown in the lower part of the same figure. Solid lines represent the fit with theoretical functions (2) and (4) presented in the figure.

References

- [1] Positronium Spin Rotation and Time Oscillation of the Normal to the Three-Photon Positronium Decay Plane in Magnetic Field. V.G.Baryshevski, Phys.Stat.Sol.(b), **124**, 619 (1984)
- [2] Oscillations of the positronium decay γ - quantum angular distribution in a magnetic field V.G. Baryshevski, O.N. Metelitsa and V.V. Tikhomirov. J.Phys. B: At.Mol.Opt.Phys. **22** (1989), 2835-2847
- [3] Nuclear Condensed Matter Physics, G. Schatz and A. Weidinger. New York, J.Wiley & Sons (1996)
- [4] Observation of time oscillation in 3γ - Annihilation of positronium in a magnetic field, D.V.G. Baryshevski, O.N. Metelitsa and V.V.Tikhomirov, S.K.Andruchovich, A.V.Berestov, B.A.Martsinkevich and E.A.Rudak, Phys.Lett.A vol 136, nr. 7,8
- [5] Hyperfine splitting in positronium measured through quantum beats in the 3γ decay. Sewan Fan, C.D. Beling, S. Fung, Physics Letters A 216 (1996) 129-136
- [6] Positronium Spin Rotation and Time Oscillations in Positron Life Time Spectrum by A.V. Berestov and all, in Materials Science Forum Vols. 363-365 (2001) pp. 649-65
- [7] Effect of the energy loss process on the annihilation of orthopositronium in silica aerogel, T. Chang, M. Xu and X. Zeng; Phys.Lett. A, vol. 126, nr. 3(1987) (189-194) and the bibliography cited herein.

Microcanonical studies on isoscaling

Ad.R. Raduta¹

¹ NIPNE-HH, Department of Nuclear Physics

A wide variety of nuclear reactions induced by projectiles whose energies range from few MeV/nucleon up to few GeV/nucleon revealed a linear behavior of isotopic yield ratios obtained from the disintegration of two equilibrated identical sources with different isospin values as a function of fragment size. This property has been called isoscaling and using grandcanonical ar-

guments was demonstrated that is possible to extract the asymmetry term of the nuclear equation of state from isoscaling slope parameters [1, 2].

Since the grandcanonical approach is not expected to offer the most reliable statistical description of a small isolated system like a multifragmenting nucleus, the aim of our work is to check to what extent isoscal-

ing is compatible with the more realistic microcanonical treatment and whether the asymmetry term of the equation of state can be extracted from the behavior of isotopic yields.

In order to offer a complete and as accurate as possible image on the subject, isoscaling was studied for a large range of source sizes ($A=40-200$), excitation energies ($E_{ex} = 2 - 15$ MeV/nucleon) and freeze-out volumes ($V = 3V_0 - 10V_0$) in both primary and asymptotic stages of the decay.

The results indicate that despite in all considered cases the logarithm of the isotopic yields corresponding to the two different sources have a linear behavior as a function of Z and N , the slope parameters are strongly dependent on most observables characterizing the state of the sources (see Fig. 1). The only observable not affecting α and β is the freeze-out volume. This result could be of particular importance for experiments aiming to extract the asymmetry term of the binding energy using multifragmentation data, since most probably equilibrated excited systems formed in heavy ion collisions have a distribution of volumes and the event separation as a function of volume is not by far possible. The isoscaling slope parameters are affected also by sequential particle emission.

Deviations from strict isoscaling have been observed for heavy clusters originating from large multifragmenting systems and light clusters emitted by light systems and were interpreted as finite size effects (see Fig. 2) [4]. Such deviations from grandcanonical predictions are expected to manifest especially for small systems and stress the importance of using approximations suitable to the physical situation.

The accuracy of isoscaling parameters is essential for obtaining correct information on fundamental quantities like the asymmetry term of the binding energy.

- [3] Al. H. Raduta and Ad. R. Raduta, Phys. Rev. C **55**, 1344 (1997); *ibid.* Phys. Rev. C **65**, 054610 (2002).

- [4] Ad. R. Raduta, Eur. Phys. J. A **24**, 85 (2005).

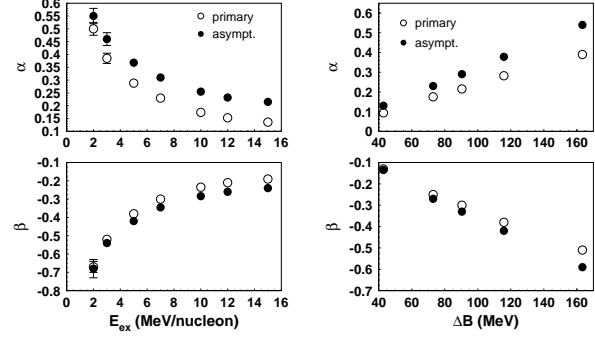


Figure 1: Slope parameters as a function of excitation energy (left panel) and difference of binding energies of the equilibrated sources (right panel) for primary and asymptotic stages of the decay. The considered nuclear systems are (200, 80) and (185, 80). The freeze-out volume is $V = 6V_0$.

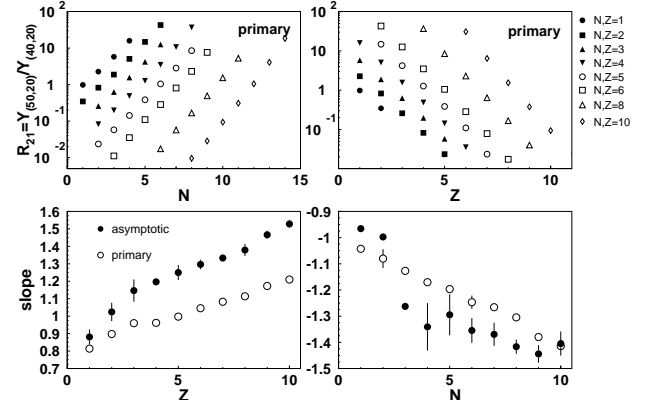


Figure 2: Upper panels: Isotopic yield ratios for the primary decay of (50, 20) and (40, 20) at $E_{ex} = 5$ MeV/nucleon and $V = 6V_0$ as a function of N (left panel) and Z (right panel). Lower panels: Dependence of the slope parameters α and β of the size of the considered emitted cluster.

References

- [1] H. S. Xu *et al.*, Phys. Rev. Lett. **85**, 716 (2000).
[2] M. B. Tsang, W. A. Friedman, C. K. Gelbke, W. G. Lynch, G. Verde and H. S. Xu, Phys. Rev. C **64**, 041603(R) (2001).

Studies of primary energy estimation and mass discrimination of cosmic rays by the EAS lateral charged particle distributions

I.M. Brancus¹, B. Mitrica¹, G. Toma¹, H. Rebel², O. Sima³, A. Haungs², A.F. Badea^{1,2}, A. Bercuci¹, J. Oehlschlaeger²

¹ NIPNE-HH, Department of Nuclear Physics

² Forschungszentrum Karlsruhe, Institut für Kernphysik

³ University of Bucharest, Department of Nuclear Physics

1 CORSIKA simulations

Using the Monte Carlo CORSIKA program a set of simulations of showers with randomly distributed angles of incidence has been performed for H, C and Fe primaries in the energy range $10^{16} - 10^{18}$ eV. The reconstruction procedure [1] is based on simulations of energy deposits per charged particle in Grande detector stations [2] based on the GEANT code. Estimates of shower observables are made by fitting the lateral distribution of charged EAS particles shown in Fig. 1 with analytical functions (LDF). [3]

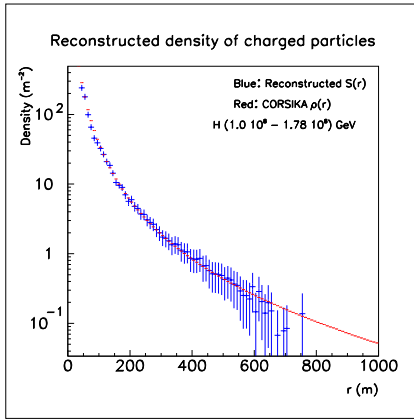


Figure 1: Lateral distribution of charged EAS particles

2 Energy estimation and mass discrimination

The reconstructed charged particle density at 500 m - 600 m, represented by $\langle \lg S_{500/600} \rangle$ or with better statistical accuracy the average $\langle \lg N_{ch400-600} \rangle$ exhibits a linear relation with the $\lg E_0$, which proves to be independent on the primary mass (Fig.2). This suggests these quantities to be an energy estimator. The region at 100 - 200 m exhibits features for mass discrimination especially in correlation with muon component observables. As observed in Fig. 3, the $N_\mu^{40-700} - N_{ch}^{100-200}$ correlation is suggested as a relevant correlation for mass discrimination in KASCADE-Grande observations. The mass discrimination fea-

tures is investigated in more detail by applying non-parametric statistical techniques for analysing multivariate distributions [4].

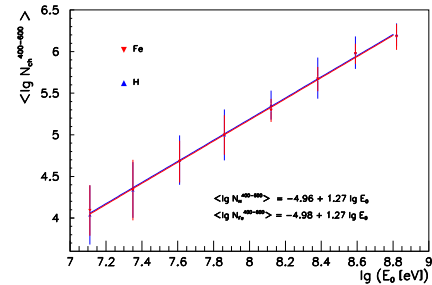


Figure 2: The energy variation of $\langle \lg N_{ch}^{400-600} \rangle$ as reconstructed for KASCADE-Grande (Linsley LDF)

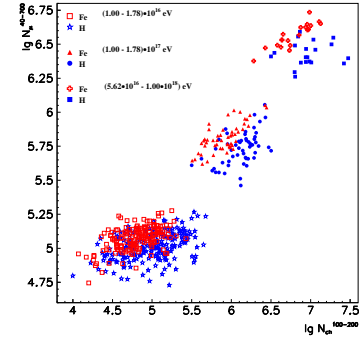


Figure 3: The $\lg N_\mu^{400-700} - \lg N_{ch}^{100-200}$ correlation reconstructed for KASCADE-Grande (Linsley LDF)

References

- [1] O.Sima, I.M.Brancus, H.Rebel and A.Haungs, FZKA-Report 6985, (2004)
- [2] A.Haungs et. al., KASCADE-Grande collaboration, Proc.28 ICRC (Japan) 2 (2003) 985
- [3] J.Linsley et. al., Journ.Phys.Soc.Japan 17 (1962) A-III, A.M.Hillas et. al., Proc.12th ICRC (Hobart, Australia) 3 (1971) 1001
- [4] A.A. Chilingarian, G.Z. Zasian, Nuovo cim. 14 (1991) 355

Wood-Saxon two-center shell model

M. Mirea¹

¹ NIPNE–HH, Experimental Physics Departement

The supersymmetric two-center shell model [1] was used to quantify single particle effects in alfa-, cluster- decays and fission [2, 3, 4, 5]. This model is constructed on the basis of modified harmonic oscillator, and contains different type of corrections. Unfortunately, calculating the potential barrier of transactinide the model predicts a very hight second barrier [5]. Therefore, in order to improve the calculations in the frame of the microscopic-macroscopic model, a new model for single-particle levels is under construction. The nuclear shape parameterization is given by two ellipses smoothly joined with a neck region given by rotating an arc of circle around the axis of symmetry. The Hamiltonian in cylindrical coordinates is given by the next ansatz:

$$H(z, \rho) = H_{as}(z, \rho) + \Delta H_{WS}(z, \rho) + H_{ls} + H_c \quad (1)$$

where $H_{as}(z, \rho)$ is the eigenvector system given by the two-center oscillator potential, $\Delta H_{WS}(z, \rho)$ is Wood-Saxon correction, H_{ls} is the spin-orbit coupling and H_c the Coulomb potential for the proton level scheme.

In the frame of the model, a test is realized in order to determine the potential energy surface for the parent ^{225}U . The potential surface for fixed eccentricities of the fragments in the plane given by elongation and necking is plotted in Fig. 1. Within this new potential barriers in better agreement with experimental ones can be obtained. In the study of Ref. [5] the high of the second barrier was obtained to be about 12 MeV but in the actual model we reach 6 MeV.

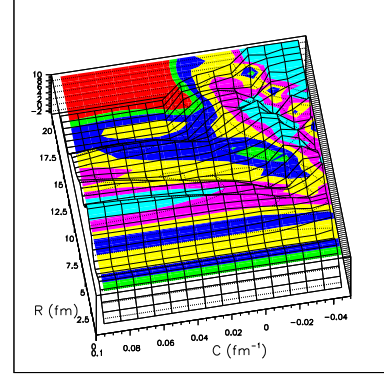


Figure 1: Potential energy surface as function of the elongation R and the necking C . The high of the second barrier is approximately 6 MeV.

References

- [1] M. Mirea, Phys. Rev. C54, 302 (1996).
- [2] M. Mirea, Phys. Rev. C57, 2484 (1998).
- [3] M. Mirea, Europ. Phys. J. A4, 335 (1999).
- [4] M. Mirea, Phys. Rev. C63, 034603 (2001).
- [5] M. Mirea, L. Tassangot, C. Stephan, C.O. Bacri, Nucl.Phys A735, 21 (2004)

Portable intelligent tritium in air monitor

L. Purghel¹, M.R. Călin¹, D. Bartos¹, L. řerbina¹, A. Lupu², F. Lupu², D. Lupu²

¹"Horia Hulubei" National Institute for Physics and Nuclear Engineering, Str. Atomistilor No. 407, 077125 Bucharest, Romania,

²S.C. Tehnoplus S.R.L. Bucharest, Romania

The tritium detection method used for this monitor is original, patented in Romania. The detection unit consists of a single ionization chamber, a special, fast preamplifier and a dedicated software associated to the detection unit, for signals processing. Some results

concerning the tritium in relative strong gamma-ray fields are presented.

Paper presented at 7-th International Conference on Tritium Science and Technology, 12-14 sept. 2004, Baden Baden, Germany;

Health and Environmental Physics

Accreditation of the "ACTIVA-N" and "IRM" laboratories

Em. Cincu¹, R. Macrin¹, S. Brancovici¹, S. Bercea¹, V. Manu¹

¹"Horia Hulubei" National Institute of Physics and Nuclear Engineering, Bucharest-Magurele

The "ACTIVA-N" Laboratory (DFNA) - involved in applications of the gamma-ray spectrometry and INAA techniques, and the Ionising Radiation Metrology (IRM) from IFIN-HH have elaborated and implemented the whole Quality Management System (QMS) required by the national and international standards, based on two projects approved in the frame of the National Programme for Research-Development and Innovation "INFRAS".

At present, the two (analytical and metrological) laboratories are in the final stage of preparation for getting Accreditation, after two steps of assessment Audit performed during this year by the IAEA Expert Dr. Michael Woods - President of the International Committee of Ionising Radiation Metrology and Counsellor (Emeritus NPL Fellow) of the Ionising Radiation from National Physical Laboratory - UK.

The accreditation will be afforded by RENAR - the Accreditation Association acknowledged by the Romanian Government as the National Accreditation Body.

RENAR has been already performed the pre-assessment Audit of the two laboratories, following that, after some modifications to be operated into the QMS documentation requested by the Audit team, the Accreditation Certificates to be approved by the National Accreditation Council.

The accreditation of the "ACTIVA-N" and IRM Laboratories according to the international Standards' requirements available in UE by RENAR - who is a member of the European Association of Accreditation (EA), is a performance, not only for IFIN-HH, but at the national level in the nuclear field; for this reasons, the Ministry of Research and Education awarded the two Laboratories for their results, within the frame of the "CONRO" National Exhibition (september 2003), by a certificate of Excellency - prize III.

The Accreditation Certificates afforded by RENAR will be acknowledged in the whole UE area, thus opening a large area for applications and services, including countries from Central Europe and the third world.

Using WOFOST crop model for data base derivation of tritium and terrestrial food chain modules in RODOS

A. Melintescu¹, D. Galeriu¹, A. Marica²

¹"Horia Hulubei" National Institute for Physics and Nuclear Engineering, P.O.Box MG-6 , Bucharest-Magurele, Romania, e-mail ancameli@ifin.nipne.ro galdan@ifin.nipne.ro

²National Institute for Meteorology and Hydrology, Bucharest

The European Commission Project RODOS is developing a coherent methodology for a Real-time Online Decision Support System for Nuclear Emergency across Europe. Within this system there is a special module to model the transfer of triated water from releases to terrestrial foods. In order to model the transfer of tritiated water from air to various plants, the conversion to organically bound tritium, and the partition to edible parts of the plant, both the mean dynamics of leaf area index and a physiological description of canopy photosynthesis are required. The

WOFOST crop growth model has been selected as a basis for deriving tritium transfer dynamics to plants. Its ability to reproduce site-specific biomass growth of various plants (not only from Europe) is demonstrated in this paper, as well as its compatibility to other photosynthesis models. We have tested that this model can simulate limited fertilisation situations via the adaptation of two important parameters. After adaptation of model parameters to site-specific plant growth data, multi-annual mean dynamics can be obtained using meteorological data for subsequent years.

The derivation of tritium transfer parameters for farm animals on the basis of a metabolic understanding

D. Galeriu¹, A. Melintescu¹, N.A. Beresford³, N.M.J. Crout²

¹ National Institute for Physics and Nuclear Engineering, P.O.B. MG-6, Bucharest-Magurele, Romania

² Centre for Ecology and Hydrology, Merlewood Research Station, Grange-over-Sands, Cumbria, LA11 6JU, UK

³ School of Life and Environmental Science, University of Nottingham, Nottingham, NG7 2RD, UK

In contrast to many radionuclides (which often have no biological function) 3H has a stable analogue which is an elemental component of major nutrients, animal tissues and drinking water. Therefore concepts used to predict the transfer of other radionuclides are not valid for 3H . We present an approach for the derivation of tritium transfer parameters which is based on the metabolism of hydrogen in animals. The derived transfer parameters separately account for transfer, to and from, free (i.e. water) and organically bound tritium. A novel aspect of the approach is that tritium transfer can be predicted to any animal product for which the required metabolic input parameters are available.

Predicted equilibrium transfer coefficients are compared to available independent data. Agreement is good ($R_2=0.97$) with the exception of the transfer from tritiated water to organically bound 3H in ruminants. This may be attributable to characteristics of ruminant digestion.

Tritium transfer coefficients will vary in response to the metabolic status of an animal and the use of a single transfer coefficient from diet to animal product is inappropriate. However, we demonstrate that concentration ratios are less subject to metabolic variation and are a more useful parameter than transfer coefficients.

RODOS, a real-time on-line decision support system for off-site emergency management in Europe. Some applications to Romania

D. Slavnicu¹, D. Galeriu¹, Gh. Mateescu¹, D. Vamanu¹, D. Gheorghiu¹, A. Gheorghiu¹, A. Melintescu¹

¹ IFIN-HH, Department of Applied Physics

A comprehensive decision support system (RODOS) has been developed under the EC aegis with applicability across Europe. The system can support decision on a wide range of potentially useful countermeasures (e.g. sheltering and evacuation of people, issue of iodine tablets, food and feedstock restrictions, relocation, decontamination, restoration, etc.) for mitigating the health, environmental and economic consequences of a nuclear accident. It is applicable to accidental releases to atmosphere and to various aquatic environments.

The RODOS system has 4 levels of information: the operating subsystem (OSY), the analyzing subsystem (ASY), the countermeasure subsystem (CSY) and the evaluating subsystem (ESY).

Based on the experience gained in exercises and during its operational use, the existing version of RODOS (PV5.0) was customized to be applied on Romanian conditions.

The customization of RODOS system to Romanian conditions has been focused on:

- the development of a specialist module for the assessment of consequences in an accidental tritium release from CANDU Cernavoda NPP, FDMH, and its full integration in ASY;
- - the evaluation of accident scenarios in nuclear risk zones like Cernavoda and Bechet - Kozloduy;
- - the assessment of the impact on environment during VVRS IFIN-HH research reactor decommissioning;
- - development of geographic and radioecological databases dedicated to Romanian nuclear risk zones, and a source term database for different accident scenarios.

Some results concerning an accidental release of tritium in an accident scenario at Cernavoda CANDU NPP and an evaluation of doses due to Kr-85 in an accidental release scenario during VVRS research re-

actor decommissioning are presented in Fig.1 and respectively, Fig.2.

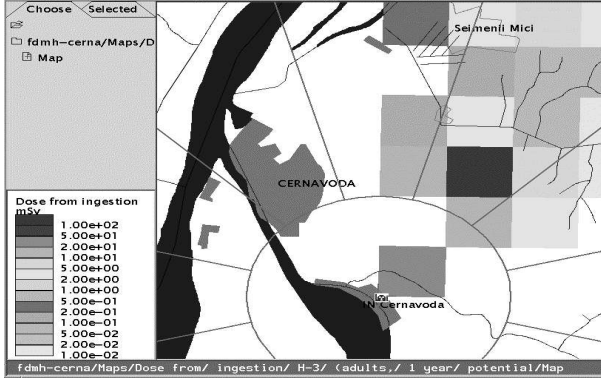


Figure 1: Evaluation of tritium ingestion dose in an accident scenario at CANDU NPP

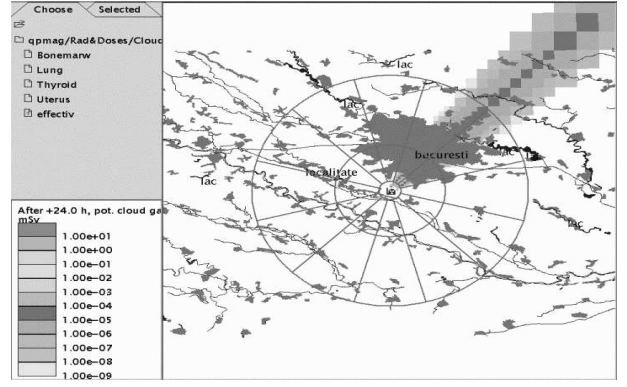


Figure 2: Assessment of dose due to emission of Kr-85. Accident scenario at VVRS reactor

The RODOS system is prepared to reach full practical and operational applicability in national emergency centers.

Aerosol generator

Gh. Giolu¹

¹ "Horia Hulubei" National Institute of Physics and Nuclear Engineering, Bucharest-Magurele

Special equipments are necessary to determine the quality of the filtered air supplied by the air treatment units. The tests are aimed at assessing air quality as well as the quality of the environment thereby achieved.

To determine the correct installation and quality of the air filters, a system consisting of an aerosol generator and a particle detector is used. The filters that are required for such tests are HEPA and ULTRA filters made of special materials and designed for retaining very fine particles ranging from $0.3\text{--}0.5\mu\text{m}$ up to $3\mu\text{m}$. There are several facilities in the structure of our institute that are provided with such filters and operate at airflow rates of $5,000\text{ m}^3/\text{h}$ to $75,000\text{ m}^3/\text{h}$.

The institute has a particle detector that is capable of identifying and measuring aerosols within the range $10^{-4}\text{ }\mu\text{g/l} \div 100\text{ }\mu\text{g/l}$ for particles of $0.3\mu\text{m}$.

Measurements are conducted using the aerosol particle detector and aerosol generator in order to determine the quality of the filters and filtering systems. These measurements are used to determine the leak rate at the filter installation gasket and the filtering efficiency of every filter in the system or to identify leaks at the joints of the system's ventilation and filtering components.

To make a filter-checking system, an aerosol generator is necessary. The device creates a cloud of about 10^8

impurifying particles of submicron dimensions that is injected into the main airflow. Using the particle detector, impurified air samples are collected upstream and downstream from the filtering system and the filtering efficiency value is displayed.

For an accurate determination of the filtering efficiency, one should use aerosols in which submicron particles account for at least 95% of the overall number of particles and the aerosol concentration should range between $20\text{--}60\text{ }\mu\text{g per liter}$ of main airflow. Consequently, the generator must be able to generate particles covering a broad range of aerosol flow rates. In addition, impurifying particles of $0.3\text{ }\mu\text{m} \div 0.5\text{ }\mu\text{m}$ are necessary to carry out the tests. Particles of these dimensions should prevail in the aerosol cloud. A minimum 75% is usually required, but the device works better if particles of $0.3\text{ }\mu\text{m} \div 0.5\text{ }\mu\text{m}$ account for as much as 95%.

In view of these technical requirements, accurate technical solutions and an advanced technology are needed to build the device.

To generate the fine particles required, a compressed-air ejection nozzle is used. The size and size distribution of the particles depend on the dimensions of the nozzle. Experience has shown that nozzles do not alter particle parameters (diameter and number) unless compressed air pressure drops to half its normal value

and/or the fluid level drops due to consumption. The device performance may be flawed if the compressed air has not been filtered. Non-filtered compressed air may clog the nozzle, thereby reducing the aerosol flow rate and changing the dimensions of the particles.

To meet quality assurance requirements, the size distribution of the particles must be determined as a function of compressed air pressure and the deviations that may occur must be identified.

Synthesys of 1, 2-t-testtosterone and 1, 2, 5, 6-t-dihydrotestosterone by selective hydrogenation of testosterone acetate

L. Matei¹, C. Postolache¹, E. Condac²

¹ National Institute of Research and Development for Physics and Nuclear Engineering "Horia Hulubei", Magurele, Bucharest, Romania, e-mail: lidiamatei@personal.ro

² Faculty of Biology, University of Bucharest, Romania, e-mail: adin@bio.bio.unibuc.ro

Labeling of testosterone and dyhydrotestosterone with tritium was necessary for the caring out of radiometric and molecular biology studies concerning androgen dependent diseases.

Testosterone was labeled by selective hydrogenation of 1,2 dihydrotestosterone acetate. forerunner was synthesized in two steps: 1) esterification of testosterone using acetic anhydride, and 2) selective dehydrogenation with 2,6-dichloro-3,5-dicyan-1,4 quinone of the ester formed in the first step. Testosterone acetate was synthesized and purified with yields of 73%, and respectively 80%. The dehydrogenation process was characterized by yields of 82% for synthesis and 33% for purification.

The tritium labeled hormones was obtained in two

steps: 1) selective hydrogenation of Δ^1 - testosterone acetate in the presence of T_2 gas, at low pressure, and 2) hydrolysis of the ester at basic pH. The raw labeled compounds were purified by preparative thin layer chromatography, using the system: silicagel GF 254 activated at 110°C for one hour and chloroforme: acetone (9:1v/v) mixture as eluent.

Radioactive concentration, radiochemical purity, chemical concentration and specific activities of labelled products was determined.

Hydrogenation reaction was also analysed by quanto chemical methods. Were determinated total binding energies of reactants, transitional state and reaction products.

Synthesis and stability studies of acyclovir labelled with tritium

C. Postolache¹, L. Matei¹, N. Vâlceanu², N. Negoita¹

¹ National Institute of Research and Development for Physics and Nuclear Engineering "Horia Hulubei", Magurele, Bucharest, Romania, e-mail: cristianpostolache@yahoo.com

² Health Ministry, National Drug Agency, Bucharest

Acyclovir, $C_8H_{11}N_5O_3$ is a biologically active compound, with antiviral properties. The use of the radioisotopic labelled compound, accompanied by radiometric measurements in biological samples is recommended in pharmacokinetic and pharmacodynamic studies for promoting pharmaceutical products.

The labelled Acyclovir was obtained by isotopic exchange reaction in heterogeneous catalysis, using Acyclovir as substrate and T_2 as labeling agent. Pd/C and $Pd/BaSO_4$ were used as catalyst and the mixtures dioxane-water-acetic acid or dimethylformamide-

phosphate buffer as solvents. Reaction time was 20-25 hours. The raw labelled compound was purified by preparative thin layer chromatography, using the system: silicagel GF 254 activated at 110°C for one hour and n-buthylic alcohol: acetic acid: water (4:1:1v/v).

The labelled compound was conditioned as aqueous solution. Characterization of labelled compound was accomplished by determination of chemical and radioactive concentrations and purities.

Radiolytical processes were evaluated by quanto chem-

ical methods. Were analyzed the primary and secondary radiolytical effects. For energetically minimized molecular structure with charge +1 and multiplicity 1 was evaluated the primary effect by analysis of binding energies and LUMO orbital distribution. Secondary effects were evaluated by analysis of radical $HO\cdot$ attack over neutral molecular structure.

The values of binding energies associated with LUMO orbital distribution indicate a radiolytical fragmenta-

tion especially for guanidic C-N bond.

Secondary effects study was developed by analysis of reactions between acyclovir (in fundamental, excited, ionized states) water and active species from radiolytical act. We analyzed the reaction enthalpies and activation energies.

The results also indicate the radio sensibility of guanidic C-N bond. The experimental results sustain the results obtained from radiolytical simulation.

Elemental analysis of airborne particulate matter, lichen bioaccumulators and total deposition after 12 months of exposure

A. Pantelică¹, V. Cercasov², E. Steinnes³, P. Bode⁴, H.TH. Wolterbeek⁴

¹ NIPNE-HH, Department of Applied Nuclear Physics

² Institute of Physics and Meteorology, University of Hohenheim, Stuttgart, Germany

³ Department of Chemistry, Norwegian University of Science and Technology, Trondheim, Norway

⁴ Interlaboratory Reactor Institute, Delft University of Technology (IRI-TUDelft), The Netherlands

The air pollution in seven locations of Romania (one of them being a reference site) was investigated using transplants of *Evernia prunastri* and *Pseudevernia furfuracea* lichens as trace element bioaccumulators during 12 months exposure [1]. This research represents a completion of a previous study based on 6 months of lichen exposure [2]. The results obtained for bulk deposition collected during 12 months, as well as those for the airborne particulate matter sequentially collected on filters during the second semester of experiment at three locations (2 months collection each, in parallel with the reference site) were also included. As analytical techniques, INAA at IRI TU Delft (The Netherlands) on lichens, filters and bulk deposition, and at IFIN-HH in Bucharest (Romania) for filters (long-lived radionuclides), XRFA at the University of Hohenheim in Stuttgart (Germany) for lichens and filters, as well as ICP-MS at Trondheim University (Norway) for lichens were applied. The investigated elements were: Ag, As, Au, Br, Ca, Cd, Co, Cr, Cu, Fe, K, Mn, Ni, Pb, S, Sb, Se, V, and Zn.

Similar with the case of 6-months exposure, significant enrichments (difference to "zero level") for all the studied elements, except for Br, Ca, K, and Mn, were found in both lichen species after 12-month exposure. Small lichen enrichments were determined for

Mn and Ca, especially at Galati (metallurgical industry) as well as for Br at all locations. Concerning the "enrichment factors" (ratios to "zero level"), both lichen species presented the highest values at Copsa Mica for Pb, Cd, Ag, Zn, Sb, As and Cu. For the suspended matter in air, relative to the background zone Fundata the highest concentration ratios were determined as follows: Ag, As, Cd, Cu, Pb, S, Sb, and Zn at Copsa Mica; Au and Se at Baia Mare; Br at Afumati and Baia Mare; Ca at Galati and Oradea; Co, Fe and K at Galati; Cr and Mn at Deva; Ni and V at Oradea (urban site, most probably due to the oil burning). This research was performed in the frame of the ICA1-CT-2000-70023 Center of Excellence EU Project IDRANAP/ WP2 ("Air pollution monitoring by sampling airborne particulate matter combined with lichen bioaccumulator exposure").

References

- [1] Report WP2 IDRANAP 52-03/2003, <http://idranap.nipne.ro/scientific.html>
- [2] Report WP2 IDRANAP 28-02/2002, <http://idranap.nipne.ro/scientific.html>

Contamination of crop vegetation with trace elements from a fertiliser plant: an INAA study

A. Pantelica¹, C. Oprea², M. Frontasyeva², I.I. Georgescu³, E. Pincovschi³, L. Catana⁴

¹ NIPNE-HH, Department of Applied Nuclear Physics

² Joint Institute for Nuclear Research (JINR), Dubna, Russia

³ University "Politehnica" Bucharest (UPB), Bucharest, Romania

⁴ Institute for Horticultural Products Processing and Marketing "HORTING", Romania

Instrumental Neutron Activation Analysis (INAA) was used to determine various trace elements in crop vegetation (potato, carrot, and maize) grown around a phosphate fertiliser plant in Romania.

INAA using long-lived radionuclides was applied at NIPNE in Bucharest, and based on short-lived radionuclides at JINR in Dubna. The results for Na, Mg, Cl, K, Ca, Mn, Fe, Zn, As, and Hg were compared with Romanian norms for the alimentary products [1,2], as well as with literature data [3-5]. Concentration ratios to control samples for both soil and crop as well as concentration factors of crop to host soil were assessed.

Relative to the control zone, significantly higher concentrations were found for various elements in carrot and potato, and to a lower degree also in maize grown in the vicinity of the fertiliser plant. Both potato and carrot pulp were found to accumulate Sc, Fe, Th, Ce, Cr, Cs, Sb, and Hf, their concentration ratio to control samples ranging between 2.1 (Sb) and 51 (Sc) for the potato and ranging between 1.6 (Hf) and 137 (Sc) for carrot samples. In addition, carrot pulp was found to accumulate Co, As, Sm, Tb, Ta, La, Se, U, Eu, Ca, Ag, Zn, Sr, Br, K, and Na (concentration ratios between 1.4 for Na and 78 for Co).

Fe, Mg, Mn, Ca, Cl, and K concentrations in carrot pulp, as well as Fe and Cl in potato pulp were found to exceed the normal levels [1,4]. As, Zn, and Hg concentrations in potato and carrot pulp were found to

be lower than the maximum allowable levels in Romania (except for As in carrot pulp which was 1.5 times higher)[2]. In the vicinity of the fertiliser plant ratios below unity were determined for Br, Cs, and Rb in all maize samples examined (except for cob from zone 2, which showed near to unity ratios for Cs and Rb).

References

- [1] I. Milcu, Rational Alimentation of the Healthy People (in Romanian), Editura Medicala, 1978.
- [2] Hygienic-sanitary norms for aliments (in Romanian), Ordinul Ministerului Sanatatii No. 975/1998, Monitorul Oficial No. 268 /1999
- [3] L. Catana, Researches concerning the accumulation of the mineral elements in horticultural products, particularly regarding the heavy metals, and modification of their content during the industrial processing (in Romanian), Ph.D. Thesis, 2003
- [4] S.W. Souci, H. Bosch, Die Zusammensetzung der Lebensmittel, Wissenschaftliche Verlags-gesellschaft, Stuttgart, 1972
- [5] A.V. Gorbunov, M.V. Frontasyeva, S.F. Gundorina, T.L. Onischenko, B.B. Maksjuta, Chen Sen Pal, Sci. Total Environ., 122 (1992) 337

Experimental model for radon monitor

M.R. Călin¹, N. Vâlcov¹

¹ "Horia Hulubei" National Institute of Physics and Nuclear Engineering

Measuring atmospheric radon is a highly interesting area of environmental radiation protection. As is well known, radon penetrates the human organism along with atmospheric air through breathing. The element is emitted from the ground due to processes

involved in chain nuclear disintegration and can also be produced by other sources such as building materials, underground stations, coal pits, salt works, quarries, etc. In the circumstances, it is quite important that the volume activity of radon and its progenies

be checked, which accounts for the broad diversity of methods that have been developed for this purpose. One of the most widespread such methods is based on measuring the average ionization current generated by radon circulation through an ionization-chamber detector. This paper presents the development of a lab device for monitoring radon concentration using a radiation detector of ionization chamber type (in 3 different variants). It is a pulsed mode device, in which the measurement of the average value of the ionization current is complemented with, or replaced by, a recording of the ionization current pulses generated

by alpha disintegration within the useful volume of the detector. The ionization chamber thus operates as a 4π counter, in which radon and its progenies are the alpha source. The paper provides a mathematical evaluation of the efficiency of the method and of the measuring device, based on a data acquisition system and a special calculation program, which make it possible to study the time and amplitude distributions of the pulses produced by alpha radiation in the ionization chamber. Early results have indicated the volume activity of radon and its descendants can be measured with a 4% –5% uncertainty margin.

New intelligent monitor for tritium in air measurements - experimental model

L. Purghel¹, M.R. Călin¹, D. Bartoş¹, L. Ţerbina¹, A. Lupu², D. Lupu¹

¹ Horia Hulubei National Institute of Physics and Nuclear Engineering

² Tehnoplus, Bucharest-Magurele, Romania

The statistical discrimination method is an original one, developed and patented in IFIN - HH Bucharest, Măgurele, Romania. In frame of the National Research and Development Program MENER, was financed the research for manufacturing and certifying a portable monitor. The method is based on the dependence of the resulting k - factor on the relative values of the ionization current components in a mixed radiation field. The instrumentation consists of a gas flow-

ing ionization chamber (integrated in a sampling circuit), a preamplifier, a data acquisition system and a microcomputer. A special designed software allows for running the monitor on tritium gas (vapors of tritiated water) and on the associated radiation field (i.e. natural radiation background or gamma-ray field). Some performances of the monitor concerning the tritium in relative strong gamma-ray fields are performed and presented.

The dynamics of tritium - including OBT- in the aquatic food chain

D. Galeriu¹, R. Heling², A. Melintescu¹

¹ NIPNE-HH, Department of Life and Environmental Phisic

Tritiated water spills by nuclear installations result in uptake in aquatic organisms. The radionuclide uptake model BURN (developed by NRG, modified), considers not only tritium as tritiated water (HTO) but also the conversion into organically bound tritium (OBT).

Comparison with the original BURN mode showed that the modified model gave more realistic results in terms of concentration levels, and consequently for dose assessment as result of ingestion of fishery products. For more accurate modelling, seasonal effects and half-life estimates as a function of body weight

and water temperature must be taken into account. A first attempt is given, although limited empirical data gives reason to further investigation of this significant effect.

At present there are no dynamic models which take into account the metabolic regulation of tritium in plants and animals. In the RODOS system for instance, developed in EC-project in the past decade, in biological uptake models such as LAKECO (freshwater) and BURN (marine environment) tritium is treated as other radionuclides. Previously the BURN model was modified in order to cope with the

metabolic regulation of hydrogen and tritium. In this paper the further development considering seasonality and a metabolic model for OBT loss rate in fish is presented.

The importance of considering the specificity of the tritium metabolic pathways was illustrated, by comparing the tritium uptake model with the initial BURN model, in which the behaviour of tritium is not different from other radionuclides. Using tritium model, the total tritium concentration in the organism decreased in proportion to the decrease in the river water, to a level where OBT in fish was predominant and slowly varying. Note the difference in the OBT concentration between a winter and a summer release (temperature effect). BURN predicted the integrated total tritium concentration in fish for the first year more than 200 times higher than the tritium specific model. For an extreme consumption of one kg of fish per day, a predicted dose of 4 Sv would be received in the first year, while BURN gave a value of 150 Sv. This clearly demonstrates both the importance of taking into account the tritium metabolism and the absence of bio-concentration for tritium, in contrast with trace elements. The model was run with appropriate param-

eters for the temperature dependence of the biological loss rate, for a generic lake temperature depending on latitude and generic seasonal availability of food (zooplankton and chironomides) and adapting the growth rate to initial and final fish mass. With a few exceptions, the model results deviated less than a factor of three from the measurements, despite the poor knowledge of site-specific environmental and trophic characteristics. Note that, ignoring seasonality, the model significantly over predicted the measurement in the winter period. In the proposed model (AQUA-TRIT) for the transfer of tritium in the aquatic environment, the metabolic regulation of the process was taken into account. We have demonstrated the ability of the model to cope with various environmental conditions. The approach selected to assess the biological half time in fish needs further experimental validation. From a radiological point of view, the model confirmed that the impact of aquatic release of tritium was not significant in comparison with atmospheric release, if only the tritiated water input is considered. If needed, a further study could include a full sensitivity and uncertainty study, and the incorporation of recent results of fish metabolism and growth.

¹⁴C and tritium dynamics in wild mammals: a metabolic model

D. Galeriu¹, A. Melintescu¹, N.A. Beresford², N.M.J. Crout³, H. Takeda⁴

¹ NIPNE-HH, Department of Life and Environmental Physics

² Radioecology Group, Centre for Ecology and Hydrology Lancaster Environment Centre Library Avenue, Bailrigg, Lancaster, LA1 4AP, U.K.

³ University of Nottingham, School of Life and Environmental Sciences University Park, Nottingham, UK, NG7 2RD

⁴ National Institute of Radiological Sciences, Environmental and Toxicological Sciences Research Group Chiba, Japan

The protection of biota from ionising radiations needs reliable predictions of radionuclide dynamics in wild animals. Data specific for many wild animal - radionuclide combinations is lacking and a number of approaches including allometry have been proposed to address this.

However, for ¹⁴C and ³H, which are integral components of animal tissues and their diets, a different approach is needed. Here we propose a metabolically based model which can be parameterised predominantly on the basis of published metabolic data. We begin with a metabolic definition of the ¹⁴C and OBT loss rate (assumed to be the same) from the whole body and specific organs. The mammalian body is conceptually partitioned into compartments (body water, viscera, adipose, muscle, blood and remainder) and a simple model defined using net maintenance and

growth needs of mammals. The model is tested with data from studies using rats and sheep. It provides a reliable prediction for whole body and muscle activity concentrations without the requirement for any calibration specific to ³H and ¹⁴C. Predictions from the model for representative wild mammals) are presented. Potential developments of a metabolic model for birds and the application of our work to human food chain modelling are also discussed. The key point in our model is the assessment of loss rate from compartments to the blood plasma organic pool.

Based on a published review of cellular energy utilisation and molecular origin of standard metabolic rate in mammals we advanced the working hypothesis that the energy turnover rate can be used as a surrogate for organic carbon/tritium transfer rates from organs in our model. We consider a mammal with daily energy

expenditure (DEE) required as the net energy to sustain basal metabolism, thermo-regulation and activity. To demonstrate model application we selected mammals representative of reference organism suggested for use within some of the proposed environmental impact assessment frameworks. For protection of biota we are interested in the whole body dynamics of radionuclides and integrated retention function values; for food chain modelling dynamics in muscle, as the main edible part of animals, are also useful. The whole body dynamics of 3H and ^{14}C are largely determined by the value of DEE and body composition but muscle dynamics are influenced by energy partitioning between organs. Wild mammals generally have a lower fat content than domestic animals and must adapt to variable environmental conditions. Body mass remains the major factor in describing the radionuclide transfer and small mammals have a fast dynamics. Environmental tem-

perature, taxon and diet must be also considered. We distinguish a fast and a slow component with the long halftime 6-14 times larger than the short one, reflecting the various balances between internal and peripheral organs.

Neither the short half-time nor the effective half-time are determined simply by mass (compare fox and rabbit). This is the result of the effects of taxon and diet. Based on these results allometric relationships have been derived.

When considering biota we must also include birds in the list of reference animals. To be able to expand the model for birds we must first clarify the origin of enhanced basal metabolism of passerines and to test if our SMR estimations can be used for birds. The results presented here are preliminary, if required, the model could be adapted to incorporate birds, seasonal effects and growth.

A versatile model for tritium transfer from atmosphere to plant and soil

A. Melintescu¹, D. Galeriu¹

¹ NIPNE-HH, Department of Life and Environmental Physics

The need to increase the predictive power of risk assessment for large tritium releases implies a process level approach for model development.

Tritium transfer for atmosphere to plant and the conversion in organically bound tritium depend strongly on plant characteristics, season, and meteorological conditions. In order to cope with this large variability and to avoid also, expensive calibration experiments, we developed a model using knowledge of plant physiology, agro meteorology, soil sciences, hydrology, and climatology. The transfer of tritiated water to plant is modeled with resistance approach including sparse canopy.

The canopy resistance is modeled using Jarvis-Calvet approach modified in order to directly use the canopy photosynthesis rate. The crop growth model WOFOST is used for photosynthesis rate both for canopy resistance and formation of organically bound tritium, also. Using this formalism, the tritium transfer parameters are directly linked to known processes and parameters from agricultural sciences. The model predictions for tritium in wheat are closed to a factor two to experimental data without any calibration. The model also is tested for rice and soybean and can be applied for various plants and environmental conditions. For sparse canopy the model uses coupled

equations between soil and plants.

The Aiken List was devised in 1990 to help decide which transport processes should be investigated experimentally as to derive the greatest improvement in performance of environmental tritium assessment models and was revised few years ago [1]. The importance of each process depends on case application.

We tried to improve in this paper the modeling and soil canopy resistance and to have a preliminary study of the application of sparse canopy approach for the transfer of HTO in atmosphere-plant-soil continuum. Adapting Jacobs-Calvet model for stomatal conductance and combining with the WOFOST photosynthesis model and database, we are able to make reliable predictions for the dynamics of HTO and OBT in crops under the atmospheric forces. The new parameterization for soil resistance offers more flexibility in various soil types. The extension of sparse canopy approach to HTO transfer reveals the role of vegetation-soil coupling and it needs further studies, in order to be included in operational codes. In the same time, it can give solutions for condensation dew and wet deposition for tritium transport. The present paper is not exhausting all possibilities of important processes for tritium transport.

Energy metabolism and human dosimetry of tritium

D. Galeriu¹, H. Takeda⁴, A. Melintescu¹, A. Trivedi²

¹ NIPNE-HH, Department of Life and Environmental Physics

² deceased, former at Radiation Protection Bureau, Health Canada, Ottawa

³ National Institute of Radiological Sciences, Environmental and Toxicological Sciences Research Group Chiba, Japan

In the frame of current revision of human dosimetry of ^{14}C and tritium, undertaken by the International Commission of Radiological Protection, we propose a novel approach based on energy metabolism and a simple biokinetic model for the dynamics of dietary intake (organic ^{14}C , tritiated water and Organically Bound Tritium-OBT). The model predicts increased doses for HTO and OBT comparing to ICRP recommendations, supporting recent findings.

The recent proposed model is derived only for adult human and shows increased dose after OBT intake. After a preliminary analysis we recently advanced a new approach for modeling the transfer of ^{14}C and tritium in mammals, at organs level, and successfully tested it with animal data. The model uses available information from animal metabolism, nutrition and physiology and no calibration was attempted. In this contribution we apply the model for the ingestion of dietary tritium and carbon in humans, including the gender and age dependence.

Applying the model with the parameters adapted for each case we first consider the assessment of the dose coefficients after intakes of tritiated water or dietary tritium, considering RBE=1.

There are three interesting observations to be noted. First, for OBT ingestion, our adult male estimate is marginally higher than the central estimate in the uncertainty analyses when considering only the effect of biokinetic parameters. We predict a dose coefficient of $6.33 \times 10^{-11} \text{ SvBq}^{-1}$, while the central estimate is $5.6 \times 10^{-11} \text{ SvBq}^{-1}$. Second, for adult male our integrated activity after a dietary tritium intake is very close, at 6 %, with the Richardson model estimate, while there are distinct model differences. This gives some confidence when claiming higher dose coefficients than classical ICRP recommendation. Last, our results for female confirm past estimate for an increased committed dose coefficient.

The model presented here based on energy metabolism and tested previously on animals gives close results to a more complex and conceptually different one when applied on male adult. Despite some simplification, the present model offers flexibility in application at various age and gender and can be upgraded to help interpretation of bioassay data. As was pointed before the biokinetic parameters have an important contribution to the increased dose coefficients and our results give more confidence in selecting realistic values.

Combined cytotoxic effects of ionizing radiation and magnetic field in yeasts and human lymphocytes

I. Petcu¹, M.A. Acasandrei¹, D. Savu¹, M. Radu¹, I. Prutu², T. Vassu-Dimov²

¹ IFIN-HH , "Horia Hulubei" Institute for Physics and Nuclear Engineering, Str. Atomistilor no.407, P.O.BOX MG-6, Bucharest - Magurele, RO - 077125, Romania

² Faculty of Biology, University of Bucharest, Alleea Portocalilor 1-3, sector 6, 7206, Romania

Introduction. The aim of this study was to give evidence about in vitro non-cumulative effects induced in low eukaryotic and mammalian cells by pre-exposure to low frequency (50 Hz) and low amplitude (100-300 μT) magnetic fields, upon subsequent irradiation with doses known to produce high cytotoxic effects [1, 2].

Materials and Methods. Two types of cells characterized by different radiosensitivity were investigated: i) yeast cells (*Saccharomyces cerevisiae* X310 D), the

parameter measured by cell survival test was the cell viability normalized by the viability in the control, and ii) human peripheral blood lymphocytes: PHA-stimulated whole-blood lymphocyte cultures and unstimulated (G_0) separated lymphocyte cultures. As a radiotoxicity parameter for lymphocytes the micronuclei (MN) induction was used: a) MN index, YMN = number of MN / per 1000 binucleated cells; b) cytokinesis block proliferation index (CBPI):

$$\text{CBPI} = \frac{[\text{binucleated cells}] + 2 \times [\text{multinucleated cells}]}{[\text{total cells}]}$$

The apoptosis degree of unstimulated (G_0) separated lymphocytes was observed by monitoring nuclear morphological changes under double staining with acridine orange and ethyldium homodimer.

Results and Discussion. It has been observed that a 50 Hz magnetic field of $100\mu T$ stimulates the radioresistance of *S.cerevisiae* culture upon subsequent irradiation with a dose of 2.4 kGy (1.2 kGy/h dose rate). On the contrary, when *S.cerevisiae* cultures were exposed to 200 and $300\mu T$, under the same conditions, they show an apparent radiosensitivity. In the case of human lymphocytes cultures, the combined exposures show the induction of an adaptative type reaction to G_2 irradiation subsequent to short pre-exposures (1h) at $100\text{-}300\mu T$. The effect is better expressed by the proliferation index than by the MN level. The apoptosis degree of lymphocytes after 2 Gy gamma irradiation in G_0 is lower when the cultures were pre-exposed

at $100\mu T$ magnetic field. Pre-exposure to higher inductions, i.e. $300\mu T$, will no longer protect the cells against gamma irradiation apoptosis induction.

Conclusions. The results obtained in this work assert for an epigenetical biological response of the cells, rather than the DNA self-repairing capacity of the cell.

Acknowledgements. This work has been supported under CERES 70/15.10.2001 project.

References

- [1] 1. Boreham, D. R. and Mitchel, R. E. J., 1991, DNA lesions that signal the induction of radioresistance and DNA repair in yeast, *Radiation Research*, 128, 19-28.
- [2] 2. Cregan, S. P., Brown, D. L. and Mitchel, R. E. J., 1999, Apoptosis and the adaptive response in human lymphocytes, *International Journal of Radiation Biology*, 75, 1087-1094.

FRET and the detection of membrane rafts

M.A. Acasandrei¹, V.R.E. Dale², M.J. vande Ven³, M. Ameloot³

¹ IFIN-HH , "Horia Hulubei" Institute for Physics and Nuclear Engineering, Str. Atomistilor no.407, P.O.BOX MG-6, Bucharest - Magurele, RO - 077125, Romania

² Randall Division for Cell and Molecular Biophysics, King's College London, London SE1 1UL, United Kingdom

³ Department of Cell Physiology of the Biomedical Research Institute, Limburgs Universitair Centrum, Diepenbeek B 3590, Belgium

Introduction. In this work we consider *Förster* resonance energy transfer between donor-labeled and acceptor-labeled proteins distributed within the planar surface of the cell membrane. Considering these proteins as raft components, we have developed FRET models for rafts that may be applied to a putative raft situation.

Results and Discussion. A geometric model for the distribution of label with respect to the plane of confinement of separately donor- and acceptor randomly surface-labeled spherical proteins is developed and expressed in numerical integral form, the proteins being considered both located in confinement areas of dimensions very much larger than R_0 (the characteristic *Förster* separation), and concentrated in circular discs of dimensions commensurate with R_0 (as a model for putative rafts). Raft constituents probed are modeled as being preferentially, but not fully, incorporated into raft areas for two different physical mechanisms of control of raft formation: i) the fraction of membrane f_R occupied by rafts is constant, and the proteins of

interest distribute into them with partition coefficient K_p , and ii) f_R depends on expression of the protein of interest. Transfer from donors both within and outwith the rafts to acceptors both within and outwith, respectively, are taken into account. These models are compared with the predictions of the simplest aggregation model, that for dimer formation of the probed proteins. Analogously to the raft models delineated above, transfer not only within hetero-dimers (one monomer D-labeled, the other A-labeled), but also from monomer donors as well as those appearing in both hetero- and homo-dimers, to all acceptors, are included. It is shown that, provided a great enough overall cell surface concentration range of bound acceptor-label is available, these three models are well distinguished by measurements of energy transfer efficiency, and that the overall acceptor concentration scale, proportional to the intensity of directly-excited acceptor or donor-alone, is then self-calibrating. Limitations on the estimation of raft dimensions are shown to arise in the lack of ability of either model to distinguish

experimentally between larger rafts containing lower concentrations of the probed proteins and smaller ones with higher concentrations. This issue is further complicated for small rafts by the appreciable extent of transfer from donors within them to acceptors outside as well as within. The results of analyses, according to each of these models, of a set of data from the literature [1], kindly made available in original form by the authors, are presented. The experimental transfer efficiencies, based on intensity measurements, appear to be evidencing a saturation plateau at relatively low efficiencies, compatible with all three models, each of which describes the measurements equally well within their noise limitations. However, they do so only on the basis of significantly different overall concentration scales.

Conclusions. The analysis carried out for these models indicate that an accurate calibration procedure for overall concentration as a function of measured inten-

sity would suffice to distinguish between, or eliminate, them.

Acknowledgements. This work was supported by the project BILOO/40 in the frame of Bilateral (international) scientific and technological cooperation between the Flemish Community and Romania. The authors gratefully acknowledge the kind provision by Professors Anne Kenworthy & Michael Edidin of their data [1] in original form to enable the analyses presented, and thank Professor Enrico Gratton for his modification of the GLOBALS analysis program (Globals Unlimited) to accommodate the particular nature of these analyses.

References

- [1] 1. A. K. Kenworthy, and M. Edidin (1998), *J. Cell Biol.*, 142, 69-84.

Validation of the testing protocol in microbiological examination of pharmaceutical products

M. Ene¹, M. Buzoianu¹

¹ NIPNE-HH, IRASM Center

Because of recent tendency of lining up to European regulations, the pharmacovigilance field in Romania gains more and more consideration, as much for drug manufacturers as for control authority.

For a laboratory that activates in microbiological control of pharmaceuticals, the preparatory stage of routine tests becomes an essential factor that influences the quality of the final results. When a new product is to be tested, the testing protocol must be first of all correctly designed and than confirmed as not just a right step, but as the optimum selection of the testing method. In fact, this preparatory part become a research stage, leading to the validation of a well defined testing protocol.

The present paper discusses certain issues – some

of them with no practical solution yet – to consider in the validation plan: the necessity/obligation of doing a validation experiment, main problems concerning suitability of the testing method, culture media, other chemical or mechanical treatments for contaminants „extraction” or recovery, optimum incubation time and temperature etc.

References

- [1] *Romanian Pharmacopeia*, X-th edition (chapt: *Microbial contamination*)
- [2] *European Pharmacopeia*, 4-th edition (chapt 2.6.12, *Microbiological examination of non-sterile products*)
- [3] *British Pharmacopeia*, 1998, appendix XIV (*Tests for microbial contamination*)
- [4] SR EN ISO 11737

Assays for production of an AMF and nitrogen fixing bacterias based biofertiliser

M. Ene¹, M. Buzoianu¹

¹ NIPNE-HH, IRASM Center

Growing media and soil improvers for plants are subjected to very strict regulation concerning safety of users, environment and plants. Following the European standard CR 13455:1999, we identified the necessity of any substrate, used either for plant multiplication, either as base for final preparation, to comply with absence of any animal or plant pathogens. In this paper we report a step in a more complex strategy for obtaining a soil improver based on Arbuscular Mycorrhizal Fungi (AMF) and nitrogen fixing bacteria.

Two substrates - perlite and peat (mixed or taken alone) - were chosen as first candidate for AMF host-

plant cultivation and/or as base material for the biofertiliser, based on criterias like: reproductibility, accessibility and nutritivity. These substrates were taken as models for perfecting the gamma irradiation technology, using a Co⁶⁰ irradiation plant and a specification for that process was produced. Microbiological effects of the treatment, applied on both substrates, were confirmed by microbial contamination tests, made before and after the gamma irradiation treatment, at 5, 10 and 15 kGy for perlite and 25 and 50 kGy for peat. Results show the necessity for a low dose in case of perlite and a high dose in case of peat.

Customisation of aquatic decision support systems to Danube river

S.D. Slavnicu¹, D. Gheorghiu¹

¹ NIPNE-HH, Department of Life and Environmental Physics

The aim of EVANET-HYDRA project, in the EC FP5 was the model comparison and customisation of some hydrological models like: RODOS-HDM, MOIRA and AQUASCOPE. IFIN-HH, as a part of contract, customised these models to Danube river, focused on Cernavoda site and downstream. The following steps have been followed: - The loading and the running of the systems on default version - The collection of necessary hydrological data to develop a specific database for RIVTOX (a part of RODOS - HDM) and MOIRA - The tests of programs based on accident scenario specific to CANDU NPP - The comparison of the results and the recommendations for the best use of each system - The encountered problems during the running of the systems and the notification to the developers. The case study : - Source after accidental release : Early Core Disassembly with Hydrogen Burn scenario in RODOS - ADM (Prognosis Mode) - Meteorological conditions: wind speed 1m/s, stability class-D, two cases: rain and no rain (10 mm/h) - Deposition after no rain case was used as RIVTOX input. For comparison tests, the rain case was used for all three models. For rain-case, tests have been performed with Cs-137 and Sr-90. The results of radionuclide concentration versus time in one point of Danube near to NPP show a similar concentration at the be-

ginning of contamination (0.3 d), 7.79 E+03 Bq/l - RODOS, 1.55 E+04 Bq/l - AQUASCOPE and 1.18 E+03 Bq/l - MOIRA. After a period of time (10 d) the concentration decreases drastically in RODOS - 0.36 Bq/l, rather slowly in AQUASCOPE - 9.27 E+03 Bq/l and twice in MOIRA - 5.83 E+02 Bq/l. Differences from this benchmark are obvious and the reasons are: - RIVTOX values decrease rapidly compared with MOIRA and AQUASCOPE results due to the fact that in the river model of MOIRA/AQUASCOPE runoff transport is included. - RIVTOX output ends at 10 days. Reason is that the domain from the other models: where MOIRA's model is a middle and long term river model using 20 compartments and AQUASCOPE is a long term river model using one compartment, RIVTOX is a short-term model based on the solution of 1D dispersion-advection equation. For a better comparison of the models is recommended to use RETRACE-RIVTOX (RODOS) modules taking into account the catchment area. Another general remark is the use of different database and GIS format and translated this to the RODOS and MOIRA format e.g. AutoCAD and Shape files to MOIRA format, as well as Dbase, ODB, Access format to ASCII for RIVTOX.

Chromosomal radiosensitivity in secondary-progressive multiple sclerosis patients

I. Petcu¹, D. Savu¹, A. Vral², H. Thierens², L. De Ridder²

¹ National Institute for Physics and Nuclear Engineering IFIN-HH, Bucharest, Romania

² University of Gent, Belgium

In the present work we investigate chromosomal radiosensitivity of secondary progressive (SP) phase multiple sclerosis (MS) in comparison to a group of healthy individuals. Chromosomal radiosensitivity was assessed in vitro with the G2 assay and the G0-micronucleus (MN) assay. For the G2 assay PHA stimulated blood cultures were irradiated with a dose of 0.4 Gy $^{60}Co \gamma$ rays in the G2 phase of the cell cycle. For the MN assay unstimulated blood cultures were exposed to 3.5 Gy $^{60}Co \gamma$ rays delivered at a high dose - rate (HDR = 1 Gy / min) or low dose-rate (LDR = 4 mGy / min). This study shows that concerning the spontaneous formation of chromatid breaks there is no difference between MS patients and healthy individuals. On the contrary, the mean spontaneous micronucleus yield is higher in MS patients compared to healthy individuals. This observation was further sustained by the finding of an increased frequency of cells with multiple-micronuclei in MS patients. In our study the most prominent results were obtained with the LDR MN assay. The mean MN value as well as the frequency of multi-micronucleated cells was significantly lower in MS patients, pointing to an increased

radioresistance in MS patients compared to healthy controls. This increased radioresistance could not be demonstrated with HDR MN assay or with the G2 assay. With the HDR MN assay no difference was observed between MS patients and healthy controls. With the G2 assay a higher mean radiation induced G2-index of 1.21 was obtained in MS compared to healthy control group (1.09) but this difference is not statistically significant ($p=0.11$). The distribution of individuals responses concerning the G2 index is also rather similar in the group of SPMS and the healthy controls. The radioresistance observed at LDR irradiation in the lymphocytes of SPMS patients may be due to an adaptive like response induced by the in vivo protracted oxidative stress exposure of lymphocytes associated with the AP stage of the disease. The modulation of radiosensitivity could also be due to abnormalities in cytokine signaling characterizing the MS pathology.

Acknowledgement. This work was supported by the project BILOO/40 in the frame of Bilateral (international) scientific and technological cooperation between the Flemish Community and Romania.

Experimental model for the study of effect of ionizing radiations on membrane proteins using a fluorescence method

M. Nae¹, D. Gazdaru¹, A. Acasandrei², M. Radu³

¹ University of Bucharest, Faculty of Physics, Department of Biophysics, Bucharest, Romania

² Horia Hulubei National Institute of Physics and Nuclear Engineering, Department of Health and Environmental Physics, PO Box MG-6, Bucharest-Magurele, 077125, Romania

³ corresponding author, address: Horia Hulubei National Institute of Physics and Nuclear Engineering, Department of Health and Environmental Physics, PO Box MG-6, Bucharest-Magurele, 077125, Romania, Fax: 004 021 4574432, E-mail: mradu@ifn.nipne.ro

Results related to the effects of ionizing radiations (gamma rays) on the structure of a membrane model (liposomes doped with gramicidin A) are reported. The liposomes were qualitatively characterized by turbidimetric measurements. The presence of gramicidin A molecule in the lipid bilayer of liposomes was analyzed by means of UV and fluorescence spectrometry (excitation: 270 nm, emission: 350 nm). The ex-

ponential decrease of the tryptophan emission intensity in respect to increasing doses of irradiation (0-250 Gy) proves the partially damaging of the tryptophan residues from the peptide. There is still a residual fluorescence of 38% suggesting that not all the tryptophan residues are accessible to the radiation damage. The effect has a decay constant of 80 Gy. Removing of the molecular oxygen or adding of ethanol prevent at least

partially, the decay of tryptophan fluorescence emission, proving the important role of the indirect action of the radiation (water radiolysis). The ethanol effect is depending of the concentration, 10% of ethanol increasing the residual fluorescence up to 90%. The exposure of liposomes to a given dose (50 Gy) produced by different dose-rate (0 -10 Gy/min) induced a decrease of the effect with the increase of the dose-

rate (inverse effect of dose-rate). This result sustains more the hypothesis according to the lipid peroxidation process (where the inverse dose-rate effect occurs) in mainly involved in the membrane bound protein damage by irradiation. To characterize in detail the radiation-induced modification in the gA structure further experiments with gA analogues (having only one Trp residue in a known position) are necessary.

Waste Management

Maintenance program for a safe prolonged wet storage of the nuclear spent fuel at IFIN-HH Bucharest-Magurele site

C.A. Drăgolici¹, A. Zorliu¹, C. Petran¹, I. Mincu¹, G. Neacșu¹

¹ National Institute of R&D for Physics and Nuclear Engineering "Horia Hulubei" (IFIN-HH), Bucharest-Magurele, Romania

Fuel is considered as spent nuclear fuel regardless of burnup when it is discharged from the reactor core for the final time. It is then normally placed in pools for cooling and interim storage until a final disposition is made. As a result of 40 years of intense utilization of the VVR-S reactor from IFIN-HH, 223 fuel assemblies of burned fuel were produced and stored in special ponds. Some of this aluminum-clad spent fuel has been in water storage for more than 30 years and remains in pristine condition until two years ago. Corrosion concerns on the spent fuel have been minimal over the years of fuel storage. The water in these basins is currently being maintained but no special issues were applied to improve water quality. Some pitting was reported on aluminum outer surface of some fuel assemblies, but this was attributed to material defects and fabrication concern. An intensive effort was made at our department to understand the corrosion problems and to be able to improve the basin storage conditions for extended storage requirements. A complex maintenance program was formalized but due to lack of funds it was delayed to be carried out. Even

so, despite financial problems some parts of this program were implemented to improve the water quality. Since March 2003 a completion of the initial programme was possible due to US financial assistance to make it feasible.

As part of the contract between National Atomic Energy Agency (ANEA) and Department of Energy (DOE), a scheduled operational maintenance program was issued. This program contains:

1. Baseline characterization and storage life prediction;
2. Formalize water characterization program;
3. Formalize corrosion surveillance program;
4. Visual examination of longest stored assemblies (EK-10 and S-36);
5. Identification and disposition of the failed fuel assemblies in Pool #3;
6. Vacuum silt and water change;
7. Relocate fuel from reactor cooling pond to AFR (Away from Reactor) Pool #1;
8. Formalize corrosion surveillance program;
9. Pool water level monitoring program.

The main goal of this strategy is to ensure that the fuels are maintained in a safe stable state until the shipment to origin country becomes available.

Structure investigations on Portland cement paste by small angle neutron scattering

C.A. Drăgolici¹, A. Len²

¹ Institute of Research and Development for Physics and Nuclear Engineering "Horia Hulubei", 77125 Bucharest-Magurele, Romania

² Research Institute for Solid State Physics and Optics, 1121 Budapest, Hungary

Portland cement pastes consist of many crystalline and non-crystalline phases in various ranges of sizes (nm and μm scale). The crystalline phases are embedded in amorphous phases of hydration products. We investigated the structural changes of hydrating phases in the time interval of 1-30 days at Budapest Neutron Center's SANS diffractometer.

The small angle neutron scattering of Portland cements prepared with a water-to-cement ratio from 0,3 to 0,8 gave us information about the microstructure changes in the material. Fractals were a suitable way for structure modelling. The variation of fractals size depending on the preparation-to-measurement time interval and water-to-cement ratio could be observed.

Decommissioning of research nuclear reactor VVR-S Magurele-Bucharest work stage

Em. Drăgulescu¹, M. Drăgușin¹, V. Popa¹, A. Boicu¹, C. Țucă¹, I. Iorga¹, C. Mustață¹

¹ "Horia Hulubei" National Institute of Physics and Nuclear Engineering, Bucharest-Magurele

A decommissioning project is performed on a nuclear facility research reactor VVR-S Magurele-Bucharest to remove the radioactive and hazardous materials so that there is no longer a risk to human health and the environment. The project involves four phases have named: assessment, development, activities implementation and closeout:

Assessment. There are two major parts to the assessment phase: preliminary characterisation and the review and decision-making process. Characterisation is needed to develop project baseline data, which should include sufficient chemical, physical, and radiological characterisation to meet planning needs. Based on the conclusions of these studies, possible decommissioning alternative will be analyzed and the best alternative chosen, final goal is identified, risk assessments are evaluated, regulations supporting assessment, land use considerations, financial concerns, disposal availability, public involvement, technology developments.

Development. After a decommissioning alternative is chosen, detailed engineering will begin following appropriate regulatory guidance. The plan will include characterisation information: review of decommissioning alternatives; justification for the selected alternative; provision for regulatory compliance; predictions of personnel exposure, radioactive waste volume, and cost. Other activities are: scheduling, preparation for decommissioning operations: coordination, documentation, characterization, report, feasibility studies, Decommissioning Plan, project report day to day, radiological survey, airborne sampling records, termination survey of the site.

Operations. The key of operations are: worker protection, health and safety program, review of planning work, work area assessment, work area controls, personal protection and monitoring, environmental pro-

tection: air quality, surface water, ground water, shipments, effluent sampling and monitoring, environmental monitoring, site release criteria.

Closeout. The final chemical and radiological surveys, as well as a Project Final Report, are produced at the conclusion of the decommissioning project.

Project stage

1. Documentations: - Urbanism licence by Ilfov Prefecture; - Feasibility study for 16 years and 3 months approved, for green-field stage decommissioning; - Will be elaborated technical documentation for building abolish, for obtaining of Unic Agreement from Ilfov Prefecture - finish in December 2003; - Decommissioning Plan revision 5 - which develop immediate dismantling strategy (16 years and 3 months) - will be finished in Dec. 2003; - Concerning with MECT financing "Technical Project" and "Execution Documentation" will be made by CITON in 2004; - Decommissioning Plan revision 5 in English for AIEA Technical Assistance Contract ROM 04/029 2003-2006;
2. Preparing activities for starting of decommissioning process. Clean-up activities, radiological characterisation, up-grading of storage conditions at nuclear spent fuel by air filtering, maintaining and monitoring of water parameters from water pools nuclear spent fuel storage, work protection and nuclear safety for Nuclear Reactor concerning ANL - SUA agreement for Sept 2003 - Sept 2005 period with prolong 1 year possibility, 500 kUSD value.
3. Specific activities in preservation stage of Nuclear Reactor: surveillance, radiological monitoring, maintaining and improvement of nuclear surveillance, improvement of nuclear surveillance of AFR, and finally implementation of CNCAN disposition by license stipulation.

Hydrophylic superabsorbants and hydrophobic absorbants for environmental protection and minimization of industrial risks

Em. Drăgușin¹, M. Drăgușin¹, V. Popa¹, A. Boicu¹, C. Țucă¹, I. Iorga¹, C. Mustață¹, E. Ionescu¹

¹ "Horia Hulubei" National Institute of Physics and Nuclear Engineering, Magurele, Str. Atomistilor, nr. 407, Bucharest-Magurele

The superabsorbants obtained by gamma Co-60 processing with swelling capacity from 40g/g to 500g/g have been used in the:

1. land management; 2. toxic and hazardouse materials in aqueouse state management in emergencies situations; 3. deuterated and tritiated water accidentally spreading in tha variouse places.

The hydrophylic absorbants obtained from rigid polyurethane reused from wastes have been used in the management of risks when petrol and derivated - petroleum materials, all in liquid state, are spreaded on

the soil, surface of water (rivers, lakes, sea etc.) or in work places. The absorbant capacity are min 4g/g and max 10g/g.

All absorbents hydrophylic and hydrophobic are in bulk form or in pillows (40x40x10)cm; tubes ($\Phi = 30$ cm (max), Length = 3 m (max)) with fast catching/detaching systems for emergency situations.

In case of the forest and wood buildings fires have been prepared ecological systems based on aqueouse polymeric solutions and esters fatty ascid.

The institutional radioactive waste evidence database

V.I. Manu¹, G. Matei¹, D. Matei¹, C. Turcan¹, Gh. Rotărescu¹, N.F. Drăgolici¹

¹ "Horia Hulubei" National Institute for Physics and Nuclear Engineering, Bucharest-Magurele

This set of applications serves for keeping the records about the radioactive waste products collected by IFIN-HH. This records cover all the levels involved, beginning with the by-product's processing at STDR, to their final destination - the dispozal at DNDR-Baita Bihor.

This applications include several user-friendly interfaces for data inputs, data editing and modifications and quering. It provides secure access for both levels: reading and/or writing. Is included here a set of security systems, most of them originally ones to insure

the database's integrity. Also some special tools were developed in order to display the current situations when viewing the database and also for measurement unit conversion.

The program consists of management applications, tables containing the main longlive izotopes, providers and utilities for reports editing.

STDR worked in conjunction with the IT Department (DIC) from IFIN-HH to elaborate this project.

Studies of radiolytical and self-radiolytical processes in polyacrylic hydrogels using RES spectrometry

C. Postolache¹, R. Georgescu¹, C. Ponta¹, L. Matei¹

¹ National Institute of R&D for Physics and Nuclear Engineering "Horia Hulubei", Magurele, Bucharest, Romania

Due to remarkable capacity of water retain, polyacrylic (PAA) hydrogels represent an interesting alternative for tritium (tritiated water-HTO) liquid wastes trapping. The study was developed on radiolytical processes in PAA:HTO systems derivated from irradiation of polymeric network by disintegration of tritium atoms from HTO. The aim of these studies is the identification of polymeric structures and optimal storage conditions.

RES studies of radiolytical processes were realized on dry polyacrylic acid (PAA) and polyacrylic based hydrogels irradiated and determined at 77 K.

In the study we observed the effect of swelling capacity of hydrogel on the formation of free radicals. In RES spectres of irradiated PAA were identified a signal with quintet structure attributed, in conformity with literature, to radical from α position referred to carboxylic group. We also identified a triplet attributed

to a radical resulted by fragmentation of polymeric main chain. In case of PAA hydrogels were identified signals attributed to HO· radical resulted form water radiolysis, R-OO· radicals resulted from the presence of atmospheric O₂ in samples and a signal with quintet structure more less spilted like dry polymer. The signal is attributed to a radical from the polymeric main chain in α position referred to carboxylic group. The decrease of split parameter is determined by tension of main chain as result of swelling, associated with increase of θ angle between p_x axis of C α radical and the C α C β H β plane. RES analysis of labelled hydrogels indicate the presence of HO and COO radicals resulted from internal primary effect. RES analysis of PAA:HTO samples indicate the preponderant role of the internal primary effect in selfradiolytical effects in concordance with the role of secondary effects stopped in RES study due to freeze material.

Durability of cemented waste in repository and under simulated conditions

F. Dragolici¹, M.B. Nicu¹, L. Lungu¹, C.N. Turcanu¹, Gh. Rotărescu¹

¹ NIPNE-HH, Radioactive Waste Management Department

The research activities performed by the Department of Radioactive Waste Management are focused on the aqueous low level waste (LLAW) treatment products obtained by chemical precipitation and on the conditioning of these products by cementation. The individual mechanisms involved in the chemical precipitation process are directly dependent on the precipitate properties and structure, which are connected with the initial system composition and the precipitation procedure, i.e. reagent concentration, rate and orders of chemical addition, mixing rate and time and ageing conditions. In the case of conditioning by

cementation, the chemical nature and proportion of the sludge or concentrates affect both the hydrolysis of the initial cement components and the reactions of metastable hydration constituents, as well as the mechanical strength and chemical resistance of the hardened cemented matrix. Generally, the study of the precipitation products and their behaviour during cementation and the long-term disposal is extremely difficult because of the system complexity (phase composition and structure) and the lack of non-destructive analytical methods.

Technical aspects regarding the upgrading of the roumanian national repository for low and intermediate level radioactive waste, Baita, Bihor county (DNDR)

F. Dragolici¹, Gh. Rotărescu¹, I. Paunica¹, C. Turcanu¹

¹ NIPNE-HH, Radioactive Waste Management Department

The proper application of the nuclear techniques and technologies in Romania started in 1957, once with the commissioning of the Research Reactor VVR-S from IFIN-HH-Magurele. During the last 40 years, appear thousands of nuclear application units with extremely diverse profiles (research, biology, medicine, education, agriculture, transport, all types of industry) which used radioactive sources in their activity and produces nuclear wastes. The Radioactive Waste Treatment Plant (STDR) from IFIN-HH was committed in collaboration with companies from United Kingdom and became operational in 1975, being the only authorized and specialized institution for the management of the non-fuel cycle radioactive wastes from all over Romania.

In 1985 was built and given in operation the National Repository for Low and Intermediate Radioactive Waste (DNDR) - Baita, Bihor county, sited in Apuseni mountains, in an old exhausted uranium mine. Using the existing concepts at '80 years level concerning the final disposal of the low and intermediate level radioactive wastes, and, rely on internal standards and international recommendations the underground constructions were dimensioned to dispose about 21.000 standard drums.

To choose the emplacement of DNDR was used the experience gained by the countries that develop nuclear programs, which show that the most proper modalities for radioactive waste disposal are the underground facilities in geological formations without water table or infiltration's. The site selection was based on preliminary studies concerning the geology, hydrogeology, seismic, meteorological and radioactivity of the area, and also on mining technical studies.

Therefore, by construction and functioning of the capacities for treatment and final disposal, in Romania was solved the management of the low and intermediate level radioactive wastes, providing the protection

of the people and environment.

In present, in the DNDR galleries are finally disposed more than 6.000 standard drums, which means about 30Both facilities were designed and built according to the philosophy of '60's and '70's, common to ex socialist countries, excepted for some West-European imports.

Beginning in 1990, many experts' missions visited STDR and DNDR under the auspices of AIEA and EEC technical co-operation projects. Nearly all experts while recognizing the scientific level and experience of personnel, strongly recommended corrective measures and up-grading of facilities and operational practices, as follows:

- a national policy addressing the management of radwaste at national level for at least the next 10 years should be established;
- elaboration of comprehensive safety analysis addressing the management of anticipated arising waste should be performed;
- refurbishment of processing and control systems is needed;
- amending of operational practices taking into account ICRP recommendations on dose limits for workers and public is also needed.

Taking in consideration all the problems mentioned above is obvious that before starting the decommissioning program is necessary to up-grade the waste management facilities. In this sense, once with elaboration of the decommissioning project were started studies on up-grading the waste management facilities in order to be able to collect, treat, condition and dispose finally the resulted wastes.

It was agreed that the first necessary step is to update DNDR to reach the national demands and international recommendations.

Studies on cement matrix used at the radioactive waste treatment plant for radwaste conditioning

F. Dragolici¹, L. Lungu¹, M. Nicu¹, Gh. Rotărescu¹, C. Turcanu¹

¹ NIPNE-HH, Radioactive Waste Management Department

The research activities performed by Department of Radioactive Waste Management is focused on the LLAW treatment products obtained by chemical precipitation and on the conditioning of these products by cementation.

The individual mechanisms participating on the chemical precipitation process are directly dependent on the precipitate properties and structure, which are connected with the initial system composition and the precipitation procedure, i.e. reagent concentration, rate and orders of chemical addition, mixing rate and time and ageing conditions.

In the case of conditioning by cementation, the chemical nature and proportion of the sludges or concentrates affect both the hydrolysis of the initial cement components and the reactions of metastable hydration constituents, as well as the mechanical strength and chemical resistance of the hardened cemented matrix. Generally, the study of the precipitation products and their behaviour during cementation and the long-term disposal is extremely difficult because of the system complexity (phase composition and structure) and the

lack of non-destructive analytical methods.

The experience accumulated by the countries who developed nuclear programs in military and socio-economic fields and which produced important volumes of radioactive wastes, lead us to study some of mineral additives to be used in the conditioning and disposal technology. It is well known that mineral additives are diminishing the leaching rate of the radionuclides in the disposal environment.

The studies have the purpose to obtain the most propitious mixture of cement-bentonite and cement-volcanic tuff, which have the mechanical properties similar to the cement paste used for the conditioning of radioactive waste.

Taking in consideration the characteristics of these mineral binders: very good plasticity and capacity of adsorption, which lead at the decrease of porosity, in the future, the mixture is wished to be used at the Radioactive Waste Treatment Plant - NIPNE-HH - Bucharest, Magurele for the conditioning of the radioactive waste.

Preliminary studies on the elaboration of technologies for long term storage of radium spent sealed sources

Gh. Dogaru¹, C. Ivan¹, F. Dragolici¹, Gh. Rotărescu¹

¹ NIPNE-HH, Radioactive Waste Management Department

The continuous progress in the knowledge of hazard associated with the use of radium sealed radioactive sources requested a well planned and carefully collection and ongoing management of these kind of radioactive materials. The paper contains the technical information and recommendations on the management of radium spent sealed radioactive sources. The information refers to the preparation of spent radium sealed radioactive sources on the user site and them

conditioning and long term storage in the radioactive waste storage facility of RWTP Magurele. The paper contains the regulation framework and emphasizes the necessity of development of the national radium inventory. Also, in the paper are presented the safety considerations regarding the handling, packaging for transport and packaging for long term storage of spent radium sealed sources and the personnel requirements and quality assurance.

Environmental impact analysis after 15 years of operation of the roumanian national repository for low and intermediate level radioactive waste, Baita-Bihor county

F. Dragolici¹, C.N. Turcanu¹, Gh. Rotărescu¹

¹ NIPNE-HH, Radioactive Waste Management Department

The proper application of the nuclear techniques and technologies in Romania started in 1957, once with the commissioning of the Research Reactor VVR-S from IFIN-HH-Magurele.

Using the existing concepts at '80 years level concerning the final disposal of the low and intermediate level radioactive wastes, and rely on internal standards and international recommendations, in 1985 was built and given in operation the National Repository for Low and Intermediate Radioactive Waste (DNDR) - Baita, Bihor county, sited in Apuseni mountains, in an old exhausted uranium mine.

Therefore, by construction and functioning of the capacities for treatment and final disposal, in Romania was solved the management of the low and intermediate level radioactive wastes, providing the protection of the people and environment.

In present, in the DNDR galleries are finally disposed more than 6,000 standard drums, which means about

30% of the repository capacity.

National Institute for Physics and Nuclear Engineering "Horia Hulubei", pursuit in a dynamic way, by radioactivity measurements and potentially radioactive elements migration, the efficacy of the applied methods regarding to assure the nuclear security of population and environment.

The methodology is applied from 1985, and it consists of soil, water and vegetation sample prelevation, radiometric measurements, chemical and spectrometric analyses to detect in real time the radiological statement changes in the area.

Radiometric measurements carried out during the last 15 years on gamma external irradiation level and radiochemical analysis of soil, water and vegetation samples shows that DNDR activity is developed without irradiation risks for population and environment.

Technical aspects regarding the management of radioactive waste from decommissioning of nuclear facilities

F. Dragolici¹, C.N. Turcanu¹, Gh. Rotărescu¹, I. Paunica¹

¹ NIPNE-HH, Radioactive Waste Management Department

The treatment and conditioning of non-fuel-cycle radioactive waste commenced in STDR nearly 26 years ago, and disposal activities started in DNDR 16 years ago. Both facilities were designed and built according to the philosophy of '60's and '70's, common to ex socialist countries, excepted for some West-European imports.

Regarding radioactive waste management resources at IFIN-HH, to face future needs and reactor decommissioning, a "Technical analysis of STDR", was completed by CITON (a nuclear design company) in December 1997 include:

- a technical analysis of the present status of STDR systems
- suggestions for both refurbishing of the existing installation for treating, decontamination and conditioning of reactor decommissioning wastes, with the

objective of meeting state-of-the art techniques and international recommendations.

Decommissioning of the Magurele research reactor will create additional waste streams for a short period, which will be treated in the Waste Treatment Plant. Taking in consideration all the problems is obvious that before starting the decommissioning programme is necessary to up-grade the waste management facilities. In this sense, once with elaboration of the decommissioning project were started studies on up-grading the waste management facilities in order to be able to collect, treat, condition and dispose finally the resulted wastes.

Another major issue is the management of wastes such aluminium, graphite and long life spent sources, which require special technologies and must be kept in special storage until will be find the proper solution for

them.

Distribution of some major and trace elements in Danube delta lacustrine sediments and soil

L.C. Dinescu¹, E. Steinnes², O.G. Dului³, C. Ciortea¹, T.E. Sjobakk², D.E. Dumitriu¹, M.M. Gugiu¹, M. Toma¹

¹ NIPNE-HH, Radioactive Waste Management Department

² Norwegian University of Science and Technology, Department of Chemistry

³ University of Bucharest, Department of Nuclear Physics

Sediment cores collected from lakes Mesteru and Furtuna (eastern part), Sontea channel and soil samples collected from Caraorman bar, all located in the Danube Delta, were analyzed for 42 elements (Ag, Al, As, Be, Na, Mg, P, S, K, Ca, Sc, Ti, V, Cr, Mn, Fe, Co, Ni, Cu, Zn, Ga, As, Se, Br, Rb, Sr, Y, Mo, Ag, Cd, In, Sn, Sb, Cs, Ce, Hf, Hg, Tl, Pb, Bi, Th, U) by instrumental neutron activation analysis (INAA), thick target proton induced X-ray emission (TT-PIXE) and inductively coupled plasma-mass spectrometry (ICP-MS). The INAA and TTPIXE yielded total concentrations whereas the ICP-MS data reflected the fractions soluble in 14M HNO₃. The ICP-MS data exhibited surface enrichment relative to the lower part of the sediment core of Cu, Zn, As, Ag, Cd, In, Sn, Sb, Hg, Tl, Pb, and Bi, most prominently by Cd and Hg. Their vertical distribution in the investigated cores generally reflected the pollution history of recent sediments in Danube delta, showing a steady increase until

the end of the 1980s followed by a slow decrease after 1990. The vertical profiles of most remaining elements were characterized by a relatively uniform distribution along the cores. In some cases, the concentrations of As, Cd, Cu, Cr, Mn, Ni and Pb exceeded minimum thresholds of safety, as defined by the Romanian regulations. The elemental composition of the sediment below 20 cm depth (total concentrations) was similar to that of the upper continental crust (UCC) for most elements. Values distinctly higher than UCC were observed for As, Sb (factor ~ 5) and Cr, Ni, Cu (factor 2 to 3). The nitric acid soluble element concentrations in the soil samples in some cases showed increased values at the surface as compared to 30 cm depth, either due to air pollution or to the action of plants. In no case a large contribution to the topsoil from atmospheric deposition was evident, indicating that the surface contamination of the sediments was mainly by riverine transport.

New data concerning the efficiency calibration of a drum waste assay system

M. Toma¹, L. Dinescu¹, O. Sima²

¹ NIPNE-HH, Radioactive Waste Management Department

² Universitatea Bucuresti, Department of Nuclear Physics

The study is focused on the efficiency calibration of the gamma spectroscopy system for drum waste assay. The measurement of a radioactive drum waste is usually difficult because its high volume, the varied distribution of the waste in the drum and its increased self attenuation. To solve this problems, a complex calibration of the system is required. For this purpose, a calibration drum provided with seven tubes, placed at different distances from its center was used, the rest of the drum having been filled with Portland cement.

For the efficiency determination of a uniform distributed source, a linear source of ¹⁵²Eu was used. The linear calibration source was introduced successively in the seven tubes, the gamma-spectra were collected while the drum was translated and simultaneously rotated. Using the GENIE-PC software, the gamma-spectra were analyzed and the detection efficiencies for shell-sources were obtained. Using this efficiencies, the total response of the detector and the detection efficiency appropriate to a uniform volume

source were calculated.

For the efficiency determination of a non-homogenous source, supplemental measurements in the following geometries were made. First with a point source of ^{152}Eu placed in front of the detector, measured in all seven tubes, the drum being only rotated. Second with the linear source of ^{152}Eu placed in front of the detector, measured in all seven tubes , the drum being only rotated.

For each position the gamma spectra was recorded and the detection efficiency was calculated.

The obtained values for efficiency were verified using GESPECOR software, which has been developed for the computation of the efficiency of Ge detectors for a wide class of measurement configurations, using Monte-Carlo method.

Miscellaneous Applications

High energy proton degradation in optical transmission materials (EURATOM project)

B. Constantinescu¹, R. Bugoi¹, P. Ioan¹, M. Drăgușin¹, D. Stan¹, M. Brașoveanu², M. Nemțanu²

¹ National Institute for Nuclear Physics and Engineering "Horia Hulubei", Bucharest-Magurele

² National Institute for Lasers, Plasma and Radiation Physics

Studies on gamma and high-energy proton irradiation-induced modifications in ultraviolet transmission properties on KU1 quartz glass samples are presented. The optical transmission components of the future thermonuclear reactor will be expected to maintain their transmission properties under high levels of ionizing radiations ($\approx 5 \text{ Gy/h}$) during hundreds of hours. KU1 quartz glass is known to be radiation-resistant. This type of silica glass, presently examined within the ITER program, has been studied under Co-60 gamma and 3 MeV proton irradiation at room temperature. For this, 0,8 mm thick samples provided by IAE Kurchatov (Moscow) have been gamma irradiated with 0.2 to 2 Mrad doses at a 20 kCi Co-60 irradiator and implanted using the Bucharest HVEC Tandem accelerator with 8×10^{13} and $1,5 \times 10^{14}$ protons, respectively. The UV transmission properties have been measured with a Cary 4 VARIAN spectrophotometer. For gamma irradiated samples two main absorption peaks were observed: 215 nm (produced by E' type defects) and 240 nm (ODC II - oxygen-deficient center

type defects). A dose dependence of these peaks intensity is discussed. As concerning the proton implanted samples, absorption peaks at 215 nm and 240 nm, similar in shape, but smaller in intensity to gamma irradiation case, can be observed. In the upper region of UV spectrum ($\geq 350 \text{ nm}$), same small peaks are also presented, possibly due to defects as OH^- produced by the implanted hydrogen. The 3 MeV protons produce considerable ionization, which is the main cause of the energy loss at such low energies. The protons and the knock-on ions produce ionization. The result of the overall ionization is the 215 nm band. As concerning the number of induced defects, our doses, equivalent to $4'10^{15} \text{ p/cm}^2$ and $7,5'10^{15} \text{ p/cm}^2$ produced $4'10^{-6}$ and $7,5'10^{-6} \text{ dpa}$, respectively, in the 3 MeV protons range in quartz (80 mm), equivalent to $5'10^{-4}$ and $9'10^{-4} \text{ dpa}$ for 1 cm. At that damage level, we have considerably defects formation, which gives an undefined general absorption. This is the explanation for the aspect of our absorption curves in the region above 450 nm.

Filtered backprojection algorithm in RPCs based PET

I. Cruceru¹, I. Manea¹, C. Nicorescu¹, F. Constantin¹

¹ National Institute for Physics and Nuclear Engineering "Horia Hulubei", P.O.B. MG-6, Bucharest-Magurele, Romania

The basis of PET consists on the administration of a radioactive isotope attached to a tracer that permits to reveal its molecular pathways in a human body. A 3-D Complete-Body-Scan is desired in order to minimize the radiation dosage to the patient and to sensitive increase of the axial field of view (FOV). A major candidate for gamma pair detection in 3-D Complete-Body-Scan are the RPCs (Resistive Plate Counters). They consist in a longitudinal microstrip grid 1.5 mm thick, spaced at 1 mm; the grid is placed between a large electric resistive glass anode ($\rho=10^{12} \Omega \text{ cm}$) and

an aluminum cathode; the gap, around $300 \mu\text{m}$ is filled with a special gas and is polarized at around 6 kV. Several detecting structures based on Resistive Plate Counters (RPCs) are evaluated for the use in a positron emission 3 Dimensional Complete Body Scan tomograph. The coincidence matrix is built for the specific detecting structure by means of random gamma pair rays generation, and then the filtered backprojection algorithm is used to reconstruct the original picture. The accuracy of image reconstruction is examined for the four different detecting structures.

Evaluation of bonding energies in organic compounds by quantum mechanical methods

C. Postolache¹, L. Matei¹

¹ "Horia Hulubei" National Institute of Physics and Nuclear Engineering, Bucharest-Magurele, e-mail: cristianpostolache@personal.ro

In this paper we proposed a quantum mechanical evaluation model for bonding energies in organic compounds. Values of bonding energies were determined as homolytic dissociation energies.

The molecular structures were built and geometry optimized in first stage using MM2, MM+, AMBER molecular mechanic. Energetically minimizations were refined using semiempirical methods. In concordance with choose molecular structure we used, methods like CNDO, INDO, PM3, AM1.

Binding energies were evaluated by simulation of homolytic dissociation processes. Using quanto-mechanical methods we characterized molecular structures and fragments resulted from dissociation of chemical bond. Were determinated and analyzed total binding energies (TBE) of unoptimized fragments, those geometrical minimized post-fragmentation, transitional state and initial molecular structures. Enthalpy of re-

action (ΔH) were determined from difference between fragments TBE and TBE of system. The values of activation energy (Ea) is indicated by the difference between transitional state TBE and TBE of system. ΔH and Ea are correlated with binding energy.

Method accuracy and application fields of different evaluation modalities (optimized, non-optimized, transition states) were achieved by intercomparison of obtained values with those experimental found in literature.

More than 74 organic and inorganic compounds (alkans, alkenes, alkynes, aromatic structures, halogenated compounds, alcohols, peroxides, aldehydes and ketones, carboxylic acids, ammines, nitro derivatives, nitrates, nitrites, thyols, thyoethers, water, hydrogen peroxide, ammonium, hydrazine etc.) were analyzed.

Studies of radiolytical processes in siloxanic polymers using RES spectrometry

C. Postolache¹, R. Georgescu¹, L. Matei¹

¹ National Institute of Research and Development for Physics and Nuclear Engineering "Horia Hulubei", Magurele, Bucharest, Romania, e-mail: cristianpostolache@yahoo.com

Radioluminescent sources based on tritium labeled polymers represent a modern technological variant with applications in defense industry, nanotechnologies. Obtaining of radioluminescent, sources with high luminances impose the identification of synthesis methods of labeled polymers with superior specific activities and high raw radioactive material using. Radioluminescent sources, which contain as excitant agent tritium labeled ethyl-siloxan polymers, represent one of the most studied constructive variants. High specific activities needed, induce significant autoradiolytic

processes in labeled polymers, those study being necessary for technological, radiobiological and radioecological reasons.

RES study followed identification of free radicals resulted from primary radiolitical act in irradiated siloxanic polymers. The study was conducted on irradiated dimethyl, ethyl, phenyl and ethyl-phenyl siloxanic structures and measured at 77 K. Results were inter compared with literature results and with those obtained by quantum-mechanical simulation and from radiometrical studies on tritium labeled polymers.

Evaluation of absorbed doses at the interface: solid surfaces - tritiated water solutions

C. Postolache¹, L. Matei¹

¹ National Institute of Research and Development for Physics and Nuclear Engineering "Horia Hulubei", Magurele, Bucharest, Romania, e-mail: cristianpostolache@yahoo.com

Studies concerning the isotopic exchange H/D/T in the system: elemental hydrogen - water and in the presence of platinic metals on hydrophobic supports as catalyst were carried out at ICSI Rm. Valcea Romania. Due to the very low energy of β -radiation emitted by tritium, the direct measurements of dose absorbed by the isotopic exchange catalyst using classical methods is practically impossible.

For this purpose an evaluation model was developed. The volume of tritiated water which can irradiate the catalyst was represented by a semi sphere with the radius equal to the maximal rate of β -radiation emitted by tritium. The catalyst surface is represented by a circle with a $0.2\mu\text{m}$ radius and the same centre as

the circle of the semisphere secant plane. Flow rate of absorbed dose is computed with the relation: $d = (1/100)(\Phi \cdot Em/m)$, where d = dose flow rate, expressed in rad/s; Φ = total radiation flux which interacts with the catalyst surface, expressed in erg; m = catalyst weight, in grams. Total flux of available radiation, Φ , was determined as a function of three parameters: a) total flow of tritium β -radiation emitted in the semi sphere of tritiated water, dependent on the volume and radioactive concentration; b) emission coefficient on the direction of the catalyst surface; c) attenuation coefficient (due to self-absorption) of the tritium β -radiation in the tritiated water body.

MO calculations of vibrational spectra of some ureides and thioureides; theoretical contributions to C=S group localization on IR spectra

C.A. Simion¹

¹ "Horia Hulubei" National Institute for Physics and Nuclear Engineering, P.O.Box MG - 6, Magurele, Bucharest

Using computational Chemistry program HyperChem 5.02 [1], two series of compounds starting with urea (ureides) and thiourea (thioureides) have been investigated.

Simulation stages on HyperChem 5.02. Program:

- "building" of compound structure
- "constraints..." on N atoms to tetrahedral and on C(O,S) atoms to trigonal
- "restraints..." for H intramolecular bond formation and for the phenyl orientation between parallel and perpendicular positions relatively to the six membered pseudo heterocycle plane H-N-C(S, O)-N-C-O
- introducing "Periodic Box" conditions
- geometry optimization using MM⁺: Polak-Ribiere optimizer, RMS (Gradient) of 0.1 kcal/mol. \AA ; single point calculations

- geometry optimization using semi empirical AM1/PM3 methods: Polak-Ribiere optimizer, RMS (Gradient) of 0.1 kcal/mol. \AA (then 0.01 kcal/mol. \AA), accelerated convergence, singlet state, RHF, total charge zero, spin multiplicity of one; single point calculations
- calculating vibrations and performing a vibrational analysis (all normal modes of vibration must have only positive values for a molecule reaching minima on EPS).

The aim of the MO calculations was a theoretical study of band positions of the C=S group in the vibrational spectra of thioureides. For a correct attribution of signals, the homologues in ureide serie were taken into account. The presentation consists in a number of original data concerning a general characterization of the molecules, frequencies assignments by type of bonding in i.r.spectra versus literature data, and a comparative table with C=O and C= S bond values [2, 3]. In all compounds, the thiocarbonyl signals

appear in the generally accepted interval data tables. For the carbonyl group, a combined signal has been obtained over 1850 cm^{-1} associated with the corresponding signal in amido-acids. For all compounds, the ν_{CO}/ν_{CS} ratio still remains in the interval 1.14 - 1.60 as suggested by literature data [4, 5].

References

- [1] HyperChem; Release 5.02. For Windows 95/NT. Molecular Modeling System, Hypercube, Inc., 1997
- [2] Mecke H., Mecke R. and Lüttringhaus D., Z. Naturforsch., 1955; 10B: 367-375
- [3] Bellamy L.J., The Infra-red Spectra of Complex Molecules, Edited by London: Methuen & Co. Ltd.; New York: John Wiley & Sons, Inc., 1959
- [4] Jones R.N., Infrared spectra of organic compounds: Summary charts of principal group frequencies", NRC Bulletin No. 6, Ottawa, 1959
- [5] Avram M. and Mateescu Gh. D., Infrared Spectroscopy. Applications in Organic Chemistry, Wiley Interscience, New York, 1972

Contributions to the online software for ATLAS test beam data acquisition system

E. Bădescu¹, M. Caprini¹

¹ NIPNE-HH, Department of Applied Nuclear Physics

The ATLAS experiment is one of four experiments at the Large Hadron Collider (LHC) particle accelerator that is currently being built at CERN and is scheduled to start data taking in 2007.

The large amount of ATLAS detector data requires the design of a very efficient Data Acquisition (DAQ) with a three level trigger system.

The Online Software is the global system software to configure and control the DAQ, as well as to share information within the DAQ system, it excludes however the processing and transportation of physics data. It has interfaces to the DataFlow system (being responsible for the transportation of the data from Readout Drivers to Mass Storage), to the different triggers as well as to the Detector Readout Crates controllers and the Detector Control System (DCS).

The Online Software consists out of three main packages which in terms contain several components - Configuration (Configuration Database, Online Bookkeeper), Control (Run Controller, DAQ Supervisor, Process Manager, Resource Manager, Graphical User Interface), Information Sharing (Information Service, Message Reporting Service, Online Histogramming Service, Event Monitoring Service).

The new design of the Online Software is presented in the document Technical Design Report for ATLAS High-Level Trigger Data Acquisition and Controls (1).

In order to study important performance aspects like alignment and calibration as well as to proceed on the way to the final ATLAS DAQ system, a Test Beam Facility at Super Proton Synchrotron (SPS) accelerator at CERN has been setup for the different detectors

of ATLAS. In 2003 four out of six sub-detectors of the Atlas detector were using the Online Software for their DAQ system to perform their data taking: the Hadronic Tile Calorimeter (TileCal), the Pixel Detector, the Muon Detector and Semiconductor Tracker (SCT) (2).

A combined beam test of all 4 detectors, with more than 20 controllers and running on 30 workstations, was configured and controlled successfully by the Online Software.

The full functionality of the Online Software was available for the Test Beam DAQ system and used by the sub-detectors.

A system with more than two hundred workstations was used to study the scaling behaviour of individual components and of the integrated system (3). These activities are providing important feedback into the development cycle.

In order to support the Test Beam users, the Online Software includes a Training package which allows the user to learn about the different components of the Online Software and their usage. Furthermore detailed descriptions about the installation and the usage are available at URL <http://atlas-onlsw.web.cern.ch/Atlas-onlsw/training/training.htm>.

The main functionalities of the Online Software are provided without the need of commercial packages and the software is available for users by download at URL <http://atlas-onlsw.web.cern.ch/Atlas-onlsw/download/download.htm>

The Bucharest group contributed in the design and implementation of some components used in the test

beam configuration (Message Reporting System, Integrated Graphical User Interface), in the software releases testing and component integration activities and in the preparation of the documentation and exercises for the Training package.

Work performed under contracts no. 72/2001 and 11/2002 in the frame of the CERES Programme supported by the Romanian Ministry of Education and Research.

References

- [1] Atlas Collaboration - ATLAS High-Level Trigger Data Acquisition and Controls - Technical Design Report, CERN/LHCC/2003-022, ATLAS TDR 016, 30 June 2003, ISBN 92-9083-205-3
- [2] J.Flammer, I.Alexandrov, ..., E.Badescu, ..., M.Caprini, ... - Online Software for the ATLAS Test Beam Data Acquisition System - The 13th Real Time Conference 2003, Montreal, Canada, May 2003, Proceedings of the 13th IEEE NPSS Real Time Conference, ISBN 0-7803-7986-1, ATL-DAQ-2003-044, to be published in IEEE Transactions on Nuclear Science
- [3] D.Burckhart-Chromek, M.Caprini, ... - Large Scale Performance Tests January 2003, ATL-DQ-ES-0012 (2003), https://edms.cern.ch/file/392827/1/ScalTestsReportJan2003_V1.pdf
- [4] A.Kazarov, I.Alexandrov, ..., E.Badescu, ..., M.Caprini, ... - Verification and Diagnostics Framework for ATLAS Trigger and Data Acquisition - 2003 Conference for Computing in High Energy and Nuclear Physics CHEP03, La Jolla, USA, March 2003, ATL-DAQ-2003-033

Hetero-junction laser diodes under neutron irradiation

D. Sporea¹, I. Vata², R. Sporea¹

¹ National Institute for Lasers, Plasma and Radiation Physics

² NIPNE-HH,Cyclotron

Key words: hetero-junction; laser diode; neutron irradiation;radiation effects.

Laser diodes are good candidates to be included into remote handling and sensing systems operating in adverse environments. A set of applications of interest for semiconductor lasers constitutes their use under irradiation conditions in nuclear power plants, radiation processing facilities, high energy physics accelerators, nuclear waste management sites, or even space crafts. Our investigation concerns the evaluation of neutron irradiation on two types of laser diodes for their possible operation in nuclear fusion installations, and the development of a radiation effects database. The devices were subjected to neutron fluences between 10^{10} and $10^{13} n.cm^{-2}$ at room temperature, while the measurements were done off-line. Optical, electrical and optoelectronic characteristics were assessed. The major radiation effects which affect laser diodes are in these environments are: the ionization and/or the displacement damage [1-3]. Our aim was to develop procedures for the evaluation of laser diodes degradation under various irradiation conditions and to contribute to a radiation effects database. The present investiga-

tion focused on the evaluation of neutron irradiation on two commercially available, low power, CW laser diode emitting in the near-IR range. Electrical, optical and optoelectronic characteristics were assessed off-line, after each irradiation step, up to a fluence of $1.2 \cdot 10^{13} n.cm^{-2}$. The paper was accepted as oral presentation at 13th International Conference on Nuclear Engineering Beijing, China, May 16-20, 2005. The authors wishes to acknowledge the financial support of the European Union and of the Romanian Ministry for Education and Research, in the frame of the Fusion Programme, grant No. ERB 5005 CT 990 101/1999.

References

- [1] Compton, D.M.J. and Cesena, R.A., 1967, IEEE Trans. Nucl. Sci., Vol. 14, p. 55.
- [2] Johnston, A.H., Miyahira, T.F. and Rax, B.G., 2001,IEEE Trans. Nucl. Sci., Vol. 48, p. 1764
- [3] Johnston, A.H. and Miyahira, T.F., 2003,Proceedings of RADECS 2003

Evaluation the measurement uncertainty of absorbed dose for ECB dosimetry system at IRASM

R. Georgescu¹

¹ NIPNE-HH, IRASM Center

ECB dosimetric system is used for evaluating absorbed dose in the gamma irradiated product at irradiation facility IRASM. In order to use it in process validation and in process control for radiation treatment of products, the calculation of the uncertainty associated with the dose measurement is required. In this paper, the identification of specific sources of uncertainty and the evaluation of their contributions to the combined standard uncertainty of measured absorbed dose are presented, using analysis of variance ANOVA. Using one-way ANOVA with equal group sizes, the uncertainty components associated with the variability in readout oscilometric equipment and with the dosimeter-to-dosimeter scatter for (10...50) kGy dose range were determinated. The uncertainty due to polynomial fit to actual dosimetry calibration data was evaluated by using the 95 % confidence interval about the fit. The combined relative uncertainty for the dosimetric system is dose dependent. For the specific dose range, the relative combined standard uncertainty of the calibrated system varies from 2.0 % ($D_x=30.0$ kGy) to 3.3 % ($D_x=10.0$ kGy), and the combined relative uncertainty of measured absorbed dose value D_x , from 2.2 % ($D_x=30.0$ kGy) end 3.4 % ($D_x=10.0$ kGy).

References

- [1] ISO 15563:1998, *Use of the Ethanol-Chlorobenzene Dosimetry System*
- [2] ISO 15556:1998, *Guide for Selection and Calibration of Dosimetry System for Radiation Processing*
- [3] Razem D. and Dvornik I. (1972) The Application of Ethanol-Chlorobenzene Dosimeter to Electron-Beam and Gamma-Radiation Dosimetry: II. Cobalt-60 Gamma Rays, *Dosimetry in Agriculture, Industry, Biology and Medicine*, p.405, IAEA/STI/PUB 311. IAEA, Vienna
- [4] V. Stenger (1981) Unified Control Methods in Dosimetry for High-Activity Irradiation Facilities in Hungary, *High-Dose Measurements in Industrial Radiation Processing*, p. 80, Technical Report series No. 205, IAEA, Vienna
- [5] ISO 15572:1998, *Guide for Estimating Uncertainties in Dosimetry for Radiation Processing*
- [6] SR 13434:1999, *Ghid pentru evaluarea si exprimarea incertitudinii de masurare*
- [7] A. Miller (1998) Dosimetry Requirements Derived from the Sterilization standards. *Radiat. Phys. Chem.*, 52, no. 1-6, 533

Detection methods of irradiated foodstuffs

C.C. Ponta¹, M. Cutrubinis¹, R. Georgescu¹, R. Mihai², M. Secu³

¹ NIPNE-HH, IRASM Center

² NIPNE-HH, Life and Environmental Physics Department

³ National Institute of Materials Physics

Food irradiation has, in certain circumstances, an important role to play both in promoting food safety and in reducing food losses. The safety and availability of nutritious food are essential components of primary health care. WHO actively encourages the proper use of food irradiation in the fight against foodborne diseases and food losses. To this end, it collaborates closely with FAO and IAEA. Food irradiation can have a number of beneficial effects, including delay of ripening and prevention of sprouting; control of insects, parasites, helminthes, pathogenic and spoilage bacteria, moulds and yeasts; and sterilization, which enables

commodities to be stored unrefrigerated for long periods. The 1990s witnessed a significant advancement in food irradiation processing. As a result, progress has been made in commercialization of the technology, culminating in greater international trade in irradiated foods and the implementation of differing regulations relating to its use in many countries. Codex General Standard for Irradiated Foodstuffs and Recommended International Code of Practice for the Operation of Irradiation Facilities Used for the Treatment of Foods regulate food irradiation at international level. At European Union level there are in power Direc-

tive 1999/2/EC and Directive 1999/3/EC. Every particular country has also its own regulations regarding food irradiation. In Romania, since 2002 are in power the Norms Regarding Foodstuffs and Food Ingredients Treated by Ionizing Radiation. These Norms are in fact the Romanian equivalent law of the European Directives 1999/2/EC and 1999/3/EC. The greater international trade in irradiated foods has led to the demand by consumers that irradiated food should be clearly labeled as such and that methods capable of differentiating between irradiated and nonirradiated products should be available. Thus a practical basis was sought to allow consumers to exercise a free choice as to which food they purchase. If a food is marketed as irradiated or if irradiated goods are sold without the appropriate labeling, then detection tests should be able to prove the authenticity of the product. For the moment in Romania there is not any food control laboratory able to detect irradiated foodstuffs. The Technological Irradiation Department coordinates and cofinances a research project aimed to establish the first Laboratory of Irradiated Foodstuffs Detection. The detection methods studied in this project are the ESR methods (for cellulose EN 1787/2000, bone EN 1786/1996 and crystalline sugar EN 13708/2003), the TL method (EN 1788/2001), the PSL method (EN 13751/2002) and the DNA Comet Assay method (EN 13784/2001). The above detection methods will be applied on various foodstuffs such: garlic, onion, potatoes, rice, beans, wheat, maize, pistachio, sunflower

seeds, raisins, figs, strawberries, chicken, beef, fish, pepper, paprika, thymian, laurel and mushrooms. As an example of the application of a detection method, in the Figure 1 there are presented the ESR spectra of irradiated and nonirradiated paprika acquired according to ESR detection method for irradiated foodstuffs containing cellulose. First of all it can be noticed that the intensity of the signal of cellulose is much higher for the irradiated sample than that for the nonirradiated one and second that appear two radiation specific signals symmetrically to the cellulose signal. These two radiation specific signals prove the irradiation treatment of paprika.

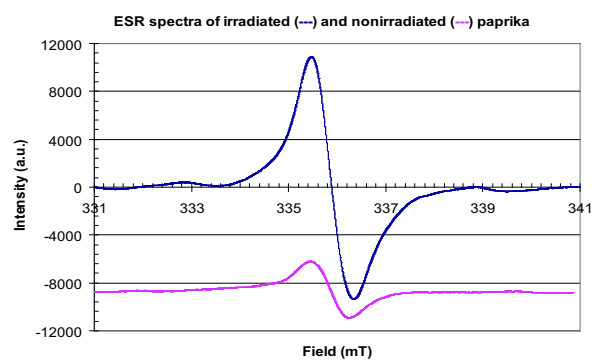


Figure 1: ESR spectra of irradiated and nonirradiated paprika

Neutron degradation of UV enhanced optical fibers for fusion installation plasma diagnostics

D. Sporea¹, I. Vata², D. Dudu², A. Danis²

¹ National Institute for Lasers, Plasma and Radiation Physics

² NIPNE-HH,Cyclotron

The design of ITER and the future operation of DEMO will require high-temperature, high-neutron flux materials to be used in plasma diagnostics, subjected to ITER requirements. A solution for remote plasma diagnostics implies the operation of various optical instruments placed apart from the critical temperature-neutron zones, with the optical signal transmitted over optical channels, for a reduction of radiation effects on the equipment, and a higher immunity to electromagnetic disturbances. Generally, data are available on the radiation effects on optical fibers used in communication applications or for transmission in the visible range. A special problem arises when optical signals have to be transmitted in the UV

region (200 nm to 450 nm), where attenuation over the distance is quite high (in the range of several meters), and the UV radiation by itself produces an increase of the attenuation upon several hours of exposure. Until now, practically no data on the radiation effects on optical fibers for fusion plasma diagnostics, operating in UV were published. In the frame of the EU's funded Fusion Programme, we focused on the evaluation of radiation induced changes in the optical transmission for different commercially available optical fibers, for their possible use in optical light guides. Pure silica optical fibers with an UV enhanced response, with various cladding/jacket materials, and core diameter of 200 μm and 400 μm were evaluated, as they are sub-

jected to neutron irradiation. The optical fiber core was of a high hydroxyl content type, and the coating was either Polymide or Al. Optical fibers with low (150°C) and high (350°C) temperature jacket materials were investigated. The optical fiber samples were irradiated at IFIN-HH U-120 Cyclotron facility. A maximum $10 \mu\text{A}$ beam of 13 MeV deuterons, when incident on the Be disk (165 mg/cm^2), produces a high neutron flux by stripping reactions. A dosimetric characterization of the neutron fields were performed prior to the radiation-damage studies. The threshold detectors (^{115}In , ^{197}Au), mica track detectors (Th and U), (^6LiF and ^7LiF) dosimeters were used to determine the neutron fluency and photon doses, and to measure the total absorbed dose angular distribution. The neutron flux at 0° (i.e. in the beam direction) was found to be equivalent to $2.13 \times 10^8 \text{ n}/(\text{cm}^2 \cdot \text{s} \cdot \mu\text{A})$, at 10 cm distance from Be target. The neutron energy spectrum shows a mean energy of 5.2 MeV. The neutron and gamma components of the mixed radiation field give rise respectively to 138 Gy/C and 2.38 Gy/C at 90 cm distance from Be target. The irradiation steps used correspond to about $6 \times 10^{10} \text{ n/cm}^2$. For the evaluation of the optical transmission degradation in optical fibers we developed a set-up enabling:

- a. the investigation on optical transmission of UV enhanced optical fibers, in the spectral range 200 - 400 nm, with spectral resolution of 1.5 nm, and 12 bits amplitude resolution of the transmission readings;
- b. the evaluation of temperature influence on optical transmission of optical fibers.

The set-up is based on a CW stabilized deuterium

source, a miniature, multi channels optical fiber spectrometer coupled to a PC via the USB link, and a programmable oven operating under the PC control. As the assessment of the optical transmission in optical fiber for the UV region is very difficult to carry out (source efficiency is very low, UV polarization effects in sampling probes are quite high, detection noise is significant in the CCD array) signal averaging and box-car smoothing were used for data processing. All the measurements were done off-line, at room temperature, between the irradiation steps. Absorption picks were observed for all the optical fibers at about 230 - 250 nm, with an amplitude increasing with the neutron flux. We noticed some absorption related recovery phenomena, induced by the fiber heating, even at ($100 - 120$) $^{\circ}\text{C}$. The paper was presented at 11-th International Conference on Fusion Reactor Materials, December 7-12, 2003, Kyoto, Japan and was published in J. Nuclear Materials, 329-333 (2004), pp. 1062-1065. The authors wishes to acknowledge the financial support of the European Union and of the Romanian Ministry for Education and Research, in the frame of the Fusion Programme, grant No. ERB 5005 CT 990 101/1999.

References

- [1] Energy spectrum of neutrons produced by deuterons on thick Be target. F. Tancu et al. Rev.Roum. Phys, Tome 28, no:10 p 857-865 (1983)

Contribution to the ATLAS online software

E. Bădescu¹, M. Caprini¹, C. Caramarcu¹, C. Gruse¹

¹ NIPNE-HH, Departament of Applied Physics

The Online Software [1] is a part of the distributed Data Acquisition System (DAQ) for the ATLAS experiment, that will start taking data in 2007 at the Large Hadron Collider at CERN.

The Online Software system is responsible for overall experiment control, including run control, configuration and monitoring of Trigger Data Acquisition System (TDAQ) and management of data-taking partitions. The system encompasses all the software for configuring, controlling and monitoring the data acquisition system, but excludes the management, processing or transportation of physics data. The Online Software is supposed to act as the "glue" of several heterogeneous data acquisition sub-systems.

The integration of the Online Software with other

sub-systems activity provides new subsequent software releases which have to be tested for functionality, performance and scalability for both CERN **afs** and local downloaded versions.

The main functionalities of the Online Software are provided without the need of commercial packages and the software is available for users by download at URL <http://atlas-onlsw.web.cern.ch/Atlas-onlsw/download/download.htm>.

Functionality tests have been performed for all four official releases issued in 2004 on both **afs** and **downloaded** installations. Performance and scalability tests have been performed at CERN on online-00-21-01 release only. The results of tests have been addressed to the Online Software developers to be taken

into account in further software versions or patches.

In order to test Online Software releases' functionality on single- and multi-host partitions, at NIPNE has been prepared a special hardware configuration. The testbed consists of five computers, on all of them have been installed the Online Software according to the specific platform (one Scientific Linux CERN version 3 server and three workstations, and one RedHat 7.3.1 workstation), C++ compilers and new Java version.

On server a **nfs** file system has been installed and accessed by all the other workstations by LAN, a special account has been created and **ssh** has been configured to access directly this account, with no password, on all of these machines, in order to allow CORBA based communication.

The downloaded versions of the working or official releases were installed in **nfs** area, on the server, therefore a lot of functionality tests were performed on local testbed. As long as all the hardware and software configurations of the data taking partitions are stored in configuration databases [2], we had to provide the configuration databases for multi-host testing partitions on the local testbed.

The Online Software has been deployed for various test beam activities at CERN [3]. In 2004 a combined beam test of all sub-detectors, with more than 60 controllers and running on 40 workstations, was configured and controlled successfully by the Online Software. Figure 1 shows the Integrated User Interface (IGUI) for one of this combined beam test run. These activities are providing important feedback into the development cycle.

Work performed under contracts no. 11/2002 and 4-1/2004 in the frame of the CERES Programme supported by the Romanian Ministry of Education and Research.

References

- [1] ATLAS High-Level Trigger, Data Acquisition and Control Technical Design Report - CERN/LHCC/2003-22, 30 June 2003
- [2] D.Burckhart-Chromek, E. Badescu, M. Capriniet al., The Configurations Database Challenge in the ATLAS DAQ System - CHEP 2004, 27th September - 1st October, 2004, Interlaken, Switzerland
- [3] I. Alexandrov, E. Badescu, M. Caprini et al., Online Software for the ATLAS Test Beam Data Acquisition System - IEEE Transactions on Nuclear Science, Volume: 51, Number: 3, June 2004, pg. 578-584

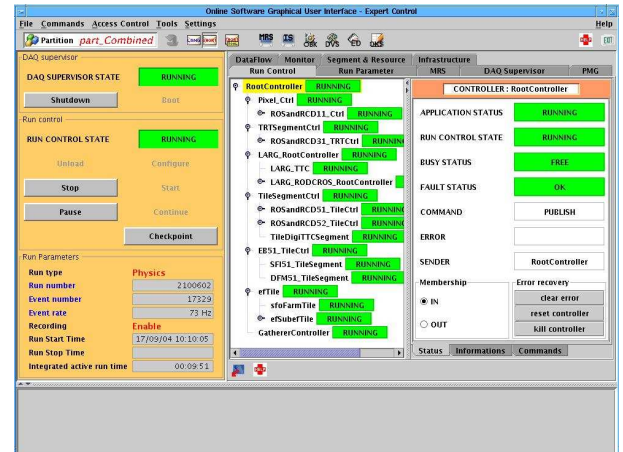


Figure 1: The IGUI for combined beam test in 2004

Appendix

Publications	109
In Journals	109
Books and Chapter in Books	113
Preprints	113
International Conferences	114
PhD Theses	118
Scientific Exchanges	119
Foreign Visitors	119
Visits Abroad	119
Seminars Abroad	120
Research Staff	121
Author Index	125

Publications

In Journals

C.S. Acatrinei

Canonical Quantization of Noncommutative Field Theory
*Phys. Rev. D*67, 045020 (2003).

C.S. Acatrinei, C. Sochichiu

A Note on the Decay of Noncommutative Solitons
*Phys. Rev. D*67, 125017 (2003).

Adam Gh., Adam S., Plakida N.M.

Reliability conditions on quadrature algorithms
Computer Physics Communications vol. 154 (no. 1), 49–64 (2003)

Adam Gh., Adam S.

Reliable software in computational physics
Romanian Reports in Physics vol. 55 (no. 4) (2003)

Plakida N.M., Anton L., Adam S., Adam Gh.

Exchange and spin-fluctuation mechanisms of superconductivity in cuprates
ZhETF vol. 124 (no. 2), 367–378 (2003) English translation: *JETP* vol. 97 (no. 2), 331–342 (2003)

Al. H. Raduta and Ad. R. Raduta

Homogeneity and size effects on the liquid-gas coexistence curve
Nucl. Phys. A 724, 233-240, 2003

F. Gulminelli, Ph. Chomaz, Al. H. Raduta, Ad. R. Raduta

Influence of the Coulomb interaction on the liquid-gas phase transition and nuclear multifragmentation
Phys. Rev. Lett. 91, 202701, 2003

T. Antoni et al. - KASCADE collaboration

Large scale cosmic-ray anisotropy with KASCADE
Astrophys.J. 604 (2004) 687

T. Antoni et al. - KASCADE collaboration

Search for cosmic ray point sources with KASCADE
Astrophys.J. 608 (2004) 865

T. Antoni et.al. - KASCADE Collaboration

Measurements of attenuation and absorption lengths with the KASCADE experiment
*Astropart.Phys.*19 (2003) 703-714

T. Antoni et.al. - KASCADE Collaboration

Preparation of enriched cosmic rays groups with KASCADE
*Astropart.Phys.*19 (2003) 713-728

T. Antoni et.al. - KASCADE Collaboration

The information from muon arrival time distributions of high-energy EAS as measured with the KASCADE detector

*Astropart.Phys.*18 (2003) 319

T. Antoni, et al. - KASCADE collaboration

The cosmic-ray experiment KASCADE
*Nucl.Instr.Meth.in Physics Research A*513 (2003)490

A.F. Badea et al. - KASCADE Collaboration

Sensitivity and consistency studies of muon arrival time distributions measured by KASCADE
Nucl. Phys. B(Proc.Suppl.) 122 (2003) 271

... E. Badescu, M. Caprini et al.

Online Software for the ATLAS Test Beam Data Acquisition System
IEEE Trans. Nucl. Sci. vol. 51, pp. 578-584, June 2004

S. Berceanu and A. Gheorghe

Differential operators on orbits of coherent states
Rom. Jour. Phys. 48, Nos. 4-5, 545-556 (2003)

S. Berceanu

On the continuity of the geometry school in Kazan
Academica 10, 55-58 (2003)

I.M. Brancus, H.Rebel, A.F.Badea, A.Haungs, C.D.Aiftimiei, J.Oehlschlaeger, M.Duma

Features of muon arrival time distributions of high energy EAS at large distance from the shower core
*J.Phys.G : Nucl.Part.Phys.*29(2003) 453

I.M. Brancus, J. Wentz, B. Mitrica, H. Rebel, M. Petcu, H. Bozdog, H.J. Mathes, A.F. Badea, A. Bercuci, C. Aiftimiei, M. Duma, A. Meli, G. Toma, B. Vulpescu

The East-West effect of the muon charge ratio at energies relevant to the atmospheric neutrino anomaly
*Nucl.Phys.A*721 (2003) 1044c

Carjan N., Rizea M., Strottman D.

Efficient numerical solution of the time - dependent Schrödinger equation for deep tunneling
Romanian Reports in Physics, vol. 55 no. 4, p. 555 - 579, 2003

A. Ramani, A.S. Cârstea, R. Willox, B. Grammaticos

Oscillating Epidemics, A Discrete time model
Physica A 333, 278 (2004)

- A. S. Carstea, A. Ramani, R. Willox, B. Grammaticos**
Discrete Painlevé II equations, Miura and auto-Bäcklund transformations
J. Phys. A: Math. Gen. **36**, 31, 8419, (2003)
- A.S. Cârstea, D. Grecu, Anca Vișinescu**
Localized and nonlocalized structures in nonlinear lattices with fermions
Europhysics Letters, **64** (4), 531-537 (2004)
- J. Satsuma, R. Willox, A. Ramani, B. Grammaticos, A.S. Cârstea**
Extending SIR epidemic model
Physica A, **369**, (2004)
- K.M. Tamizhmani, A. Ramani, B. Grammaticos, A.S. Cârstea**
Modelling AIDS epidemics dynamics and treatment with difference equations
Advances in Difference Equations, **3**, 183 (2004)
- K.M. Tamizhmani, B. Grammaticos, A.S. Cârstea, A. Ramani**
The q-discrete Painlevé IV equations and their properties
Reg. Chaotic Dynamics, **9**, 13 (2004)
- B. Constantinescu, A. Sasianu, R. Bugoi**
Adulterations in First Century B. C.: the Case of Greek Silver Drachmae Analysed by X-Ray Methods
Spectrochimica Acta, part B: Atomic Spectroscopy **58/4** (2003) 755-761
- M. Chipara, J. R. Romero, M. Ignat, B. Constantinescu**
ESR studies on collagen irradiated with protons
Polymer Degradation Stability **80**(1) (2003) 45-49
- R. Bugoi, V. Cojocaru, B. Constantinescu, F. Constantin, D. Grambole, F. Herrmann**
Micro-PIXE Study of Gold Archaeological Objects
Journal of Radioanalytical and Nuclear Chemistry vol. 257 no. 2 (2003) 375-383
- I.I.Cotăescu and M. Vișinescu**
Dirac operators on Taub-NUT space: Relationship and discrete transformations
General Relativity and Gravitation **35**, 389 (2003)
- L.-C. Crasovan, V. M. Perez-Garcia, I. Danaila, D. Mihalache, L. Torner**
Three-dimensional parallel vortex rings in Bose-Einstein condensates
Physical Review A **70**, 033605 (2004)
- L.-C. Crasovan, V. Vekslerchik, V. M. Perez-Garcia, J. P. Torres, D. Mihalache, L. Torner**
Stable vortex dipoles in non-rotating Bose-Einstein condensates
Physical Review A **68**, 063609 (2003)
- L.-C. Crasovan, Y. V. Kartashov, D. Mihalache, L. Torner, Yu. S. Kivshar, V. M. Perez-Garcia**
Soliton “molecules”: Robust clusters of spatiotemporal optical solitons
Physical Review E **67**, 046610 (2003)
- L.-C. Crasovan, J. P. Torres, D. Mihalache, L. Torner**
Arresting wave collapse by wave self-rectification
Physical Review Letters **91**, 063904 (2003)
- L.-C. Crasovan, V. Vekslerchik, D. Mihalache, J. P. Torres, V. M. Perez-Garcia, L. Torner**
Globally-linked vortex clusters
Proc. of NATO ASI "Nonlinear Waves: Classical and Quantum Aspects", p. 81-98, F. Kh. Abdullaev and V. V. Konotop (eds.), Kluwer Academic Publishers, 2004
- L. Dinescu, E. Steinnes, O.G. Duliu, C. Ciortea, T.E. Sjobakk, D.E. Dumitriu, M.M. Gugiu, M. Toma**
Distribution of some major and trace elements in Danube Delta lacustrine sediments and soil
Romanian Reports in Physics, Vol. 56, No. 4, P. 711-720, 2004
- P. Diță**
Motion on the n -dimensional ellipsoid under the influence of a harmonic force revisited
J.Phys.A: Math.Gen **36** (2003) 10159-10172
- P. Diță**
Parameterisation of unitary matrices
J.Phys.A: Math.Gen **36** (2003) 2781-2789
- M. Falcitelli, S. Ianuș, A. M. Pastore and M. Vișinescu**
Some applications of Riemannian submersions in physics
Rom. Journ. Phys. **48**, No. 5-6 (2003)
- Georgescu Rodica**
Evaluation the Measurement Uncertainty of Absorbed Dose for ECB Dosimetry System at IRASM "METROLOGIE", vol. L, nr. 2/2003
- G. Royer, C. Bonilla and R. A. Gherghescu**
Stability of rotating ^{44}Ti , ^{56}Ni and ^{126}Ba nuclei in the fusion-like deformation path.
Physical Review C **67**, 034315 (2003)
- R. A. Gherghescu and G. Royer**
Shape isomerism of rotating ^{44}Ti and ^{48}Cr
Physical Review C **68**, 014315 (2003)
- R. A. Gherghescu and W. Greiner**
Charge density influence on cold fusion barriers.
Physical Review C **68**, 044314 (2003)
- R. A. Gherghescu**
Deformed two center shell model
Physical Review C **67**, 014309 (2003)

- R. A. Gherghescu, W. Greiner and G. Muenzenberg**
Shell effects in cold fusion reactions.
Physical Review C **68**, 054314 (2003)
- C. Grama, N. Grama, I. Zamfirescu**
Jump phenomenon induced by potential strength variation and the influence of exotic resonant states
Phys. Rev. A **68**, 032723 (2003)
- D. Grecu, Anca Vișinescu**
Influence of third order dispersion on the bound state of two solitons of the NLS equation
Rom. Journ. Phys. **48** nr 5-6 (2003)
- D. Grecu, Anca Vișinescu**
Modulational instability of some nonlinear continuum and discrete systems
Nonlinear Waves, Kluwer Acad. Publish., 151-165 (2004)
- D. Grecu, Anca Vișinescu, A.S. Cârstea**
Crossover behaviour between KdV and mKdV equations in a cold plasma with negative ions
American Institute of Physics Conference Proceedings vol. 729, 332-338 (2004)
- D. Grecu, Anca Vișinescu, A.T. Grecu**
Modulational instability phenomenon of quasi-monochromatic waves propagating in dispersive and weakly nonlinear media
Interdisciplinary applications of fractals and chaos theory, ed. Academiei, 406-413 (2004)
- D. Grecu, Anca Vișinescu, I. Turcu**
Ratchet Motion and Quantum Motors in Biological Systems
Studia Universitatis Babeș-Bolyai, Physica, special Issue 2003
- D. Grecu, Anca Vișinescu**
Higher order dispersion effects on the modulational instability of NLS type equations
Romanian Reports in Physics **55** nr.4, 444-452 (2003)
- Grigore D. R., Scharf G.**
A Supersymmetric Extension of Quantum Gauge Theory
Annalen der Physik **12**, 5-36 (2003)
- Grigore D. R., Scharf G.**
The Quantum Supersymmetric Vector Multiplet and Some Problems in Non-Abelian Supergauge Theory
Annalen der Physik **12**, 643-683 (2003)
- A. Haungs et al. - KASCADE collaboration**
Large scale cosmic-ray anisotropy with KASCADE
Acta Phys. Polon. B **35** (2004) 331
- A. Haungs et.al. - KASCADE Collaboration**
Muon density spectra as a probe of the muon component predicted by air shower simulations
Nucl. Phys. B(Proc. Suppl.) **122** (2003) 384
- J. Hoerandel et al. - KASCADE Collaboration**
On the hadronic component of extensive air showers
Nucl. Phys. B(Proc. Suppl.) **122** (2003) 309
- Isar A., Sandulescu A., Scheid W.**
Lindblad master equation for the damped harmonic oscillator with deformed dissipation
Physica A **322**, 233 (2003)
- Isar A.**
Uncertainty relations in the theory of open quantum systems
Romanian J. Phys. **48**, 705 (2003)
- KyungJoong Kim, R. Cools, L. Gr. Ixaru**
Extended quadrature rules for oscillatory integrands
Appl. Numer. Math. **46**, 59 – 73, 2003
- L. Gr. Ixaru, G. Vanden Berghe, H. De Meyer**
Exponentially fitted variable two-step BDF algorithm for first order ODEs
Comput. Phys. Commun. **150**, 116 – 128, 2003
- K.H. Kampert et al. - KASCADE Collaboration**
Status of the KASCADE -Grande experiment
Nucl. Phys. B(Proc. Suppl.) **122** (2003) 422
- K.H. Kampert et al. - KASCADE collaboration**
Cosmic Rays in the "knee" region -Recent results from KASCADE
Acta Phys. Polon. B **35** (2004) 1799
- I. V. Melnikov, H. Leblond, F. Sanchez, and D. Mihalache**
Nonlinear optics of a few-cycle optical pulse: Slow-enveloppe approximation revisited
IEEE J. Selected Top. in Quantum Electron. **10**, 870-875 (2004)
- D. Mihalache, D. Mazilu, B. A. Malomed, F. Lederer**
Stable vortex solitons supported by competing quadratic and cubic nonlinearities
Physical Review E **69**, 066614 (2004)
- D. Mihalache, D. Mazilu, B. A. Malomed, and F. Lederer**
Stable vortex solitons in a vectorial cubic-quintic model
J. Opt. B: Quantum Semiclass. Opt. **6**, S341-S350 (2004)
- D. Mihalache, D. Mazilu, F. Lederer, Y. V. Kartashov, L.-C. Crasovan, L. Torner**
Stable three-dimensional spatiotemporal solitons in a two-dimensional photonic lattice
Physical Review E **70**, 055603(R) (2004)
- D. Mihalache, D. Mazilu, I. Towers, B. A. Malomed, F. Lederer**
Stable spatiotemporal spinning solitons in a bimodal cubic-quintic medium
Physical Review E **67**, 056608 (2003)

- D. Mihalache, D. Mazilu, L.-C. Crasovan, B. A. Malomed, F. Lederer, L. Torner**
 Robust soliton clusters in media with competing cubic and quintic nonlinearities
Physical Review E **68**, 046612 (2003)
- D. Mihalache, D. Mazilu, L.-C. Crasovan, B.A. Malomed, F. Lederer, L. Torner**
 Soliton clusters in three-dimensional media with competing cubic and quintic nonlinearities
J. Opt. B: Quantum Semiclass. Opt. **6**, S333-S340 (2004)
- D. Mihalache**
 Spatiotemporal optical solitons: an overview
Proceedings of SPIE **5581**, pp. 564-570 (2004)
- H. Milke et al. - KASCADE collaboration**
 Test of hadronic interaction models with KASCADE
Acta Phys. Polon. B **35** (2004) 341
- M. Mirea, L. Groza, M. Apostol and M. Ganciu**
 Energy Loss and Straggling of Electrons
Romanian Reports in Physics **55**, 609 (2003)
- G. Fares, R. Bimbot, S. Hachem, M. Mirea, R. Anne, T. Benfoughal, C. Cabot, F. Clapier, P. Delbourgo-Salvador, T. Ethvignot, A. Lefebvre, M. Lewitowitz, P. Roussel-Chomaz, M.G. Saint-Laurent, J.E. Sauvestre, J.L. Sida and Yang Yong Feng**
 Fragmentation of 95 MeV/u ^{12}C and ^{13}C . Application to Secondary-Beam Production
European Physical Journal A **19** 105 (2004)
- M. Mirea, L. Tassan-Got, C. Stephan and C.O. Bacri**
 Dissipation in Low Energy Fission
Nuclear Physics A **735** 21 (2004)
- M. Mirea, O. Bajeat, F. Clapier, E. Essabaa, L. Groza, F. Ibrahim, S. Kandri-Rody, A.C. Mueller, N. Pauwels and J. Proust**
 Exploratory Analysis of a Neutron-Rich Nuclei Source Based on Photo-Fission
Nuclear Instruments and Methods B **201**, 443 (2003)
- M. Mirea**
 Landau-Zener Effect in Superfluid Nuclear Systems
Modern Physics Letters A **18** 1809 (2003)
- G. Navarra et al. - KASCADE collaboration**
 KASCADE-Grande: A Large Acceptance High Resolution Cosmic-Ray Detector up to 10^{18} eV
Nucl. Instr. Meth. in Phys. Res. A **518** (2004) 207
- N.-C. Panoiu, D. Mihalache, D. Mazilu, F. Lederer, R. M. Osgood**
 Two-dimensional solitons in quasi-phase-matched quadratic crystals
Physical Review E **68**, 016608 (2003)
- N.-C. Panoiu, D. Mihalache, H. Rao, R. M. Osgood**
 Spatial solitons in type II quasiphase-matched slab waveguides
Physical Review E **68**, 065603(R) (2003)
- N.-C. Panoiu, D. Mihalache, D. Mazilu, F. Lederer, R. M. Osgood**
 Vectorial spatial solitons in bulk periodic quadratically nonlinear media
J. Opt. B: Quantum Semiclass. Opt. **6**, S351-S360 (2004)
- N.-C. Panoiu, D. Mihalache, D. Mazilu, I. V. Melnikov, J. S. Aitchison, F. Lederer, R. M. Osgood**
 Dynamics of dual-frequency solitons under the influence of frequency-sliding filters, third-order dispersion, and intrapulse Raman scattering
IEEE J. Select. Top. in Quantum Electron. **10**, 885-892 (2004)
- D. N. Poenaru and W. Greiner**
 Deformation Energy Minima at Finite Mass Asymmetry
Europhysics Letters **64**, 164-170 (2003)
- D. N. Poenaru, R. A. Gherghescu, W. Greiner, Y. Nagame, J. H. Hamilton, and A. V. Ramayya**
 True ternary fission.
Romanian Reports in Physics **55**, 549-554 (2003)
- D. N. Poenaru, W. Greiner, R. A. Gherghescu, and Y. Nagame**
 Advances in fission and spontaneous emission of heavy particles from nuclei.
Romanian Journal of Physics **48 Suppl. I**, 143-153 (2003)
- M. Roth et al. - KASCADE Collaboration**
 Determination of the primary energy and mass in the PeV region by Bayesian unfolding techniques
Nucl. Phys. B (Proc. Suppl.) **122** (2003) 317
- S. Stoica and Klapdor Kleigrothaus**
 Calculation of the $\beta^+\beta^+$, β^+/EC and EC/EC half-lives for Cd-106 with the second QRPA method
EUR. Phys. Journ. A **17**, 529 (2003)
- M. Toma, L. Dinescu, O. Sima**
 New data concerning the efficiency calibration of a drum waste assay system
Journal of Radioanalytical and Nuclear Chemistry, Vol. 262, No. 2 (2004) 345-354
- Anca Vișinescu, D. Grecu**
 Modulational Instability and Multiple Scales Analysis of Davydov Model
Proceedings of Institute of Mathematics of NAS of Ukraine vol.50, 1502-1510 (2004)

Anca Vișinescu, D. Grecu

Modulational instability of some nonlinear continuum and discrete systems

American Institute of Physics Conference Proceedings, vol. 729, 389-398 (2004)

Anca Vișinescu, D. Grecu

Statistical approach of the modulational instability of the discrete self-trapping equation

Eur. Phys. J. B 34, 225-229 (2003)

M. Vișinescu

Geometrie și gravitație

Academica 11, 64 (2003)

J. Wentz, I.M.Brancus, A.Bercuci, D.Heck, J.Oehlschlaeger, H.Rebel, B.Vulpescu

Simulation of atmospheric muon and neutrino fluxes with CORSIKA

Phys.Rev.D, 2003, Phys.Rev.D 67 (2003) 07320

Z. Xu, Y. V. Kartashov, L.-C. Crasovan, D. Mihalache, L. Torner

Spatiotemporal discrete multicolor solitons

Physical Review E 70, 066618 (2004)

Books and Chapter in Books

A.C. Mueller, M. Mirea, L. Tassangot

New Applications of Nuclear Fission

World Scientific 2004

Preprints

...E. Badescu, M. Caprini et al.

An on-line Integrated Bookkeeping: electronic run log book and Meta-Data Repository for ATLAS

ATL-DAQ-2004-002

I.I.Cotăescu and M. Vișinescu

The induced representation of the isometry group of the Euclidean Taub-NUT space and new spherical harmonics

hep-th/0312129, to appear in Mod. Phys. Lett. A (2004)

Grigore D. R., Scharf G.

Quantum EXtended Supersymmetries

hep-th/0303176

D. N. Poenaru, R. A. Gherghescu, Y.Nagame, and W. Greiner

Fission paths for fragmentation in three and more than three nuclei

Report WP18 65-03, IDRANAP, Centre of Excellence of EC from IFIN-HH, 2003.

International Conferences

Adam Gh.

An insight into computational physics

Cooperation between JINR and Romanian scientific centres and universities, Proceedings of the round-table meeting "Romania at JINR" held in the framework of the 49-th session of the JINR Scientific Council on 6 June 2003 (V. Kadyshevsky, A. Syssakian, D. Popescu, Gh. Stratan, Eds.) JINR-Dubna, 2003, pp. 33-40

Ad. R. Raduta and Al. H. Raduta

Fingerprints of finite size effects in nuclear multifragmentation

International Workshop on New Applications of Nuclear Fission, Bucharest, Romania, 2003

Ad. R. Raduta and Al. H. Raduta

Isoscaling in a microcanonical nuclear multifragmentation model

International Workshop on Multifragmentation and related areas, Caen, France, 2003

A.T. Grecu

Modulational instability of derivative NLS equation

Conferinta Nationala de Fizica, Pitesti, 13-16 sept. 2004

A.T. Grecu

Modulational instability of derivative NLS equation

Quantum Field Theories and Hamiltonian Systems, Calimanesti, 16-22 oct. 2004

... E. Badescu, M. Caprini et al.

Experience with CORBA communication middleware in the ATLAS DAQ - CHEP 2004

27th September - 1st October, 2004, Interlaken, Switzerland

...E. Badescu, M. Caprini et al.

Conditions Databases: the interfaces between the different ATLAS systems

CHEP 2004, 27th September - 1st October, 2004, Interlaken, Switzerland

...E. Badescu, M. Caprini et al.

Control in the ATLAS DAQ System

CHEP 2004, 27th September - 1st October, 2004, Interlaken, Switzerland

...E. Badescu, M. Caprini et al.

The Configurations Database Challenge in the ATLAS DAQ System

CHEP 2004, 27th September - 1st October, 2004, Interlaken, Switzerland

S. Berceanu, A. Gheorghe

A holomorphic representation of coherent state algebras of semidirect product type

Annual conference of communications of NIPNE, Bucharest, Romania, 17-19 December 2003

S. Berceanu

Realization of coherent state algebras by differential operators

2nd Operator Algebras and Mathematical Physics Conference, Sinaia, June 26-July 04, 2003

S. Berceanu

Geometrical phases on hermitian symmetric spaces in

*Recent Advances in Geometry and Topology
Proceedings of the The Sixth International Workshop on Differential Geometry and its Applications and The Third German-Romanian Seminar on Geometry, Cluj-Napoca - ROMANIA, Editors Dorin Andrica, Paul A.Bлага, Cluj University Press (2004)*

S. Berceanu

A holomorphic representation of the Jacobi algebra invited talk at the XXIII Workshop on Geometric Methods in Physics, 27 June - 3 July 2004, Bialowieza, Poland

I.M. Brancus et al.

Simulation of Atmospheric Neutrino Fluxes with CORSIKA

1403, ICRC2003, Tsukuba, Japan

I.M. Brancus et al.

The Charge Ratio of the Atmospheric Muons as Probe for Azimuthal Asymmetry

1187, ICRC2003, Tsukuba, Japan

I.M. Brancus for the KASCADE-Grande Collaboration

The Role of Measurements of Muon Arrival Time Distributions for the Mass Discrimination of High Energy EAS

41, ICRC2003, Tsukuba, Japan

I.M. Brancus, B. Mitrica, G. Toma, H. Rebel, O. Sima, A. Haungs, F. Badea, J. Oehlschlaeger

Studies of primary energy estimation and mass discrimination of cosmic rays by the EAS lateral charged particle distributions simulated for KASCADE Grande ECRS2004, "European Cosmic Rays Conference", Florenta, Italia, 28.08.2004 - 04.09.2004

I.M. Brancus, J. Wentz, B. Mitrica, M. Petcu, H. Rebel, A. Bercuci, C. Aiftimiei, M. Duma, G. Toma

Azimuthal asymmetry of the charge ratio of atmospheric muons as probe of the influence of the geomagnetic field

INPC2004, "International Nuclear Physics Conference", Goeteborg Suedia, 27.06.2004 - 03.07.2004

- M. Bucataru-Nicu, L. Lungu, C.N. Turcanu, Gh. Rotarescu**
Durability of cemented waste in repository and under simulated conditions
IAEA-TECDOC-1397, June 2004
- A.S. Cârstea**
Supersymmetric Solitons and Integrability
Quantum Field Theories and Hamiltonian Systems, Calimanesti, 16-22 oct. 2004
- A. Chiavassa for the KASCADE-Grande Collaboration**
KASCADE-Grande: The Grande Array
989, ICRC2003, Tsukuba, Japan
- B. Constantinescu**
XRF Analysis of Archaeological Objects from Romanian Museums
IAEA Meeting on Material Analysis using XRF Portable Equipments, Vienna, September, 2003
- L. Dinescu, O.G. Duliu, E. Steinnes, C. Ciortea, D. Fluerasu, M. Toma**
Investigation of the radioactive and heavy metal pollution of the Danube Delta lacustrine sediments and soil
Environmental Physics Conference EPC'4, 24 - 28 Feb. 2004, Minya, Egypt
- P. Dită**
Density operators on finite-dimensional spaces
Coferința Anuală IFIN-HH, 17-19 Decembrie 2003
- R. Engel et al.**
One-Dimensional Hybrid Simulation of EAS Using KASCADE Equations
511, ICRC2003, Tsukuba, Japan
- M.V. Frontasieva, O. Culicov, L. Dinescu, A. Pantelica**
Retrospective review and future prospects of russian - romanian studies in life sciences using INAA at IBR-2 reactor of Dubna
International Balkan Workshop on Applied Physics, 5-7 July 2004, Constanta, Romania
- N. Grama, C. Grama, I. Zamfirescu**
Riemann surface approach to bound and resonant states: Exotic poles and resonant states
CAIM, Conference on Applied and Industrial Mathematics, Oradea, May 29-31, 2003
- N. Grama, C. Grama, I. Zamfirescu**
Uniform asymptotic approximation of 3-D Coulomb scattering wave function
CAIM, Conference on Applied and Industrial Mathematics, Oradea, May 29-31, 2003
- N. Grama**
Parent di-nuclear quasimolecular states as exotic resonant states
International workshop "New applications of nuclear fission" NANUF03, Bucharest, September 7-12, 2003
- D. Grecu, Anca Vișinescu**
Modulational Instability of some Nonlinear Continuum and Discrete Systems
"Nonlinear Waves: Classical and Quantum Aspects", Estoril, Portugalia, 13-17 iulie 2003
- D. Grecu, Anca Vișinescu**
Randomness Effects on Modulational Instability of a Discrete Self-trapping Equation
Conferința Balcanică de Fizică BPU-5, Vrnjacka Banja, Serbia, august 2003
- D. Grecu, Anca Vișinescu, A.S. Cârstea, A.T. Grecu**
Modulational instability and soliton generation in nonlinear evolution equations
Quantum Field Theories and Hamiltonian Systems, Calimanesti, 16-22 oct. 2004
- D. Grecu, Anca Vișinescu**
Crossover behaviour between KdV and mKdV equations in a cold plasma with negative ions
International Workshop on Global Analysis, Ankara, Turkey, 15-17 April 2004
- D. Grecu, Anca Vișinescu**
IST for a completely integrable reaction-diffusion system
Physics Conference TIM03, Timișoara , november 2003
- D. Grecu, Anca Vișinescu**
Long wave-short wave resonance in complex molecular systems: Davydov's model
Conferinta Nationala de Fizica, Pitesti, 13-16 sept. 2004
- D. Grecu, Anca Vișinescu**
Modulational Instability of Quasi-monochromatic Waves Propagating in Dispersive and Weakly Nonlinear Media
"Interdisciplinary Approaches in Fractal Analysis" IAFA, p. 158-164, mai 2003
- D. Grecu, Anca Vișinescu**
Statistical Approach on modulational instability in nonlinear discrete systems
Nonlinear Physics: Theory and Experiment, Gallipoli (Lecce) Italia, 24 June- 3 July 2004
- A. Haungs for the KASCADE Collaboration**
Analysis of Air Showers at the Trigger Threshold of KASCADE
17, ICRC2003, Tsukuba, Japan
- A. Haungs for the KASCADE-Grande Collaboration**
Muon Density Measurements as Probe of the Muon Component of Air-Shower Simulations
37, ICRC2003, Tsukuba, Japan
- A. Haungs for the KASCADE-Grande Collaboration**
The KASCADE-Grande Experiment
985, ICRC2003, Tsukuba, Japan

J. Hoerandel for the KASCADE Collaboration
A Measurement of the Energy Spectrum of Unaccompanied Hadrons
101, ICRC2003, Tsukuba, Japan

Isar A.

Deformed open quantum systems

International Workshop on "New applications of nuclear fission" NANUF03, Bucharest, 2003

Isar A.

Quantum deformation in open systems

First Annual Conference on Physics - IFIN, Bucharest-Magurele, 2003

C. Ivan, F. Dragolici, Gh. Rotarescu

Preliminary studies on the elaboration of technologies for long term storage of radium spent sealed sources

Annual Conference "Horia Hulubei" National Institute of R&D for Physics and Nuclear Engineering, December 17-19 2003, Bucharest-Magurele

L. Lungu, M. Nicu, Gh. Rotarescu, C. Turcanu

Studies on cement matrix used at the Radioactive Waste Treatment Plant for Radwaste Conditioning

Annual Conference "Horia Hulubei" National Institute of R&D for Physics and Nuclear Engineering, December 17-19 2003, Bucharest-Magurele

Maier for the KASCADE-Grande Collaboration

Shower Reconstruction Performance of KASCADE-Grande

81, ICRC2003, Tsukuba, Japan

M. Dobson on behalf of the ATLAS collaboration

Integration of ATLAS Software in the Combined Beam Test

CHEP 2004, 27th September - 1st October, 2004, Interlaken, Switzerland

M. Mirea, L. Groza, O. Bajeat, F. Clapier, S. Essabaa, F. Ibrahim, A.C. Mueller and J. Proust

Analysis of a Neutron-Rich Nuclei Source Based on Photo-Fission

International Workshop New Applications of Nuclear Fission (NANUF03), Eds. A.C. Mueller, M. Mirea and L. Tassan-Got, World Scientific, Singapore 2004, p 132

M. Mirea

Dissipation in a Wide Range of Mass-Asymmetries

International Workshop New Applications of Nuclear Fission (NANUF03), Eds. A.C. Mueller, M. Mirea and L. Tassan-Got, World Scientific, Singapore 2004, p 132

O. Bajeat, S. Essabaa, F. Ibrahim, C. Lau, Y. Huguet, P. Jardin, N. Lecesne, R. Leroy, F. Pellemoine, M.G. Saint-Laurent, A.C.C. Villari, F. Nizery, A Plukis, D. Ridikas, J.M. Gauzier and M. Mirea

Optimization of ISOL UCx Targets for Fission Induced by Fast Neutrons or Electrons

International Workshop New Applications of Nuclear Fission (NANUF03), Eds. A.C. Mueller, M. Mirea and L. Tassan-Got, World Scientific, Singapore 2004, p 132

Mișicu Ș., Rizea M., Greiner W.

Electromagnetic radiation in quantum tunneling

The International Symposium on Channeling - Bent Crystals - Radiation Processes, Frankfurt am Main, Germany, 5-6 June 2003

B. Mitrica, A. Bercuci

Muon Decay, a possibility for precise measurements of muon charge ratio in the low energy range ($< 1 \text{ GeV}/c$)

NANUF 2003, Bucharest, Romania

B. Mitrica, I.M. Brancus, H. Rebel, J. Wentz, A. Bercuci, G. Toma, C. Aiftimie, M. Duma

Experimentally guided Monte Carlo calculations of the atmospheric muon and neutrino flux

ISVHECR2004, "International Symposium of Very High Energy Cosmic Rays Interactions", Pylos, Greece, 06.09.2004 - 12.09.2004

B. Mitrica, I.M. Brancus, J. Wentz, M. Petcu, H. Rebel, A. Bercuci, C. Aiftimie, M. Duma, G. Toma

Experimentally guided Monte Carlo calculations of the atmospheric muon flux for interdisciplinary applications

INPC2004, "International Nuclear Physics Conference", Goeteborg Suedia, 27.06.2004 - 03.07.2004

D. Fong, W. Greiner, D. N. Poenaru, et al.(total 26 authors)

Hot bimodal ternary fission in ^{252}Cf

oral contribution, in Fission and Properties of Neutron-Rich Nuclei, Proc. of the 3rd International Conference, Sanibel Island, Eds J. H. Hamilton, A. V. Ramayya, and H. K. Carter (World Scientific, Singapore, 2003), p. 454-459.

D. N. Poenaru, R. A. Gherghescu, W. Greiner, and A. V. Ramayya

Equilibrium shapes in cold fission phenomena

invited talk, in Proc. Jefferson Lab. and University of Georgia Workshop on Modern Sub-Nuclear Physics and JLAB Experiments, Eds W. Roberts and G. Strobel, (Jefferson Lab., 2003), p. 19-26.

D. N. Poenaru, R. Gherghescu, W. Greiner

Fission into equally sized three fragments

invited talk, in Nuclear Clusters: from Light Exotic to Superheavy Nuclei, Proc. Internat. Symposium 248. WE-Heraeus-Seminar, Rauischholzhausen, Eds R. Jolos and W. Scheid (EP Systema Bt., Debrecen, 2003), p. 283-288.

D. N. Poenaru, W. Greiner, R. A. Gherghescu, J. H. Hamilton, and A. V. Ramayya

Heavy Ion Radioactivities

invited talk, in Fission and Properties of Neutron-Rich Nuclei, Proc. of the 3rd International Conference, Sanibel Island, Eds J. H. Hamilton, A. V. Ramayya, and H. K. Carter (World Scientific, Singapore, 2003), p. 527-534.

D. N. Poenaru

Nuclear physicist point of view

invited talk, SERENATE (European Research and Education Networking) End-user workshop, IBM - Montpellier, 2003.

R. A. Gherghescu, D. N. Poenaru, W. Greiner

A new deformed two-center shell model.

oral contribution, in Fission and Properties of Neutron-Rich Nuclei, Proc. of the 3rd International Conference, Sanibel Island, Eds J. H. Hamilton, A. V. Ramayya, and H. K. Carter (World Scientific, Singapore, 2003), p. 177-182.

Gh. Rotarescu, I. Paunica, C. Turcanu

Technical aspects regarding the upgrading of the Romanian National Repository for low and intermediate level radioactive waste, Baita, Bihor County (DNDR) Workshop "Structure and Content of Safety Cases and Development of Confidence in the Safety of Near-Surface Disposal Facilities" Budapest, Ungaria, 21-25 iunie 2004

M. Roth, A.F. Badea

Test of a Hadronic Interaction Model by a Multidimensional Analysis of Lateral and Longitudinal Air-Shower Observables at KASCADE
25, ICRC2003, Tsukuba, Japan

M. Roth, H. Ulrich

Energy Spectrum and Elemental Composition in the PeV Region
139, ICRC2003, Tsukuba, Japan

G. Schatz

How Well Do We Know EAS Size Spectra
97, ICRC2003, Tsukuba, Japan

G. Toma, O. Sima, A.F. Badea, I.M. Brancus, H. Rebel, B. Mitrica, A. Haungs

Study of the Lateral and Temporal Distributions of Particles in Extensive Air Showers
"Conferinta Nationala de Fizica de la Pitesti", 09.09.2004 - 11.09.2004

M. Toma, L. Dinescu, O. Sima

Experimental and simulated studies concerning the efficiency calibration of a drum waste assay system
Annual Physics Conference, Faculty of Physics, University of Bucharest, 2004

M. Toma, L. Dinescu, O. Sima

Study concerning the efficiency calibration of a drum waste assay system
International Balkan Workshop on Applied Physics, 5-7 July 2004, Constanta, Romania

C.N. Turcanu, Gh. Rotarescu, I. Paunica

Technical aspects regarding the management of radioactive waste from decommissioning of nuclear facilities

Radioactive Waste Management Conference, Tucson, Arizona, SUA, 23-27 februarie 2003

Anca Vișinescu, D. Grecu

Modulational instability of some nonlinear continuum and discrete systems

International Workshop on Global Analysis, Ankara, Turkey, 15-17 April 2004

Anca Vișinescu, D. Grecu

Solitary waves in a 2D "zigzag" model of coupled chains

Nonlinear Physics: Theory and Experiment, Gallipoli (Lecce) Italia, 24 June- 3 July 2004

Anca Vișinescu, D. Grecu

Modulational Instability and Multiple Scales Analysis of Davydov Model

Conferința internațională "Symmetries 2003", Kiev, iulie 2003

Anca Vișinescu, D. Grecu

Modulational instability phenomenon of quasi-monochromatic waves in dispersive and weakly nonlinear media

CNF-2003, UPB, sept. 2003

Anca Vișinescu, D. Grecu

Solitary waves in a 2-D "zig-zag" model of coupled chains

Physics Conference TIM03, Timișoara, noiembrie 2003

M. Vișinescu

Dirac-type operators in curved spaces

Invited lecture at the International Conference "Selected Problems of Modern Physics", JINR-Dubna, Russia, June 8-11, 2003; to appear in Proceedings

M. Vișinescu

Killing-Yano tensors and Dirac-type operators on curved spaces

Talk at the Fifth General Conference of the Balkan Physical Union, Vrnjacka Banja, Serbia, August 25-29, 2003; to appear in Proceedings

M. Vişinescu

Supersymmetries of the Dirac-type operators
Invited lecture at the 27th Spanish Relativity Meeting "Gravitational Radiation", Alicante, Spain, September 11-15, 2003; to appear in Proceedings

M. Vişinescu

Symmetries and supersymmetries of the Dirac-type operators on curved spaces
Invited lecture at the Fifth International Conference "Symmetry in nonlinear mathematical physics", Kiev, Ukraine, June 23-29, 2003; to appear in Proceedings

M. Vişinescu

Symmetries of the Dirac-type operators in curved spaces
Invited lecture at the Balkan Workshop BW-2003 "Mathematical, theoretical and phenomenological challenges beyond standard model", Vrnjacka Banja, Serbia, August 29 - September 2, 2003; to appear in Proceedings

J. Wentz, I.M.Brancus, A.Bercuci, D.Heck, J.Oehlschlaeger, H.Rebel, B.Vulpescu

Simulations of the atmospheric neutrino fluxes with CORSIKA
INPC2004, "International Nuclear Physics Conference", Goeteborg Suedia, 27.06.2004 - 03.07.2004

J. Zabierowski for the KASCADE Collaboration

Investigation of the Muon Pseudorapidities in EAS with the Muon Tracking Detector of the KASCADE Experiment

29, ICRC2003, Tsukuba, Japan

J. Zabierowski for the KASCADE Collaboration

Muon Production Height from the Muon Tracking Detector in KASCADE

33, ICRC2003, Tsukuba, Japan

PhD Theses

Rizea M.

Numerical methods for solving some boundary problems associated to the Schrödinger equation

Scientific Exchanges

Foreign Visitors

G. Royer

SUBATECH, Ecole des Mines, Nantes, France, 2003

W. Greiner

Frankfurt Institute for Advanced Studies, J. W. Goethe University, Frankfurt am Main, Germany, 2003

H. Rebel

Universitat Heidelberg, Germany, 2003, IDRANAP support

H. Rebel

Universitat Heidelberg, Germany, 2004, IDRANAP support

H. Rebel

Universitat Heidelberg, Germany, 2004, NATO support

G. Vanden Berghe

Department of Applied Mathematics and Computer Science, Universiteit Gent, Krijgslaan 281-S9, B-9000 Gent, Belgium

J. Wentz

Forschungszentrum Karlsruhe, Institut fur Kernphysik, Germany, 2003, IDRANAP support

Visits Abroad

Ad. R. Raduta

GSI-Darmstadt

Ad. R. Raduta

IPN-Orsay

A. Bercuci

Florence, ECRS-European Cosmic Ray Symposium 2004, poster, local support, CERES nr.87

A. Bercuci

ICTP Trieste, Italy, 7th School on Nonaccelerator Astroparticle Physics, 2004, local support

I. M. Brancus

FZK, Karlsruhe, Germany, Research visit, 2004, NATO support

I. M. Brancus

FZK, Karlsruhe, Germany, Research visit, 2004, IDRANAP WP17 support

I. M. Brancus

Florence, ECRS-European Cosmic Ray Symposium 2004, poster, local support, CERES Nr.87 support

I. M. Brancus

HEAPNET-High Energy Astroparticle Physics NET-work, meeting, Paris, 2004, local support, DFN support

I. M. Brancus

INPC-International Nuclear Physics Conference 2004, Gotheborg Sweden, oral contribution, poster, CERES Nr.87 support

I. M. Brancus

ISVECHRI2004, oral contribution, local support, IDRANAP WP17 support

I.M. Brancus

10th International Conference on Nuclear Reaction Mechanisms, Invited talk, Varenna, Italy, 2003, local support, CERES Nr.87

I.M. Brancus

FZK, Karlsruhe, Germany, Research visit, 2003, grant Forschungsgemeinschaft

I.M. Brancus

ICRC-International Cosmic ray Conference 2003, oral contributions, poster, Tsukuba, Japan, 2003, IDRANAP WP17 support

L. Dinescu

Environmental Physics Conference EPC'4, 24 - 28 Feb. 2004, Minya, Egypt

R. A. Gherghescu

Bordeaux, Centre d'Etudes Nucleaires, Bordeaux-Gradignan, France, working stage, 2003

R. A. Gherghescu

Frankfurt Institute for Advanced Studies, J. W. Goethe University, Frankfurt am Main, Germany, working stage, 2003

R. A. Gherghescu

NATO Advanced Study Institute on Structure and Dynamics of Elementary Matter, Kemer, Turkey, 2003

Grigore D. R.

Institute of Theoretical Physics, Zürich University,
Switzerland

L. Gr. Ixaru

Department of Applied Mathematica and Computer
Science, Univ. Gent, Belgium

L. Gr. Ixaru

Dipartimento di Informatica, Univ. Salerno, Italy

L. Gr. Ixaru

Dipartimento di Matematica Applicata, Univ. Pisa,
Italy

M. Mirea

Institut de Physique Nucléaire – Orsay, France

B. Mitrica

Erice, Summer School Participation, oral contribution,
2004, NATO support

B. Mitrica

FZK, Karlsruhe, Germany, research visit, 2003,
IDRANAP WP17 support

M. Petcu

FZK, Karlsruhe, Germany, Research visit, 2004,
IDRANAP WP17 support

D. N. Poenaru

Frankfurt Institute for Advanced Studies, J. W. Goethe
University, Frankfurt am Main, Germany, working
stage, 2003

D. N. Poenaru

NATO Advanced Study Institute on Structure and
Dynamics of Elementary Matter, Kemer, Turkey, 2003

D. N. Poenaru

SERENATE (European Research and Education Net-
working) End-user workshop, IBM - Montpellier,
France, 2003

Rizea M.

Los Alamos National Laboratory, USA

G. Toma

FZK, Karlsruhe, Germany, Research visit, 2004, FZK
support

G. Toma

FZK, Karlsruhe, Germany, research visit, 2003, NATO
grant

G. Toma

ICTP, Trieste, Italy, Participation on summer school,
Summer School on particle Physics, 2003, local sup-
port

Seminars Abroad

Adam Gh.

Reliable scientific software

JINR-Dubna, Russia, February, 21, 2003

Ad. R. Raduta

Experimental evidences of dense neutron-rich matter
in heavy ion collisions

IPN, Orsay, 20 September 2004

Ad. R. Raduta

Fingerprints of dense neutron-rich matter in heavy ion
collisions

GANIL, Caen, 07 December 2004

P. Dita

Factorization of unitary matrices and its applications

University of Bern, June 24, 2003

N. Gramă

Starile cuasimoleculare parent ca stari rezonante exo-
tice

Academie Romana, 30 iunie 2003

Isar A.

Role of decoherence in the quantum theory of information

*Institute of Theoretical Physics, University Giessen,
Germany, November 2003*

L. Gr. Ixaru

Bounds for the local error in the CP methods for the
Schrödinger equation

*Dept. Appl. Math, Univ. Gent, Belgium, 22 October
2003*

L. Gr. Ixaru

CP methods for the Sturm–Liouville problem

*Dipartimento di Matematica Applicata, Univ. Pisa,
Italy, 13 March 2003*

L. Gr. Ixaru

Theory and applications of exponential fitting - a set
of lectures

*Dipartimento di Informatica, Univ. Salerno, Italy, 2
– 11 March 2003*

D. N. Poenaru

Saddle point shapes of nuclei

*Institut für Theoretische Physik der Justus Liebig Uni-
versität, Giessen, 2003*

M. Vișinescu

Research in quantum field theories and gravitation

Scientific Council, JINR-Dubna, Russia, June 6, 2003

Research Staff

Nuclear Physics Department

Bucurescu Dorel, Hațeganu Cornel, Calboreanu Alexandru, Buta Apostol, Borcea Cătălin, Iordăchescu Alexandru, Ionescu Bujor Manuela, Corcalciuc Valentin, Petrovici Alexandrina, Petrovici Mihai, Avrigeanu Marilena, Zamfir Nicolae Victor, Olariu Silviu, Cutoiu Dan, Schachter Leon, Avrigeanu Vlad Gabriel, Pădureanu Ion, Ivașcu Marin, Popescu Ion V., Căta Danil Gheorghe, Petrascu Marius, Bădica Teodor, Isbășescu Alina, Pantelică Ana, David Ioana, Berceanu Ionela, Brâncuș Ileana, Simion Victor, Enulescu Alexandru, Ciortea Constantin, Pentia Mircea, Pop Amalia, Pârlög Marian, Iacob Victor Eugen, Ion Mihail, Mirea Mihail Doloris, Ur .Călin Alexandru, Piticu Ion, Păpureanu Sorin, Duma Marin, Pantelică Dan, Fluerașu Daniela, Tarta Petru Dorinel, Petrache Costel, Petrascu Horia, Legrand Iosif Charles, Căta Danil Irina, Bordeanu Cristina, Nica N. Ninel, Enescu Sanda Elena, Scîntee N.Nicolae, Szilagyi Szabolcs Zoltan, Ionescu M. Remus Amilcar, Rădulescu Aurel, Răduță Adriana Rodica, Olariu Agata, Mărginean Nicolae Marius, Sabaiduc Vasile, Petris D.Mariana, Andronic N.Anton, Dumitriu M.Dana Elena, Stroe Lucian, Negoită Florin, Vaman Georgeta, Vulpescu Bogdan, Stoicea Gabriel, Aranghel Dorina, Glodariu Tudor, Badea Aurelian Florin, Radu Florin, Mărginean Raluca Maria, Aiftimie Doina, Bastea T.Sorin, Popescu I.Răzvan, Draffa George, Tabacaru Gabriel, Toader Cristian Florentin, Stetcu Ionel, Borcan Cristina, Stefanescu Irina, Dobrescu Bogdan, Bercuci Alexandru, Stefan Gheorghie Iulian, Gugiu Marin Marius, Ionescu Paul, Olariu Albert, Radu Aimee Theodora, Suliman Gabriel, Mitrică Bogdan, Toma Gabriel, Oros D.Ană Maria, Popa Gabriela, Negret Alexandru, Colci Madalina, Mihăilescu Liviu Cristian, Buta Adina-Mihaela, Preda Mitică, Radu Oana Georgeta, Penescu Liviu Constantin, Sava Tiberiu Bogdan, Ghiță Dan Gabriel, Borcea Ruxandra, Popa Gabriela, Ciocarlan Cristian, Ilie Gabriele, Gurban Dan.

Theoretical Physics Department

Poenariu Dorin, Grecu Dan, Vișinescu Mihai, Ixaru Liviu, Rădescu Eugen, Răduță Apolodor, Diță Petre, Micu Liliana, Angelescu Nicolae, Scutaru Horia, Caprini Irinel, Stratan Gheorghe, Berceanu Stefan, Grama Nicolae, Adam Gheorghe, Mihalache Dumitru, Apostol Marian, Stoica Sabin, Silișteanu Ion, Grigore Radu Dan, Delion Doru Sabin, Ceașescu N.Valentin, Cîrstoiu Florin Cornel, Vișinescu Anca, Adam Sanda, Gheorghe I.Alex Cezar, Bundaru Mircea, Rizea Mărăgărit, Mazilu Dumitru, Isar Aurelian, Săndulescu Nicolai, Gherghescu Radu, Buzatu Florin Dorian, Ursu Ioan, Baran Virgil, Mișcu erban Dragoș, Despa Florin,

Bîrsan Vasile Victor, Bulboacă Iosif, Cârstea Adrian Stefan, Crașovan Lucian Cornel, Horoi Mihai, Costin Ovidiu, Baboiu Daniel Marian, Panou Nicolae Coriolan, Schiaua Claudiu Cornel, Cune Liviu Cristian, Manoliu I. Mihaela, Doloc A.Lida, Firica Radu Gabriel, Moldoveanu Florin, Vaman Diana, Paraocanu Gheorghie Sorin, Mihut Izabela Ramona, Acatrinei Ciprian Sorin, Răduță Cristian, Negoită Gianina Alina, Pacearescu Larisa, Grecu Alexandru Tudor, Ispas Simona Giorgiana, Bora Florin.

Particle Physics Department

Ion B.Dumitru, Ponta Titus, Diță Sanda, Boldea Venerea, Coca Cornelia, Pantea Dan, Cotorobai Florin Valeriu, Petrascu Cătălina Oana, Alexa R.Călin, Răduță Alexandru Horia, Preda Titi, Iliescu Mihail, Popescu Sorina, Groza Radu Liviu, Bragadireanu Alexandru, Anghel Dragos Victor, Sirghi Diana Laura, Micu Andrei, Orlandea Marius Ciprian, Sandru Adriana Ileana, Rotaru Marina, Cheșneanu Daniela, Rusu Vadim.

Life and Environmental Physics Department

Galeriu Dan, Mateescu Gheorghe, Dorobanțu Ion, Vamanu Vasile Dan, Berinde Alexandru, Petcu Ileana, Mocanu Nicolae, Sandu Elena, Stângă Doru, Mărgineanu Romul Mircea, Slavnicu Stelian Dan, Gheorghiu Adriana, Preoteasa Eugen, Călin Marian Romeo, Pușcalău Mirela Angela, Radu Mihai, Stochioiu Ana, Moiseev Tamara, Dumitru Radu Octavian, Simion Corina Anca, Moisoi Nicoleta, Gheorghiu Dorina, Acasandrei Valentin Teodor, Apostoaei Andrei Iulian, Savu Iulia Diana, Manciu Felicia Speranța, Breban Domnica Cristina, Turcanu Catrinel Octavia, Niculae Carmen Georgeta, Acasandrei Maria Adriana, Corol Delia Irina, Melintescu Mirela Anca, Albu Nicolae Marius, Mihai Felicia, Turcin Ileana, Haranguş Livia, Vamanu Bogdan Ioan, Iordan Andreea Luminita, Olteanu Carmen Ileana, Crețu Mirela Ileana, Mitrică Ionel.

Informatics and Communications

Constantinescu Serban, Manu Valentin, Cărbunaru Octavian, Dima Mihai Octavian, Apostu Ana-Maria, Păuna Eduard Dănuț, Ciubancan Liviu Matei.

Applied Nuclear Physics Department

Constantinescu Olimpiu, Caprini Mihai, Ciobanu Mircea, Tripăduș Vasile, Caragheorgheopol Gheorghe, Rusu Alexandru, Cătănescu Vasile, Bădescu Elisabeta, Petcu Mirel Adrian, Măgureanu Constantin, Constantinescu Bogdan, Cruceru Ilie, Cincu Manuela, Stan Sion Cătălin, Constantin Florin, Gârlea Cristina, Bartoș Daniel, Lupu Mihaela, Nicolescu George, Mihai Nelu, Vasilescu Angela, Rădulescu Mihaela, Crăciun Liviu, Ioan Petre, Enăchescu Mihaela, Todor A.Aurel

Dorin, Ilaș Dănuț, Ivan P.Adrian, Arsenescu N.Remus, Bugoi Roxana Nicoleta, Radu Alina, Rusu Claudiu, Dănilă Bogdan, Militaru Otilia, Ianculescu M.Cristian, Alexandreanu Bogdan, Minca Mariana, Popescu Lucia-Ana, Muresan Ofelia, Serban Alin Titus, Dogaru Marius Stefan, Manea Ioana, Petre Alexandru Bogdan, Pavel Carmen, Cucoaneș Andi Sebastian, Ochesanu Silvia, Mihai Constantin, Gruse Cătălina, Caramarcu Costin, Ghiță Ionica Alina, Buda Stelian Ioan, Cirstea Cristina Diana, Voiculescu Dana.

Nuclear and Vacuum Engineering Department

Duță Viorel, Mateescu Gheorghe, Giolu Gheorghe, Lucaciu Adriana, Popescu Aurora, Lungu Claudiu Teodor, Pop Dan, Mureșan Raluca Anca, Borca Camelia Nicoleta, Ilie Theodor, Crăciun Marian Virgil.

TANDEM Accelerator Group

Dobrescu Serban, Dumitru Gabriel, Dima Răzvan, Mosu Daniel Vasile.

Cyclotron Group

Ivanov Eugen, Vătă Ion, Dudu Dorin, Ploștinaru Dan, Catană Dumitru, Rusen I.Ion, Cazan Ioan Lucian, Cătana Dumitru, Postelnicu Marin.

Radioactive Waste Plant

Dinescu Lucreția, Turcanu Corneliu, Rotărescu Gheorghe, Ene Daniela, Dragolici Felicia Nicoleta, Iancu Dumitru, Rotaru Păstorita Rodica, Nicu Mihaela Daniela, Ionașcu Laura Florina, Mihai Cosmin, Matei Daniela, Stoica Paul, Haralambie Magdalena, Dogaru Gheorghe, Matei Gigel.

National Radioactive Waste Repository

Păunica Iosif, Morar Dumitru Nicolae.

Nuclear Reactor Group

Drăgușin Mitică, Popa Victor, Tucă Carmen Alexandra, Boicu Alin, Mustață Carmen Georgeta, Lupescu Henrieta, Badea Silviu Laurentiu, tefan Violeta, Iorga Ioan, Zorliu Adrian, Mincu Gh.Ion, Isbășescu Mihai, Dragolici Cristian, Ionescu Evelina, Copaciu Vasile.

IRASM – Technological Irradiations

Ponta Corneliu, Moise Ioan Valentin, Cutrubinis Mihalis, Georgescu Rodica Maria, Bratu Eugen, Negut Constantin Daniel, Postelnicu Mihaela, Buzoianu Mioara, Aron Anuța Gabriela, Chiritea Daniel Romeo.

Radioisotope Research and Production Department

Sahagia Maria, Borza Virginia, Postolache Cristian, Fugaru Viorel, Chiper Diana, Luca Aurelian, Ionescu Simona Eugenia, Neacșu V.Elena, Cîmpeanu Cătălina, Razdolescu L. Ana-Maria, Mihăilescu Gabriela, Barna Cătălina Mihaela, Niculae (Mihancea) Dana, Lungu Valeria, Grigorescu Leon, Petrașcu Anca Maria, Ivan Constantin, Duță Elena, Matei Lidia, Negoită Nicolae, Tuta Stelian Cătălin, Șerban Violeta, Drăgan Radu Gabriel.

Design, Development, and Technological Transfer Department

Serbina Leonardo, Rădulescu Laura, Udup Emil.

Radioprotection

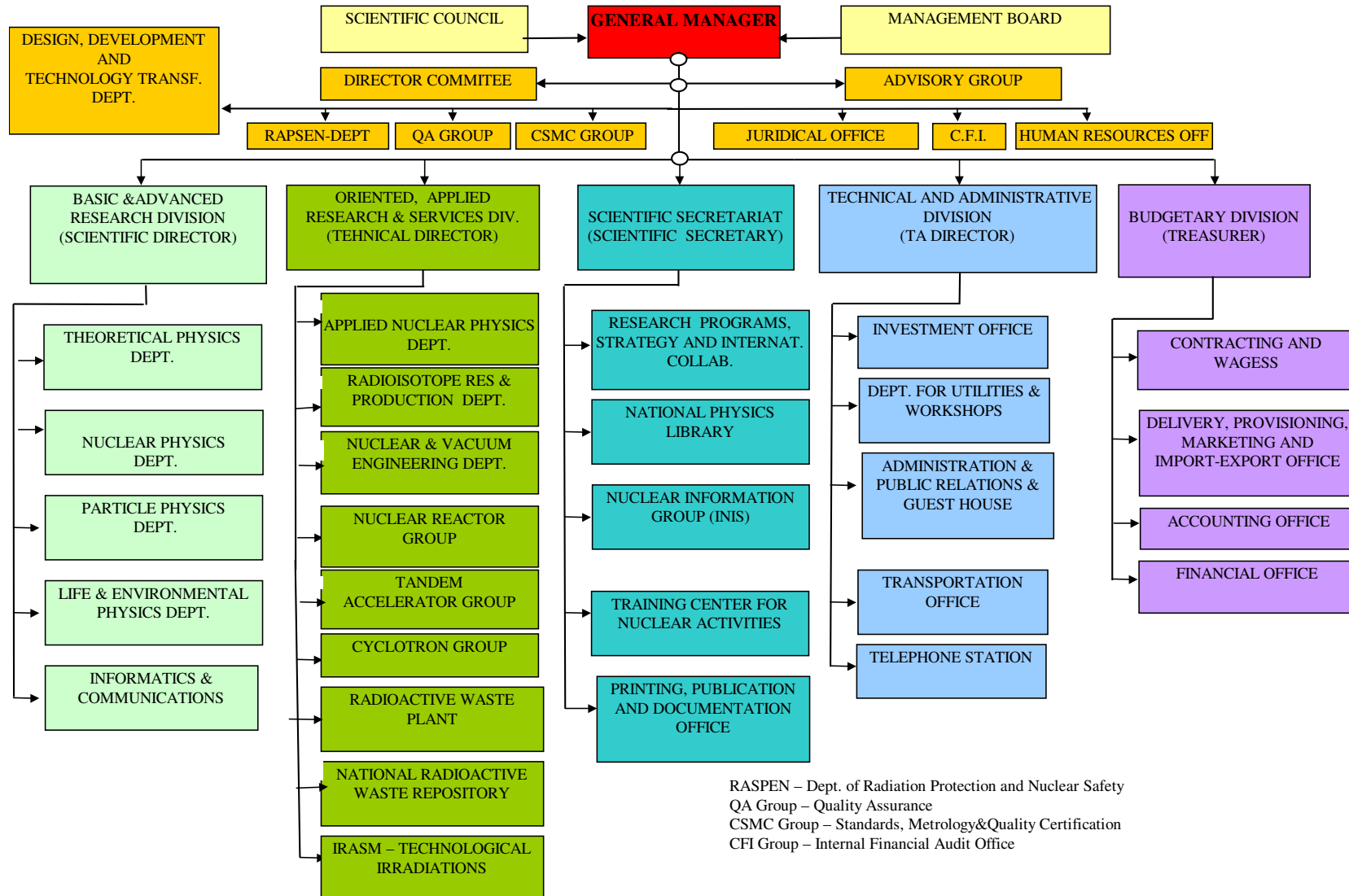
Floare Gabriel, Frăjinoiu Cătălin, Preda Mihaela, Ciort Codruța Adriana, Virgolici Marian, Filimon Andrei Daniel.

Standards, Metrology and Quality Certification

Bercea Sorin, Purghel Lidia, Lira Cristian, Macrin Rodica, Iancso Georgeta, Celarel Aurelia, Iliescu Elena, Hurezeanu Dorina, Iancu Rodica, Cenusu Z.Constantin, Costin Aurelia Monica.

"HORIA HULUBEI" NATIONAL INSTITUTE OF
PHYSICS AND NUCLEAR ENGINEERING

INTERNAL ORGANIZATION



Author Index

Acasandrei,A.	80	Cojocaru,V.	43, 45
Acasandrei,M.A.	76, 77	Collaboration,DIRAC	52
Achouri,N.	49	Condac,E.	70
Adam,Gh.	14	Constantinescu,A.	44
Adam,S.	14	Constantinescu,B.	43, 47, 97
Aiftimiei,C.	56	Constantinescu,S.	41
Aitchison,J.S.	32	Constantin,F.	41, 42, 46, 47, 97
Alexa,C.	41	Cools,R.	13
Ameloot,M.	77	Cotăescu,I.I.	19, 20
Angélique,J.C.	49	Courtin,S.	49
Anton,L.	14	Crăciun,L.	45, 49
Badea,A.F.	55, 62	Crasovan,L.C.	10–12, 28, 30, 31
Bădescu,E.	41, 100, 104	Crout,N.M.J.	67, 74
Badica,T.	45	Cruceru,I.	42, 44, 47, 97
Baiborodin,D.	49	Cutrubinis,M.	102
Balaceanu,M.	58	Dale,V.R.E.	77
Bartoş,D.	41, 46, 47, 64, 73	Danaila,I.	30
Baumann,P.	49	Danis,A.	57, 103
Berceanu,S.	15	Daugas,J.M.	49
Bercea,S.	67	Delion,D.S.	12
Bercuci,A.	56, 62	Dessagne,P.	49
Beresford,N.A.	67, 74	Dinescu,L.	92
Bode,P.	71	Dinescu,L.C.	92
Boicu,A.	85, 86	Diță,P.	17, 18, 41
Boldea,V.	41	Diță,S.	41
Borcea,C.	49	Dlouhy,Z.	49
Braic,M.	58	Dobrescu,S.	50
Braic,V.	58	Dogaru,Gh.	90
Brancovici,S.	67	Drăgolici,C.A.	85
Brancus,I.M.	55, 56, 62	Dragolici,F.	88–91
Brașoveanu,M.	97	Drăgolici,N.F.	87
Buchsteiner,A.	48	Drăgușescu,Em.	85, 86
Bucurescu,D.	41	Drăgușin,M.	85, 86, 97
Bugoi,R.	43, 47, 97	Dudu,D.	57–60, 103
Buță,A.	49	Duliu,O.G.	92
Buzatu,D.	9	Duma,M.	56
Buzatu,F.D.	9	Dumitriu,D.E.	43, 92
Buzoianu,M.	78	Ene,M.	78
Calboreanu,Al.	42	Enescu,S.E.	54
Călin,M.R.	64, 72, 73	Frontasyeva,M.	71
Calin,R.	46	Galeriu,D.	67, 68, 73–75
Caprini,I.	41	Gazdaru,D.	80
Caprini,M.	41, 100, 104	Gentils,A.	54
Caragheopol,Gh.	47	Georgescu,I.I.	71
Caramarcu,C.	104	Georgescu,R.	87, 98, 101, 102
Carjan,N.	25	Gheorghe,Al.	15
Catana,D.	58–60	Gheorghiu,A.	68
Catană,L.	71	Gheorghiu,D.	68, 79
Cârstea,A.S.	15, 35	Gherghescu,R.A.	21–23
Cercasov,V.	71	Giolu,Gh.	46, 69
Cincu,Em.	45, 67	Gramă,C.	17
Ciortea,C.	92	Gramă,N.	17

Grambole,D.	43	Micu,L.	41
Grammaticos,B.	35	Miehé,C.	49
Grecu,D.	15, 33, 36	Mihai,R.	102
Greiner,W.	12, 21–23, 25	Mihalache,D.	9–12, 28–32
Grévy,S.	49	Mincu,I.	85
Grigore,D.R.	18	Mirea,M.	63
Gruse,C.	104	Mișicu,Ș.	25
Gugiu,M.M.	92	Mitrica,B.	55, 56, 62
Guillemaud-Mueller,D.	49	Morimoto,K.	44
Guță,T.	41, 46	Mrazek,J.	49
Haungs,A.	55, 62	Mureșan,O.	49
Heling,R.	73	Mustață,C.	85, 86
Herrmann,F.	43	Münzenberg,G.	23
Huckaby,D.A.	9	Nae,M.	80
Ioan,P.	97	Neacșu,G.	85
Ionescu,E.	86	Neelmeijer,C.	47
Ionescu,P.	53, 54	Negoita,A.G.	27
Iorga,I.	85, 86	Negoită,F.	49, 53, 54
Isar,A.	19	Negoita,N.	70
Ivan,C.	90	Nemțanu,M.	97
Ivanov,E.A.	59, 60	Nicorescu,C.	42, 97
Ixaru,L.Gr.	13	Nicu,M.	89
Kartashov,Y.V.	11, 28, 30	Nicu,M.B.	88
Kim,KyungJoong	13	Oehlschlaeger,J.	55, 62
Kiss,A.	58	Olariu,A.	45
Kivshar,Yu.S.	11	Oprea,C.	71
Knipper,A.	49	Orr,N.A.	49
Kobayashi,T.	44	Osgood,R.M.	9, 11, 32
Leblond,H.	29	Panoiu,N.C.	9, 11, 32
Lecolley,F.R.	49	Pantea,D.	41
Lecouey,J.L.	49	Pantelică,A.	71
Lederer,F.	9, 10, 12, 29–32	Pantelică,D.	53, 54
Len,A.	85	Paunica,I.	88, 91
Lewitowicz,M.	49	Paun,V.P.	27
Lienard,E.	49	Penionzhkevich,Yu.E.	49
Lukyanov,S.M.	49	Penția,M.	52
Lungu,L.	88, 89	Perez-Garcia,V.M.	11, 30
Lupu,A.	46, 47, 64, 73	Petcu,I.	76, 79
Lupu,D.	64, 73	Petcu,M.	56
Lupu,F.	64	Péter,J.	49
Macrin,R.	67	Peticila,M.	49
Malomed,B.A.	10, 12, 29, 31	Petran,C.	85
Manea,I.	42, 97	Petrascu,M.	44
Manu,V.	67	Petre,M.	45
Manu,V.I.	87	Pieper,J.	48
Marica,A.	67	Pietri,S.	49
Marqués,F.M.	49	Pincovschi,E.	71
Mateescu,Gh.	68	Plakida,N.M.	14
Matei,D.	87	Plostinaru,D.	45, 58–60
Matei,G.	87	Poenaru,D.N.	21–23
Matei,L.	70, 87, 97, 98	Poirier,E.	49
Mazilu,D.	9, 10, 12, 29–32	Ponta,C.	87
Melintescu,A.	67, 68, 73–75	Ponta,C.C.	102
Melnikov,I.V.	29, 32	Popa,V.	85, 86
De Meyer,H.	13	Popeneciu,G.	41
Meyer,J.D.	50	Popescu,I.V.	45

Popovici,M.	43, 49	Stiebing,K.E.	50
Postolache,C.	70, 87, 97, 98	Stochioiu,A.	46
Preda,T.	41	Stoica,S.	27
Prutu,I.	76	Strottman,D.	25
Purghel,L.	64, 73	Takeda,H.	74, 75
Racolța,P.M.	45	Tanihata,I.	44
Radu,M.	76, 80	Thierens,H.	79
Raduta,Ad.R.	61	Thome,L.	54
Ramani,A.	35	Timiș,C.	49
Rao,H.	11	Toma,G.	55, 56, 62
Rebel,H.	55, 56, 62	Toma,M.	92
De Ridder,L.	79	Torner,L.	10–12, 28, 30, 31
Rizea,M.	25, 26	Torres,J.P.	10, 11
Rotărescu,Gh.	87–91	Towers,I.	10
Rusu,Al.	46, 47	Tripăduș,V.	48, 49
Sanchez,F.	29	Trivedi,A.	75
Săndulescu,A.	12, 19	Țucă,C.	85, 86
Satsuma,J.	35	Turcan,C.	87
Savu,D.	76, 79	Turcanu,C.	88, 89
Schachter,L.	50	Turcanu,C.N.	88, 90, 91
Scheid,W.	19	Vamanu,D.	68
Scintee,N.	53	Vanden Berghe,G.	13
Secelean,D.	43	vande Ven,M.J.	77
Secu,M.	102	Vasiliu,F.	53
Serban,A.	48	Vassu-Dimov,T.	76
Serbina,L.	47	Vata,I.	57, 59, 60, 101, 103
Şerbina,L.	64, 73	Vâlcceanu,N.	70
Sima,O.	55, 62, 92	Vâlcov,N.	72
Simion,C.A.	99	Vekslerchik,V.	11
Sjobbekk,T.E.	92	Vișinescu,A.	15, 33, 36
Slavnicu,D.	68	Vișinescu,M.	19, 20
Slavnicu,S.D.	79	Voiculescu,D.	45
Sporea,D.	101, 103	Vral,A.	79
Sporea,R.	101	Walter,G.	49
Stan,D.	97	Wentz,J.	56
Stanga,D.	46	Willox,R.	35
Stănoiu,M.	49	Wolterbeek,H.TH.	71
Stefanescu,I.	45	Xu,Z.	28
Stefan,I.	54	Zamfirescu,I.	17
Steinnes,E.	71, 92	Zorliu,A.	85